Development of Microsphere-based Molecular and Serodiagnostics and Their Clinical Utility

YILIN WANG

Doctoral program in Biomedicine
Department of Virology
Medicum, Faculty of Medicine
University of Helsinki
Helsinki, Finland

ACADEMIC DISSERTATION

To be presented, with the permission of the Faculty of Medicine of the University of Helsinki, for public examination in Porthania, Suomen Laki-Sali, Yliopistonkatu 3, Helsinki, on Friday 3rd of April 2020, at 12 noon.

Helsinki 2020

SUPERVISOR

Klaus Hedman, MD, PhD, Professor
Department of Virology
Medicum
University of Helsinki
and
Department of Virology
Helsinki University Hospital Laboratory
Helsinki, Finland

REVIEWERS

Tero Soukka, PhD, Professor
Department of Biotechnology
University of Turku
Turku, Finland

Laura Kakkola, PhD, Docent
Institute of Biomedicine
University of Turku
Turku, Finland

OPPONENT

Matti Lehtinen, MD, PhD, Docent, Visiting scientist
Department of Laboratory Medicine,
Karolinska Institute
Stockholm, Sweden
and
Faculty of Medicine
University of Tampere
Tampere, Finland

ISBN 978-951-51-5934-2 (paperback)
ISBN 978-951-51-5935-9 (online)
Picaset Oy

Helsinki 2020

The Faculty of Medicine uses the Urkund system (plagiarism recognition) to examine all doctoral dissertations.

“博学，审问，慎思，明辨，笃行” —— 子思《中庸》

"Study Extensively, Enquire Accurately, Reflect Carefully, Discriminate Clearly, Practice Earnestly"

—— Zisi, Doctrine of the Mean

Table of Contents

ABSTRACT

Microbial infections share many symptoms in common, rendering diagnosis difficult solely on clinical grounds. Thus, rapid, cost-effective and reliable tests are necessary for the diagnosis of infectious diseases. While the traditional diagnosis is mostly confined to detection of one pathogen at a time, a multiplex array could be a feasible alternative to improve the efficiency in the detection of infections. The Luminex xMAP-based high-throughput platform can provide simultaneous analysis of multiple analytes from the same sample by utilising differentially dyed microspheres. In this thesis, I developed xMAP-based Suspension Immuno Assays (SIAs) for the determination of IgG antibodies, IgM antibodies, as well as the avidity of IgG against the human cytomegalovirus (HCMV), *Toxoplasma gondii (T. gondii)* or human parvovirus B19 (B19V). Moreover, I also developed xMAP-based multiplex DNA assays for 13 human polyomaviruses (HPyVs).

Primary infections by HCMV, *T. gondii* and B19V during pregnancy can result in severe consequences to the foetus. The serological status of the mother is critically important in counselling and recognition of infections. Hereby, I developed and evaluated SIAs for IgG, IgM and IgG-avidity against these three important pathogens. Diagnostic performances of the new assays were assessed with more than 1000 well-characterised serum samples. All the newly developed assays exhibited excellent performance compared to corresponding high-quality reference methods. The positive and negative percent agreements of the antibody-SIAs in comparison with high-standard reference assays were 92-100% and 95-100%, respectively. Kappa efficiencies between SIAs and corresponding reference assays were 0.94-1. Intra-assay and inter-assay coefficients of variations ranged between 2-12% and 1-19%, respectively. Among clinical samples from individuals with primary infection, the IgM- and IgG-SIAs served as highly sensitive screening means for detection of acute infections and immune status; and IgG-avidity-SIAs as a highly specific confirmatory approach for separation of primary infections from long-term B-cell immunity.

On the other hand, during the past 12 years, a dozen viruses have joined the known family members of HPyVs. Serological studies have shown that HPyV infections occur at young age and most of the viruses circulate widely in the general population. Although HPyV infections are generally asymptomatic, severe complications can arise due to virus reactivations in immunocompromised or elderly individuals. HPyVs can persist lifelong after primary infection; however, their tissue specificities, persistence sites and transmission routes are still unclear. Also, the clinical manifestations of HPyVs with regard to immune suppression are largely unidentified. To this end, I developed xMAP-based multiplex DNA assays for all 13 HPyVs

known before 2017, by using primer pairs and probes targeting the respective HPyV major capsid protein VP1 genes.

The xMAP-based multiplex assays allowed for simultaneous detection of all the HPyVs with detection limits of 1-100 copies/µl. At high copies (10^5 copies/µl) each of the 13 target sequences were identified correctly with no cross-reactions. With this novel and specific assay, the extent to which the lymphoid system plays a role in the HPyV infection and persistence was assessed. The frequency of occurrence of HPyV viral genomes was explored in 78 lymphoid tissues from children and adults with tonsillar diseases. HPyV-DNA was found in 17.9% (14/78) of tonsils: JC polyomavirus (JCPyV, n=1), WU polyomavirus (WUPyV, n=3), Merkel cell polyomavirus (MCPyV, n=1), human polyomavirus 6 (HPyV6, n=6), trichodysplasia spinulosa polyomavirus (TSPyV, n=3). The observed frequent occurrence of HPyVs in human tonsils suggests the lymphoid tissue plays an important role as a potential transmission route and a location of persistence for these viruses. However, whether or not the undetected HPyVs share the same infection route requires more investigation with different sample types. Furthermore, to determine the occurrences in skin and clinical associations of HPyVs, I studied their genoprevalences in biopsies of premalignant [squamous cell carcinoma in situ (SCCis) or actinic keratosis (AK)] lesional vs. benign skin from 126 liver transplant recipients (LiTRs); as well as in healthy skin of 80 immunocompetent adults. Multiplex screening was followed by singleplex qPCRs of positive samples, for reference and quantification of the viral DNAs. In total, five dermal HPyVs – MCPyV, HPyV6, human polyomavirus 7, TSPyV, and Lyon IARC polyomavirus (LIPyV) – were found in 26.2% (58/221) skin biopsies. The prevalences and quantities of MCPyV in premalignant vs. benign skin of LiTRs were similar to those in healthy skin of controls. TSPyV was found in a single skin lesion at very low copies. The other three HPyVs occurred exclusively in benign skin. Overall, in 10 out of 12 SCCis/AK patients the viral DNA findings in skin were alike. Thereby, the occurrences of HPyVs in the skin of LiTRs and controls speak against a role for any of HPyVs in SCC development.

The work presented in this thesis shows that the xMAP-based serological approaches exhibit excellent diagnostic performances compared to corresponding conventional methods. Moreover, the developed xMAP-based multiplex PCR for 13 HPyVs could be applied successfully in a variety of clinical materials. Altogether, the newly developed systems provide a powerful tool for medical diagnosis and research.

LIST OF ORIGINAL PUBLICATIONS

This thesis is based on the following publications:

I. **Wang Y**, Hedman L, Perdomo MF, Elfaitouri A, Bolin-Wiener A, Kumar A, Lappalainen M, Söderlund-Venermo M, Blomberg J, Hedman K: Microsphere-based antibody assays for human parvovirus B19V, HCMV and *T. gondii*. *BMC Infect Dis* 2016, 16:8.

II. **Wang Y**, Hedman L, Nurmi V, Ziemele I, Perdomo MF, Söderlund-Venermo M, Hedman K: Microsphere-based IgM and IgG avidity assays for human parvovirus B19V, HCMV and *T. gondii*. *mSphere 2020. In press*

III. Sadeghi M*, **Wang Y***, Ramqvist T, Aaltonen LM, Pyöriä L, Toppinen M, Söderlund-Venermo M, Hedman K: Multiplex detection in tonsillar tissue of all known human polyomaviruses. *BMC Infect Dis* 2017, 17(1):409. *Equal contribution

IV. **Wang Y,** Keinonen A, Koskenmies S, Pitkanen S, Fyhrquist N, Sadeghi M, Mäkisola H, Söderlund-Venermo M and Hedman K: Occurrence of newly discovered human polyomaviruses in skin of liver transplant recipients and their relation with squamous cell carcinoma in situ and actinic keratosis - a single-centre cohort study. *Transpl Int*. 2019, 32(5):516-22.

ABBREVIATIONS

AK	actinic keratosis
AI	avidity index
B19V	human parvovirus B19
BKPyV	BK polyomavirus
CLIA	chemiluminescent immunoassay
CMIA	chemiluminescent microparticle immunoassay
ELFA	enzyme-linked fluorescent assay
CNS	central nervous system
DALY	disability-adjusted life year
dsDNA	double-stranded DNA
EDC	1-ethyl-3-[3-dimetylaminopropyl] carbodiimide hydrochloride
EIA	enzyme immunoassay
ETS	epitope-type specificity
HCMV	human cytomegalovirus
HIV	human immunodeficiency virus
HOT	hands-on-time
HPV	human papilloma virus
HPyV10	human polyomavirus 10
HPyV12	human polyomavirus 12
HPyV6	human polyomavirus 6
HPyV7	human polyomavirus 7
HPyV9	human polyomavirus 9
HPyV	human polyomavirus
HUSLAB	Helsinki University Central Hospital Laboratory
ICTV	International Committee on Taxonomy of Viruses
IFA	immunofluorescence assay
Ig	immunoglobulin
ITR	inverted terminal repeat
JCPyV	JC polyomavirus
KIPyV	Karolinska Institute polyomavirus
LED	light-emitting diode
LIPyV	Lyon IARC (International Agency for Research on Cancer) polyomavirus
LiTR	liver transplant recipient
LTAg	large tumour antigen

MCC	Merkel cell carcinoma
MCPyV	Merkel cell polyomavirus
MFI	median fluorescence intensity
mRNA	messenger RNA
MTAg	middle tumour antigen
MWPyV	Malawi polyomavirus
MXPyV	Mexico polyomavirus
NCCR	non-coding control region
NHS	N-hydroxysulfosuccinimide
NIHF	nonimmune hydrops fetalis
NJPyV	New Jersey polyomavirus
nt	nucleotide
PCNV	proliferating cell nuclear antigen
PML	progressive multifocal leukoencephalopathy
post-tx	post-transplant
PP2A	protein phosphatase 2A
PVAN	polyomavirus-associated nephropathy
qPCR	quantitative PCR
SAPE	streptavidin-R-phycoerythrin
SCCis	squamous cell carcinoma in situ
SD	standard deviation
SG	StabilGuard® immunoassay stabilizer
SIA	suspension immuno assay
ssDNA	single-stranded DNA
STAg	small tumour antigen
STLPyV	Saint Louis polyomavirus
T. gondii	*Toxoplasma gondii*
TAT	total assay time
TSPyV	trichodysplasia spinulosa polyomavirus
VLP	virus-like particle
VP1	virus protein 1
VP1u	unique region of virus protein 1
WHIM	warts, hypogammaglobulinemia, infections and myelokathexis
WUPyV	Washington University polyomavirus

FOREWORD

Infectious diseases are responsible for approximately 15 million deaths annually. Due to ecological changes, population growth, migration and travelling, emerging and re-emerging pathogens are rapidly rising and presenting an ever-increasing burden to public health. In the battle against infectious diseases, timely and accurate diagnosis is pivotal in making treatment decisions and improving patient prognosis. Even more importantly, diagnostic tests can help to control infection transmission via identifying the transmission route and potential infection risks and mechanisms.

Over the years, a variety of methods have been developed for the diagnosis of infectious diseases. Traditional diagnostic methods, for example cell culture, has played an essential role in the early development of clinical microbiology. However, the majority of diagnostic methods have transited to serological and molecular determinations due to the increased diagnostic performance and reduced turn-around time. While there are diversified molecular and serological methods for the detection of infections, most of them are based on monoplex format (detect one pathogen at a time). Today, advanced technologies offer the platform for high-throughput multiplex detection which can save cost, time, labour and sample volume, without compromising diagnostic sensitivity and specificity. This high-throughput setting can significantly facilitate the diagnosis efficiency in resource-limited settings, particularly in the sample volume and time-limited conditions.

The first part of the literature review of this thesis focuses on the traditional and advanced technologies in the diagnosis of infectious diseases. Luminex xMAP technology offers simultaneous determination of multiple analytes from the same sample by utilising dyed microspheres. This part provides a detailed description of xMAP technology, xMAP microspheres and detection instruments—and furthermore—introduces the previously developed xMAP-based multiplex applications for detection of infectious diseases.

The second part of the literature review emphasises the microbial infection and antigen-antibody interactions. This part gives the presentation of the vertically transmitted infections, followed by the fundamental knowledge of the infections by parvovirus B19, human cytomegalovirus and *Toxoplasma gondii* and host immune responses to these infections. The focus of this part is on the serodiagnosis and clinical significance of maternal infections by these three important pathogens.

The last section of the literature review deals specifically with all currently known human polyomaviruses. The section focuses on the biology, epidemiology, discovery, pathogenesis and disease association of human polyomaviruses. To date, 14 human polyomaviruses have been found. The prototype human polyomaviruses JC and BK were discovered in 1971, but

the 12 others are new members of this family since 2008. The rapid discoveries of these novel viruses, on one hand, present a fascinating world of human polyomaviruses; on the other hand, raise many important questions regarding these newly found viruses.

REVIEW OF THE LITERATURE

1. Diagnosis of infectious diseases

Throughout human existence, infectious diseases have always had significant impacts on public health (1). The World Health Organization (WHO) estimates 13-15 million deaths attributed to infection annually until 2030 (2, 3). Despite the advances in the development of vaccines and treatments, infectious diseases are still the dominant cause of morbidity and mortality across the world, particularly in resource-limited countries.

When fighting against infectious diseases, lab-based diagnosis plays an essential role to help the aetiology identification, appropriate treatment, controlling of outbreaks, disease surveillance and discovery of new pathogens. Over the years, various methods have been developed in clinical microbiology. Classical diagnostic techniques like culture and microscopy were heavily used in the early development of clinical laboratories. However, culturing is a prolonged process, which often requires from few days to weeks to produce results. In many cases, viruses grow poorly or not at all in the culture systems. Direct examination by microscopy is restricted to pathogens able to be visualised at low magnification. Current diagnostic methods have focused on the development of antigen detection, antibody detection and nucleic acid detection.

1.1 Traditional diagnosis

1.1.1 Antigen detection

Diagnosis of infection can be obtained in the early stages of a disease by detection of microbial antigen in the clinical specimen. One of the classical methods for antigen detection is immunofluorescence (4). Immunofluorescence relies on the use of an antibody, linked to a fluorescent compound as a probe, to target a specific antigen on the surface of microbes or in cells present in the infected tissue. An antibody bound with a fluorochrome that absorbs light of a defined wavelength and then emits light at a higher wavelength offers optical detection with a special microscope. Immunofluorescence has been widely applied in diagnosis, particularly in respiratory infection in which a clinical specimen may contain microbial aggregates in sufficient amount to be seen microscopically (5). Another approach, latex agglutination, utilising the antibody bound to latex particles, can also offer rapid antigen detections in body fluids (6).

1.1.2 Antibody detection

Infection and antibodies

Microbial infections can trigger immune responses and defence mechanisms in the host. During infection, the host responds with production of antibodies, known as immunoglobulins (Igs), to help defend against foreign invasion. Igs are divided into five classes based on their structure: IgG, IgM, IgA, IgD and IgE. Specific IgM and IgA antibodies usually appear quickly after infection and are dominant during the first days or week after onset, followed by a switch to an increasing proportion of specific IgG antibodies (7).

The binding of antibody and antigen is a noncovalent interaction, and the binding strength involves antigenic determinants and affinity of the corresponding antibodies. The affinity is related with the ratio of the molar concentration of bound Ag-Ab complex to the molar concentrations of unbound antigen and antibody at equilibrium, which can be referred to the association constant (K_a) (7).

$$K_a = [Ag\text{-}Ab] / [Ab][Ag] = 1 / K_d$$

K_d equilibrium dissociation constant
K_a equilibrium association constant
Ag antigen
Ab antibody
Ag-Ab antigen-antibody complex

Affinity (intrinsic affinity) reflects a single binding site between antibody and antigen. In natural infection, the immune response often involves complex antigens containing multiple antigenic determinants and antibodies with bi- or multivalency (8, 9). In this case, another term, avidity (functional affinity) is chosen over affinity due to the measurement of the overall binding capacity within biological systems (10). IgG avidity testing allows for discrimination of a primary infection from a non-primary infection (i.e. past infection, exogenous reinfection, reactivation from latency). It reflects the “average” affinity of IgG antibodies. At the beginning of an infection, IgG antibodies have limited binding force towards a multiplicity of different epitopes with low avidity, but over time, under antigen-driven B-cell selection, the binding force increases through somatic hypermutations, resulting in higher avidity (11). In consequence, high-avidity IgGs predominantly exist in long-term seropositivity, whereas low-avidity IgGs are the major population shortly after primary infection (12).

Antibody detection approaches

Several techniques based on different principles have been used for antibody detection, yet

enzyme-linked immunosorbent assay (ELISA) is the most popular one. ELISA employs an enzyme as immunochemical label for the detection of analytes in clinical samples (13). A chemical reaction between enzyme (commonly used e.g. alkaline phosphatase, horseradish peroxidase and glucose oxidase react) and an appropriate substrate (chromogen or a fluorogen) allows the visualisation of analytes. When chromogen or fluorogen is triggered by an enzyme, a colourless or nonfluorescent molecule can be converted into a coloured or fluorescence end product.

For antibody detection, classical ELISA formats are indirect ELISA, competitive ELISA and IgM-capture ELISA (14). In indirect ELISA, the analyte target antibody is bound to the immobilised antigen on a solid surface. The primary antibody can be detected by a secondary antibody conjugated with an enzyme which reacts with the substrate to generate a colour. Competitive ELISA is designed either based on the labelled antibody and analyte target antibody competing for binding to an immobilised antigen or based on a soluble antigen and immobilised antigen competing for binding to the analyte target antibody. Capture ELISA is preferably used for the detection of IgM antibodies. In capture ELISA, a repertoire of IgM antibodies in serum is captured by an immobilised anti-IgM antibody on the solid surface and then the specific IgM antibodies are detected by binding to the corresponding labelled antigen (14).

For the determination of antibody avidity, approaches are in mainly two formats: One is chaotropic-based avidity assay that separates high and low avidity antibodies by a denaturing wash step, which elutes low-avidity antibodies from the antibody-antigen complex (15). Protein-denaturing reagents, i.e. urea, are commonly used in antibody-antigen dissociation. Another is competition-based avidity assay that detects low-avidity IgG directly by blocking the specific high-avidity IgG with soluble antigen and determining the concentration of the remaining marker-specific low-avidity IgG (16). Measurement of IgG avidity has been successfully applied in the diagnosis of several microbial infections (15, 17).

1.1.3 Nucleic acid test

Nucleic acid tests are laboratory tests based on the analysis of genetic parameters. Polymerase chain reaction (PCR) was initially developed by Kary Mullis and described in (18); this revolutionary technique provides the detection of a microorganism, prompting the identification of agents, especially for the ones that are difficult to culture. PCR methods can provide identification of pathogen DNA or RNA through amplification and are the essential molecular diagnostics in clinical microbiology laboratories nowadays.

The basic PCR technique uses the oligonucleotide primers and DNA polymerase to capture and amplify the target DNA molecules. Most of the PCR methods rely on thermal

cycling, which allows repeated synthesis cycles of target DNA molecules. General thermal cycling includes heat initialisation (activate hot-start DNA polymerase), DNA denaturation (separate double DNA strands), DNA annealing (allow primer binds to target DNA) and DNA extension (synthesis of new DNA strand). The more advanced PCR technique, e.g. quantitative real-time PCR (qPCR), is a trendy method in clinical laboratories. The qPCR uses target amplification in combination with fluorescence probe-based detection, providing the estimation of the amount of a given sequence in a clinical sample. Compared to traditional PCR, qPCR has progressed with regard to quantification of analysis time, assay sensitivity and working safety (no need for gel electrophoresis staining with ethidium bromide) (19). Other advanced PCR techniques, for example, digital PCR (dPCR), utilise PCR and partitioning can provide the absolute quantities of DNA targets per partition and the copy number of a given sequence in the original sample (20).

1.2 Multiplex technology

Conventional diagnostic tests are predominantly monoplex approaches, which means they are limited to one analyte at a time per assay. Combining different assays into a single run can improve diagnosis efficiency in terms of cost, labour, time and sample volume. Multiplex detection technologies that allow the simultaneous detection of different analytes have shown to be a powerful tool for the detection of proteins and nucleic acids in clinical infectious disease diagnostics (21).

Multiplexed serological assays mainly fall into two classes, planar assays and suspension microsphere assays (22). Planar multiplex assays (e.g. microspot microarray-based) consist of high-density microspots of capture ligands immobilised on a solid phase, while in suspension microsphere assays (e.g. Luminex xMAP-based), capture ligands are immobilised on colour- or size-coded microspheres. An advantage of planar assays compared with suspension microsphere assays is higher sensitivity and wide dynamic range (5 logs in planar assay vs. 3.5 logs in suspension assay). However, in comparison with planar assays, suspension assays provide improved precision as the data derived from multiple (50-100) independent measurements of each microsphere population (22). Both planar and suspension multiplex assays have diagnostic potential in clinical microbiology, yet suspension multiplex assays are the prevailing method for FDA-cleared protein measurements (23).

Technological innovations allow for simultaneous detection and identification of multiple targets. The multiplex nucleic acid tests are beneficial to identify aetiological agents, especially when a patient presents nonspecific symptoms attributable to several pathogens. PCR-based multiplex tests are based on the combination of multiple primer sets into a single PCR run for

simultaneous detection of several targets. In general, PCR-based multiplex tests are divided into three categories: excitation and detection of multiple fluorophores-labelled probes in a single PCR run; solid microarray-based detection utilising different capture probes immobilised on a solid phase; and suspension microsphere-based approach based on different capture probes chemically linked to microsphere and then sorted using flow cytometry (21). Multiplex tests based on multiple fluorophore-labelled probes, e.g. multiplex qPCR, can offer real-time detection and relative quantification of multiple analytes. These types of PCRs are done in a closed tube to avoid the risk for contamination since they do not require a separation of pre- and post-PCR steps in the assay; however, these tests have limited multiplex capacity (up to 4-6 analytes). Solid microarray-based detection can correctly identify several targets in the single specimen by using a large number of probes. These tests are often used for whole-genome expression profiling or genome-wide comparisons (21). A suspension microsphere-based approach has the ability to detect 100 or 500 different targets simultaneously, providing a high-throughput and affordable platform for identification of microorganisms (24).

1.3 Suspension microsphere assay

In the late 1990s, a new technology, Luminex® xMAP (x=analyte, MAP=Multi-Analyte Profiling) was invented (25, 26). This new technology offers a high-throughput bioassay platform for simultaneous determination of multiple analytes in a single sample by using spectrally distinct sets of microspheres. Importantly, xMAP technology allows the end-users to customise their *in-house* assays and therefore is gaining popularity in pharmaceutical, clinical and research laboratories.

Different from the microarray runs on a glass slide, xMAP identifies the analytes with different colour-coded sets of microspheres in a liquid suspension. The microsphere sets are coded internally, and each microsphere set can be determined by its unique spectral signature (different concentrations of two different fluorophores) (Fig. 1). A fluorescent reporter, for instance, streptavidin-R-phycoerythrin (SAPE) is used to detect the captured target molecule when bound on the microsphere surface (25).

1.3.1 xMAP microspheres (beads)

Each set of microspheres is dyed internally with different intensity of two or three fluorophores. The combinations of two internally-coded fluorophores can generate 100 spectrally distinct microsphere sets (Fig. 1A). The addition of a third internally-coded fluorophore allows the creation of 500 distinct microsphere sets (Fig.1B).

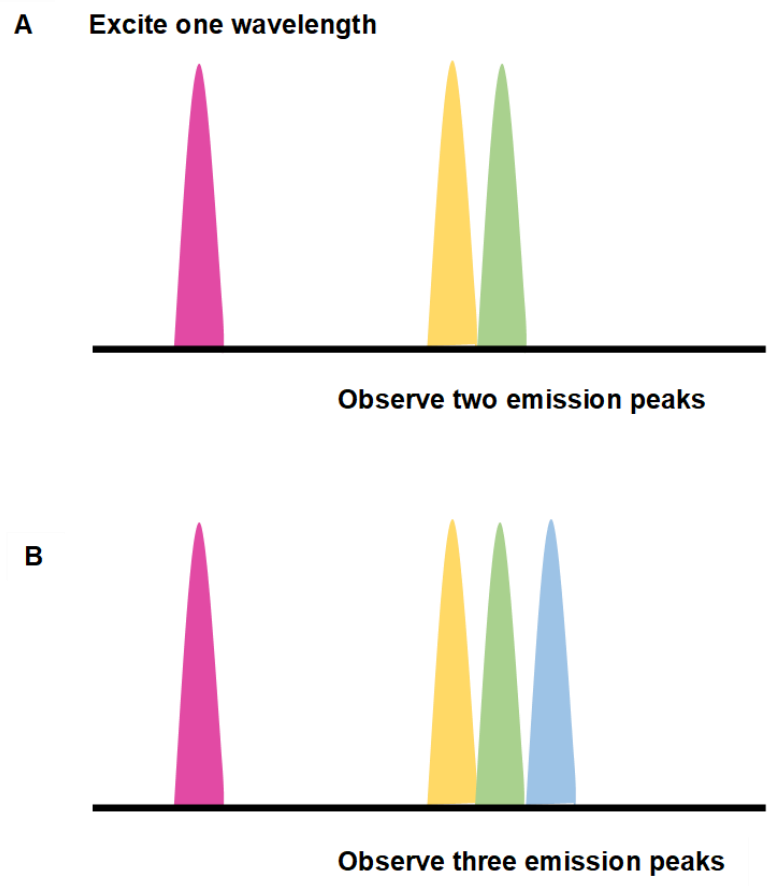

Figure 1. Each microsphere set is encoded internally with a unique internal concentration of fluorophores. Two internally-coded fluorophores generate 100 distinctly coloured microsphere sets (A) and three internally-coded yields 500 distinctly coloured microsphere sets (B).

The classical xMAP microsphere is a 5.6 µm polystyrene microparticle, the surface of which is covered by approximately 10^8 carboxyl groups (COOH) for covalent coupling. Assays with polystyrene microparticles require filter plates for washing; which however, can cause problems such as leaking, clogging and nonspecific analyte adsorption (22, 27). Implementation of the magnetic microsphere has overcome this limitation. The magnetic microsphere has the same binding feature as a polystyrene microsphere, but contains a magnetic layer and differs in size (6.5 µm) (Fig. 2). Usage of the magnetic microsphere permits easy separation from solution, improving recovery during handling and washing steps (28).

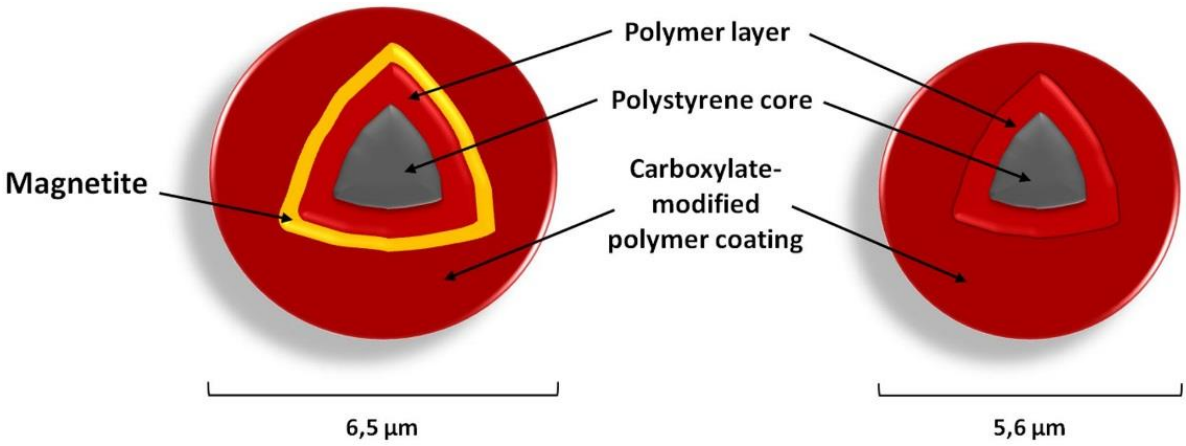

Figure 2. The structures of magnetic and non-magnetic microspheres. Reproduced with permission from Reslova et al., Front Microbiol. 2017; 8:55. Copyright 2017 Reslova, Michna, Kasny, Mikel and Kralik.

1.3.2 xMAP microspheres coupling

The surface of each xMAP microsphere allows for simple carbodiimide coupling of diverse analytes. Protein coupling involves a two-step carbodiimide chemistry while the nucleic acid coupling is a one-step process. In protein coupling, the carboxyl group is first activated with an EDC (1-Ethyl-3-[3-dimetylaminopropyl] carbodiimide hydrochloride) reagent in the presence of sulfo-NHS (N-hydroxysulfosuccinimide), forming a sulfo-NHS-ester intermediate. Then, the reactive intermediate is replaced by the primary amine, forming a covalent amide bond (Fig. 3) (29). In nucleic acid coupling chemistry, the carboxyl group on the surface of microspheres is activated and forms covalent bonds with amine-attached oligonucleotides (29) (Fig. 4)

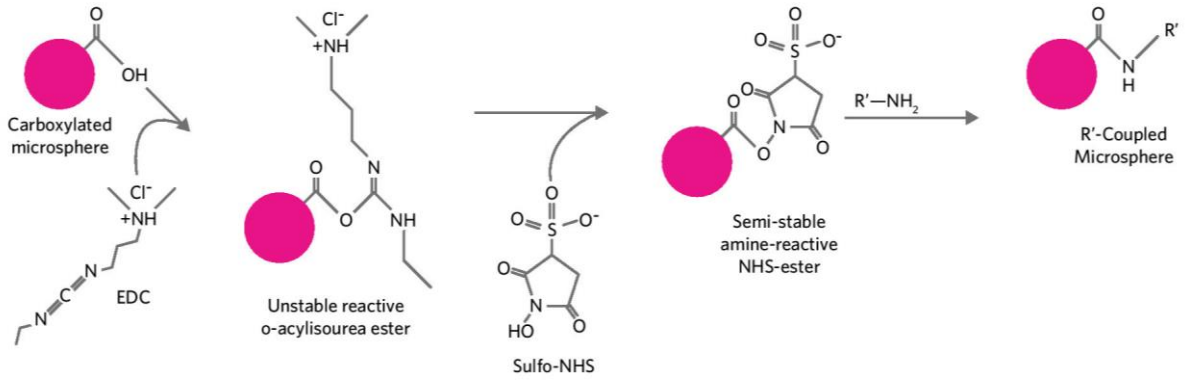

Figure 3. Protein and microsphere coupling chemistry. Adapted with permission from Angeloni S, Das S, Dunbar S, et al, Protein Coupling. In: *Luminex xMAP® cookbook 4th Edition*, Luminex Corporation, 2016: 16-25.

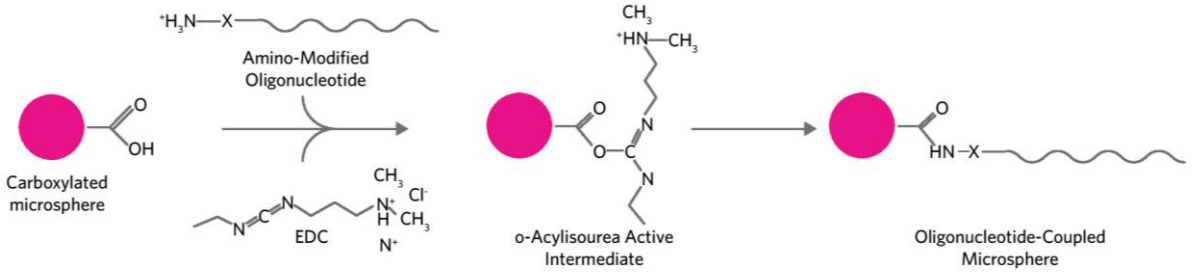

Figure 4. Nucleic acid and microsphere coupling chemistry. Adapted with permission from Angeloni S, Das S, Dunbar S, et al, Nucleic Acid Coupling. In: *Luminex xMAP® cookbook 4th Edition*, Luminex Corporation, 2016: 82-89.

1.3.3 xMAP analysis

The analysis of xMAP application requires a specific detection instrument. Those in the market are (presently): Luminex 100®/200®, FlexMAP 3D® and MAGPIX®. Luminex 100®/200® and FlexMAP 3D® are advanced instruments based on flow cytometry (25). FlexMAP 3D® is capable of measuring up to 500 analytes while Luminex 100®/200® is capable of measuring up to 100 analytes in a single sample. Besides, FlexMAP 3D® is compatible with both 96- and 384-well plates while Luminex 100®/200® is compatible with 96-well plates (25). MAGPIX® is a basic instrument only compatible with the magnetic microspheres and with a maximal reading capacity of 50 bead sets. Distinct from other Luminex instruments, MAGPIX® is based on the principle that the immobilisation of microspheres on the magnetic surface can be recognised by LEDs and charge-coupled device (CCD).

The analysis of microspheres relies on either lasers or light-emitting diodes (LEDs) (Fig. 5). The classification laser or LED (635-nm, 10mW) excites the inner fluorescence impregnated in the microspheres and allows observation of two or three separate fluorescence emission wavelengths. A second laser / LED (532-nm, 13mW) excites the SAPE (578-nm emission) that allows the detection of the captured analytes on the microsphere surface. In laser-based analysis, each microsphere is measured when it rapidly goes through a flowing fluid stream and is digitally processed when the stream passes through the imaging cuvette (Fig. 5A). Whereas in LED-based analysis, microspheres are caught by the magnetic surface and the signal intensity is detected by a CCD camera (Fig. 5B). Each bead region per sample is measured with multiple, independent measurements (typically 50–100) (22). All the independent measurements are collected, and doublets and other aggregates are excluded using side scatter measurements. The final results are obtained as mean fluorescence intensity (MFI) (30).

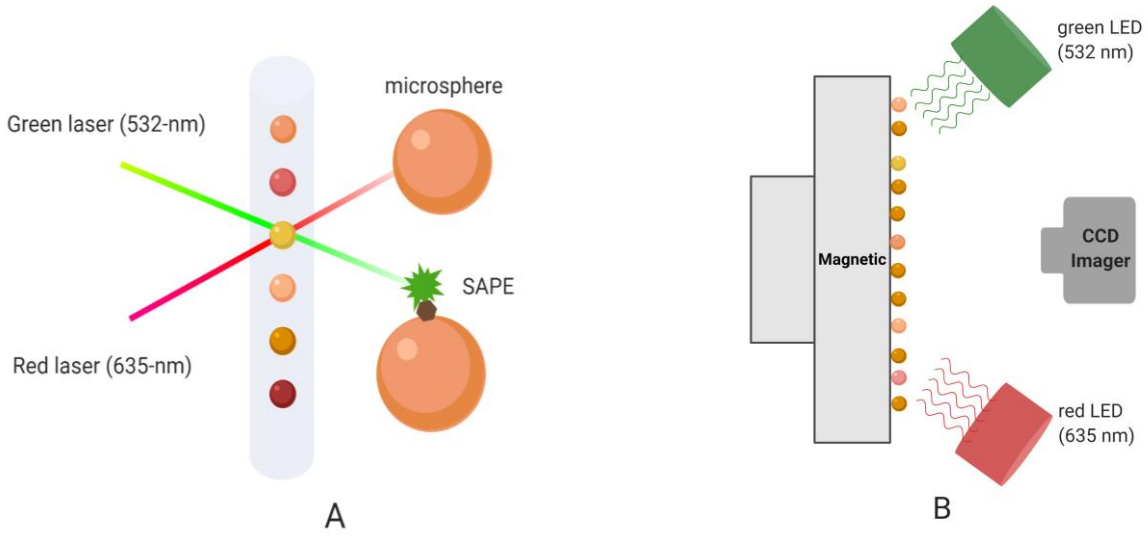

Figure 5. The microsphere is analysed by lasers (A) or LEDs (B). The red laser/LED (635-nm) excites to identify a specific microsphere set according to its internal spectral signature. The green laser/LED (532-nm) excites to detect SAPE bound to the captured analytes. In laser-based analysis, each microsphere is measured when it rapidly goes through a flowing fluid stream and is digitally processed when the stream passes through the imaging cuvette. In LED-based analysis, microspheres are caught by the magnetic surface and the signal intensity is detected by a CCD camera. LED, light-emitting diode; CCD, charge-coupled device.

1.3.4 Microsphere-based multiplex serological assay

The multiplex serological assay is a good surrogate for single-analyte ELISA, thanks to its advantage of simultaneous detection of many different analytes in a single serum sample. The adoption of xMAP technology has led to a wide range of monoplex assays to transition into multiplex assays. This conversion is efficient and cost-effective and has shown superior sensitivity and dynamic range (25). The total-assay-time (TAT) and hands-on-time (HOT) for EIA and xMAP formats have been measured in (198). The TAT for the two is similar. xMAP has a shorter HOT than EIA because of less incubation time since the equilibrium is reached sooner in the near-liquid than solid phase (26). However, the time of measurement of xMAP (80 mins per 96-well plate) is longer than that of EIA (5 min per plate). Moreover, microsphere-based assays have other characteristics which make it superior in immunological analysis: direct fluorescence opposed to colourimetric detection results in excellent sensitivity and reproducibility (198); small surface diameter (5.6 µm or 6.5 µm per bead) has lower risk of nonspecific binding (199); the covalent coupling followed by post-blocking minimises background noise (200); internal controls can monitor the assay performance in each well per run (26, 201); and a possibility to include or exclude assays according to clinical needs. In a

microsphere-based serological assay, analytes covalently linked to microspheres allow capture and quantification of the target molecule in solution.

The common multiplex serological assay formats include competitive assay, capture sandwich assay and indirect assay (29) (Fig. 6). The competitive assay is useful for analysis of small proteins with a single (or very few) epitopes, or for measurement of neutralising antibody responses against a pathogen. The capture sandwich assay is commonly used to measure enzymes, drugs and other biological molecules. And the indirect assay is suitable for the detection of specific antibodies for example to determine allergy, vaccine responses and infection status.

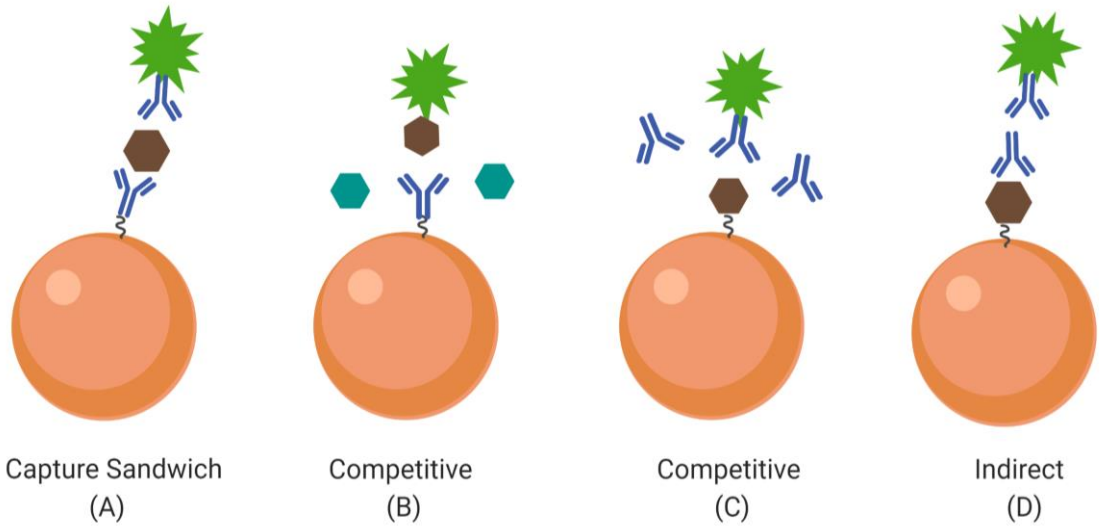

Figure 6. Common multiplex serological assay formats. (A) Capture sandwich immunoassay enables detection of an antigen with the use of a capture antibody coupled to a microsphere and a detection antibody conjugated with a fluorescent reporter. (B) Competitive immunoassay can detect an antigen with the use of a capture antibody coupled to a microsphere and a competitive-labelled antigen reversibly bound to the capture antibody. (C) Competitive immunoassay can also detect an antibody in the sample with the use of a capture antigen coupled to a microsphere and a competitive-labelled antibody reversibly bound to the capture antigen. (D) Indirect immunoassay is used to detect an antibody with an antigen coupled to a microsphere and a labelled detection antibody.

Several microsphere-based multiplex assays have been developed for multiplex detection of microbial infection. For example, a competitive immunoassay was designed for measurement of neutralising antibodies against human papillomavirus (HPV) types 6, 11, 16, 18 (31); an indirect immunoassay for antibodies against viral protein 1 (VP1) of all 14 human polyomaviruses (HPyVs) (32); for antibodies against human immunodeficiency viruses (HIV) recombinant antigens gp41, p17, p24, p31 and p66 (33); for antibodies against four recombinant proteins of hepacivirus C (34); for antibodies against Epstein–Barr virus antigens in nasopharyngeal carcinoma patients (35), and for antibodies against *Trichinella spiralis* and *Toxoplasma gondii (T. gondii)* in infected pigs (36).

1.3.5 Microsphere-based multiplex nucleic acid assay

xMAP technology allows for the development of several genomic applications including miRNA assay, gene expression analysis, SNP analysis and specific sequence detection (25). In the xMAP-based applications for detection of various pathogens, target-specific PCR sequence detection is widely used. This assay format requires the amplification of the target sequence by PCR with specific primers. Then the amplified target DNA sequences are melted and annealed to their capture probes which are chemically linked on the microspheres. Finally, SAPE is added to detect and semi-quantify the target sequences (Fig.7).

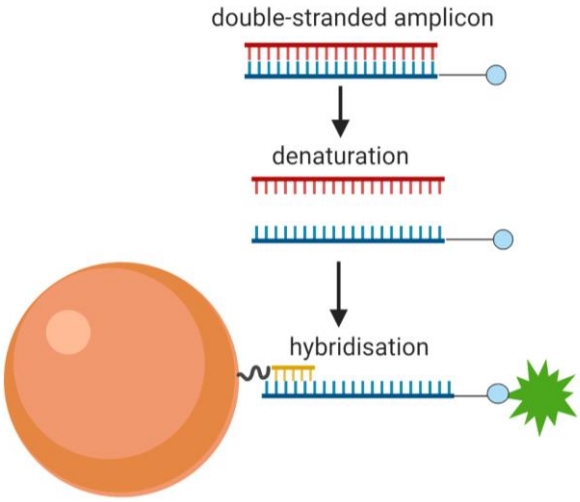

Figure 7. Target-specific PCR sequence detection. The target DNA sequence is amplified by PCR reaction when one of the primers is biotin conjugated. The amplified target DNA sequences are melted and annealed to their capture probes which are chemically linked on the microspheres. SAPE linked with biotin allows the detection and semi-quantification of the target sequences.

The microsphere-based multiplex nucleic acid assay has been successfully applied in genotyping of several microbes including viruses, bacteria, fungi and parasites. A microsphere-based commercial kit is available, for example, for detection of respiratory viruses, xTAG® Respiratory Viral Panel. This panel is intended for the simultaneous detection and identification of 20 respiratory viral targets in nasopharyngeal swabs. The test has a sensitivity of 91.2% and a specificity of 99.7% (37). Furthermore, microsphere-based *in-house* genotyping tests have been developed for genotyping of influenza virus H5N1 isolates from pharyngeal swabs and tracheal aspirates (38); for detection and genotyping of 46 mucosal HPV types associated with infections of genital, anal and oropharyngeal mucosae (39); for identification of 10 foodborne pathogens (40); and for detection of human enteric viruses in sewage and river water (41).

2. Vertically transmitted infections

Infections in pregnancy may pass to the foetus. The infections known to cause congenital defects have been denoted as “TORCH”. The acronym “TORCH” referring to *T*oxoplasma *gondii* (To), Rubella (R), *C*ytomegalovirus (C) and *H*erpes Simplex Virus (H), was first suggested by Nahmias in 1971 (42). Later, other researchers proposed to add “O” for “others” due to the increasing number of other pathogens considered significant causes of transplacental infection, e.g. human parvovirus B19 (B19V), Zika virus, varicella-zoster virus, HIV, hepatitis viruses B and C, *Treponema pallidum* for syphilis and *Listeria monocytogenes.* Vertical transmission of infection before birth (antenatal) is a major cause of foetal morbidity and mortality worldwide (43). The harmful agents may lead to severe outcomes including stillbirth, spontaneous abortion or central nervous system (CNS) defects. The mechanisms of vertical transmission of infection across the placental barrier are largely unknown. Existing studies suggest that the invasion strategies of pathogens may vary throughout gestation or with the level of maternal infection or the corresponding immune responses (43).

In the diagnosis of vertically transmitted infections, nucleic acid tests can be useful to detect the presence of the pathogen genome, however its diagnostic value may be limited due to a short detection window or pathogen persistence after the initial infection or its minor role in identification of primary infection. Therefore, the detection of pathogen-specific antibody kinetics is crucial for the diagnosis of maternal infections.

2.1 Parvovirus B19

Parvoviruses are a group of small (25-nm) (44), non-enveloped viruses with single-stranded DNA (ssDNA) genomes of 5 to 6 kb. The name “parvo” originates from the Latin *Parvum* meaning “small”. B19V was identified in 1974 during blood screening of healthy donors for the hepatitis B surface antigen (45) and is also the first known pathogenic parvovirus infecting humans. Parvovirus B19 (B19V) infections are often mild or asymptomatic; however, they do have a wide range of pathological manifestations including the childhood fifth disease, transient aplastic crisis in patients with longstanding haemolytic diseases, e.g. sickle cell disease, hydrops fetalis, persistent anaemia in immunocompromised patients, as well as post-infection arthralgia (46, 47).

B19V has a linear ssDNA genome of 5596 nucleotides (nt). The B19V genome encodes three major proteins, one non-structural NS1 (77kDa) and two structural, VP1 (83kDa) and VP2 (58kDa). Similar to other parvovirus capsids, B19V capsids have T=1 icosahedral structure assembled from 60 copies of the structural proteins. In B19V, VP1 and VP2 assemble to form a capsid, of which VP2 constitutes 90-95%. The sequences of the two

structural proteins overlap except the unique 227nt at N-terminal end of VP1 called VP1u (48, 49).

2.1.1 Intrauterine B19V infection

B19V infection can be vertically transmitted from mother to foetus. Foetal infection may cause anaemia, hypoalbuminaemia, inflammation of the liver and possible myocarditis, leading to cardiac failure and even nonimmune hydrops fetalis (NIHF) and spontaneous foetal loss (50). B19V has tropism for erythrocyte precursors of bone marrow and foetal liver. When the virus replicates in the haematopoietic system, it can destroy the host cells. Foetuses are vulnerable and susceptible to viral infection due to their immature immune response and relatively short erythrocyte life span. The virus can also lyse erythroid progenitor cells, making B19V a potent inhibitor of erythropoiesis. The consequence can be severe transient or chronic anaemia and eventually high-output heart failure (50-55).

The rate of vertical transmission has been estimated to be 25-50% and the incidence of foetal loss due to B19V, 1.7% to 12.5% (56-59). Foetal hydrops develops in up to 12.5% of infected foetuses with a peak in the second trimester (51, 60). B19V-seronegative women of childbearing age are at risk for B19V infection during pregnancy. Day-care workers, schoolteachers and mothers of B19V-infected children are also the high-risk population groups. In pregnant women, susceptibility to B19V infection has been estimated from 26 to 43.5%, with a seroconversion rate of 0.6 to 2.4% that can reach 13.5% during epidemics (61, 62).

2.1.2 Serodiagnosis of B19V infection in pregnancy

Quickly after viremia, a strong humoral response against B19V is elicited (Fig. 8). At 8 to 12 days post-infection, the anti-B19V IgM antibody tends to appear, followed by the IgG antibody. The anti-B19V IgM is secreted into blood to clear viremia, and the clearance is enhanced by anti-B19V IgG. The anti-B19V IgM usually lasts for 3 to 6 months and then gradually wanes to an undetectable level, while the anti-B19V IgG, although decreasing with time, in most individuals remains detectable for life (Fig. 8). Several immunogenic epitopes have been identified on the VP1 and VP2. Many studies have shown that the virus proteins could induce strong B cell responses (52, 63-65).

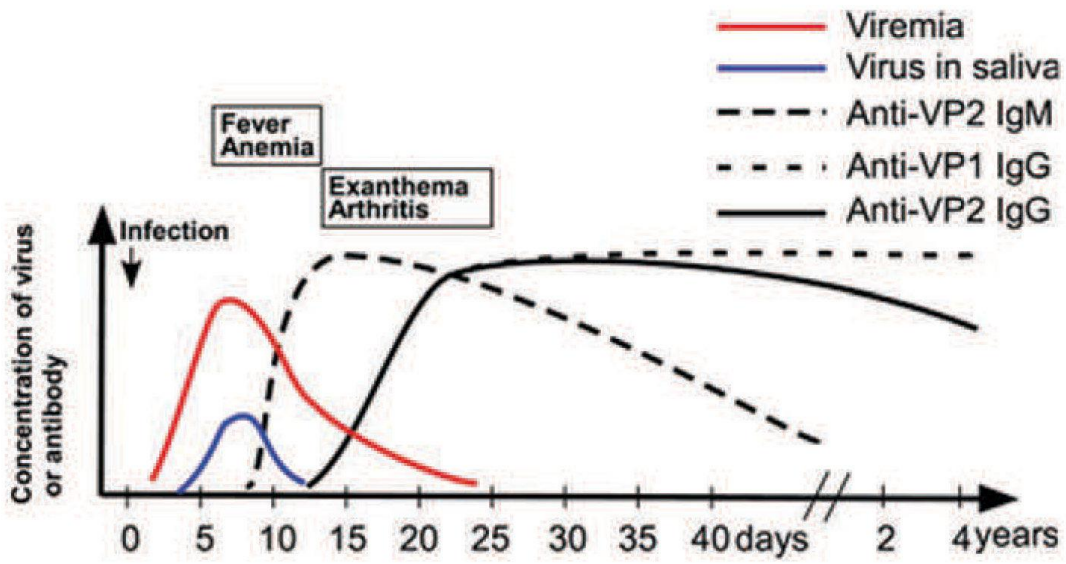

Figure 8. Humoral response to B19V viral capsid proteins at different times in human infection. Adapted with permission from Wolters Kluwer Health, Inc.: David M. Knipe, Peter Howley, *Fields Virology 6th Ed*, 2013, volume II, Chapter 57 Parvoviridae, figure 57.14, p1785.

Antibody detection is an important means for the diagnosis of maternal B19V infection. The first-line serodiagnosis is to use IgG and IgM tests. The presence of B19V IgM, 4-fold IgG-level rise or IgG seroconversion in paired samples is suggestive of a recent infection. The antibody assays for B19V have existed in various formats, the most commonly used ones being enzyme immunoassay (EIA), immunofluorescence assay (IFA) and chemiluminescent immunoassay (CLIA) (49). Recombinant VLPs expressed e.g. in insect cell culture or prokaryotic systems have been successfully applied in commercial as well as *in-house* serological tests. Conformational VP2-VLPs resembling native viral capsids can be recognised by specific IgG and IgM antibodies in recent infections as well as by IgG of long-term immunity, whereas linear VP2 epitopes can only be recognised during acute infection and early convalescence (66). The kinetic difference in the ratio of antibody reactivity towards conformational and linear epitopes has been employed in development of a unique serological assay, epitope-type-specificity (ETS) EIA, which provides useful means for differentiation of recent from past B19V infection (66, 67).

Another method of distinguishing between acute and past B19V infection is the measurement of IgG avidity. The avidity of B19V-IgG can efficiently distinguish acute from past infection. For B19V, the IgG avidity is measured by EIA with VP1, but not with VP2 because the conformational VP2 determinants are irreversibly destroyed after the denaturing treatment and the linear VP2 epitopes cannot be recognized by past-immunity IgG (66, 68). In the clinics, the combination of IgM and ETS or IgG avidity EIAs can accurately diagnose whether the B19V infection occurred within 3-4 months (69, 70).

2.2 Human cytomegalovirus

Human cytomegalovirus (HCMV), also called human herpesvirus 5, belongs to the highly host-specific subfamily *betaherpesvirinae* of family *Herpesviridae*. It is a ubiquitous virus and highly adapted to the host (71). HCMV is the biggest virus in the *Herpesviridae* family with a double-stranded (ds) DNA genome of 236,000bp. The genome has capacity to encode at least 167 gene products, with alternate messenger RNA (mRNA) splicing in certain regions (71). HCMV DNA is encapsidated inside of a highly stable icosahedral capsid (T=16) made up of 162 capsomeres. Cryoelectron microscopy in combination with computer-assisted tomographic image reconstruction (cryoEM or cryoET) has revealed HCMV to have a ~130-nm-diameter icosahedral nucleocapsid and ~200 nm-diameter mature virion particle (nucleocapsid + other structural details) (71-73). The capsid is surrounded by an envelope derived from the host cell membrane and containing viral glycoproteins. Additionally, herpesviruses have a typical thick tegument layer of virus-encoded proteins between the capsid and the envelope. The capsid and tegument are essential for attachment and entry into cells (71).

HCMV is the most significant infectious cause of congenital disease, and the most common of non-genetic childhood hearing loss and of neurodevelopmental delay (74-77). After infection, the virus can never be completely cleared and remains latent for the life of the host. Reactivation of the persistent virus is an important cause of opportunistic infection in immunocompromised individuals and also serves as a source for viral transmission.

2.2.1 Maternal transmission of HCMV

The most common transmission route of maternal infection is breastfeeding; however, transplacental transmission is the major cause of the adverse sequelae with congenital HCMV infection. The risk of intrauterine transmission is closely related to the maternal pre-existing immune response to HCMV, for example, from primary HCMV infection the risk is 30-50% (78, 79) and from a non-primary infection merely 0.5 to 3.4% (80-82). Although the mother's existing immunity cannot prevent vertical transmission, reactivated infections are less likely causes of an adverse outcome to the foetus than primary infections (71, 77, 83). Transplacental transmission is more frequent during late gestation (84-87), whereas the incidence of severe congenital disease is higher in early pregnancy (88, 89).

2.2.2 Congenital HCMV infection

Congenital HCMV infections are associated with a variety of clinical manifestations, of which CNS abnormalities are the most common severe outcomes. Neonatal death occurs in approximately 10% of symptomatic newborns, and HCMV infection has been estimated to be

the leading cause of sensorineural deafness and infectious brain damage in children in the United States (71). Based on a report from the national congenital HCMV disease registry in 1990-1993 (90), the most common non-neurological symptoms are: petechiae (54%), small for gestational age (47%), hepatosplenomegaly (40%) and jaundice at birth (38%); and the neurological abnormalities are: intracranial calcifications (37%), microcephaly (36%), hearing impairment (25%) and chorioretinitis (11%). HCMV birth prevalence was estimated at 0.7% based on 117 986 infants screened (91). Of the infected infants, 12.7% had symptomatic HCMV infection at birth, and 40-58% of the symptomatic infants at birth had permanent sequelae. Furthermore, 13.5% of the children without symptoms at birth had delayed development of permanent sequelae (91).

2.2.3 Serodiagnosis of HCMV primary infection in pregnancy

After primary infection, anti-HCMV IgM antibody is produced initially. IgM peaks at the first months after infection and then declines to an undetectable level typically within 3-6 months of onset (Fig. 9, IgM pattern A). However, persistent IgM may exist longer than 6 months in some individuals (Fig. 9, IgM pattern B). The anti-HCMV IgG level increases and peaks around 1-3 months after primary infection; the specific IgG can persist life-long (48).

The demonstration of detectable anti-HCMV IgM, seroconversion of specific IgG or more than four-fold IgG rise in a serum sample pair may indicate primary maternal infection (92). However, because anti-HCMV IgM may persist for long-term after the primary antigenic challenge and can also be elicited in non-primary infection, the IgM result alone cannot be used as a marker for HCMV acute primary infection (93). In this case, a result of reactivated IgM should be further confirmed by IgG-avidity assay. A high avidity result is suggestive of a past infection; on the contrary, a result of low-avidity IgG is an indicator of primary maternal infection occurred within last 3-4 months (94).

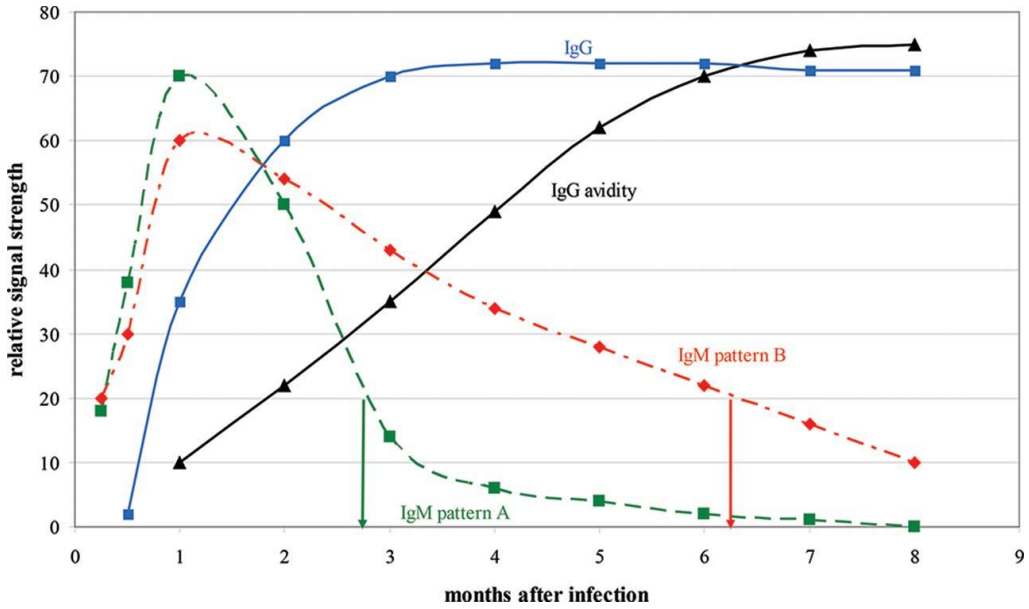

Figure 9. Kinetics of HCMV IgM, IgG and IgG avidity levels over time following HCMV primary infection. IgM pattern A shows a typical IgM response that antibody level declines within 3-6 months of onset (green arrow). IgM pattern B shows long-term IgM persistence that the persistent IgM may exist longer than 6 months in some individuals (red arrow) Low avidity index indicates primary infection within the preceding 3 to 4 months, whereas high avidity indicates a past infection with a low risk of intrauterine transmission. Modified with the publisher's permission from Prince HE, Lape-Nixon M. 2014. Role of cytomegalovirus (CMV) IgG avidity testing in diagnosing primary CMV infection during pregnancy. Clin Vaccine Immunol 21:1377-84.

2.3 *Toxoplasma gondii*

T. gondii is an obligate intracellular parasite which can infect almost all warm-blooded animals including humans, mammals and birds. The first observation of *T. gondii* as human pathogen was probably in 1914 by Castellani who described a *T. gondii*-like parasite in smears of blood and spleen from a 14-year old boy (95). However the first conclusive identification of *T. gondii* as a human pathogen was in 1939 by Wolf, Cowen and Paige (96, 97). In the 1960s, the entire life cycle was eventually identified with the discovery of the cat as a definitive host harbouring and spreading *T. gondii* oocysts through faeces (98, 99).

Toxoplasma gondii is a coccidian parasite, belonging to the order *Eucoccidiida* and family *Sarcocystidae*. It can exist in three forms: an oocyst (environmental stage, sporozoite), tachyzoite (proliferative form) and tissue cyst (slowly dividing bradyzoite). After *T. gondii* oocyst ingestion, sporozoites are liberated in the host. Sporozoites can penetrate the intestinal epithelium and further differentiate into tachyzoites, the proliferative forms of *T. gondii.* In host cells, the tachyzoites rapidly multiply inside a parasitophorous vacuole and then invade any nucleated cell and disseminate throughout the host (100).

2.3.1 Maternal transmission of T. gondii

Tachyzoites are the proliferative form of *T. gondii* and play a major role in vertical transmission. *T. gondii* primary infections during pregnancy constitute a high risk of transmission to the foetus. The mechanism of vertical transmission is not yet fully understood. A hypothesis was proposed that tachyzoites which invaded and multiplied within placental cells during transient parasitaemia are able to cross the placenta and enter the foetal circulation or foetal tissues (101-103). The transmission rate from mother to foetus varies depending on many factors, including primary maternal infection, gestational age (first, second or third trimester), maturity of the foetus, *T. gondii* strain and the maternal immune response (102, 104). In general, the risk of transmission is highest during the third trimester, but foetal infection in early pregnancy constitutes the highest risk of severe congenital diseases (105).

2.3.2 Congenital T. gondii infection

T. gondii replicating in a foetus induces strong inflammation and necrotic foci that can lead to major abnormalities in the brain and ocular tissues. In the former severe outcomes include mental retardation, hydrocephalus, deafness, seizures, microcephalus and psychomotor deficiency. In particular, *T. gondii* infection is the most common cause of posterior uveitis (106); e.g. responsible for >85% of cases in southern Brazil (107). *T. gondii* retinochoroiditis is mainly due to congenital and rarely to acquired infection. Acute retinochoroiditis could cause photophobia, scotoma and active or partial loss of vision (108). Most children with intrauterine infection are usually asymptomatic at birth, whereas the late manifestations (retinochoroiditis or neurological abnormalities) begin to show up in early adulthood (109). A longitudinal U.S. study showed 72% of infants not treated *in utero* or during the first year of life, developed eye lesions during a mean follow-up of 5.7 years (110). In 2013, WHO reported the global annual incidence of congenital toxoplasmosis to be (estimated at) 190 000 cases, corresponding to a burden of 1.2 million in disability-adjusted life years (DALYs) (111).

2.3.3 Serodiagnosis of primary T. gondii infection in pregnancy

Once *T. gondii* enters the host, IgA and IgM are produced during the first few weeks post-infection and the antibody level reaches a plateau within one month. Specific IgM declines to an undetectable level after several months to two years depending on the test used (112). Likewise, specific IgA can be detected long after infection, and thus IgM and IgA alone do not qualify for a marker of recent infection (113). Specific IgG appears after IgM and IgA and the IgG level reaches a plateau within 2-3 months. The IgG level declines and persists lifelong at a residual level (Fig. 10).

Serodiagnostic methods are useful for the detection of maternal *T. gondii* primary infection. IgG detection using a major membrane protein or whole parasite can efficiently detect infection, but the sensitivity is based on the technique used (ELISA, Sabin Feldman dye test, immunofluorescence antibody test and agglutination test) (114). The Sabin-Feldman dye test (115, 116) has been considered a gold standard for years. The test is based on parasite lysis by serum antibodies in the presence of complement. Nevertheless, it is performed only in few laboratories due to its complexity. ELISA-based detection is suitable for antibody detection and is used widely in clinical laboratories.

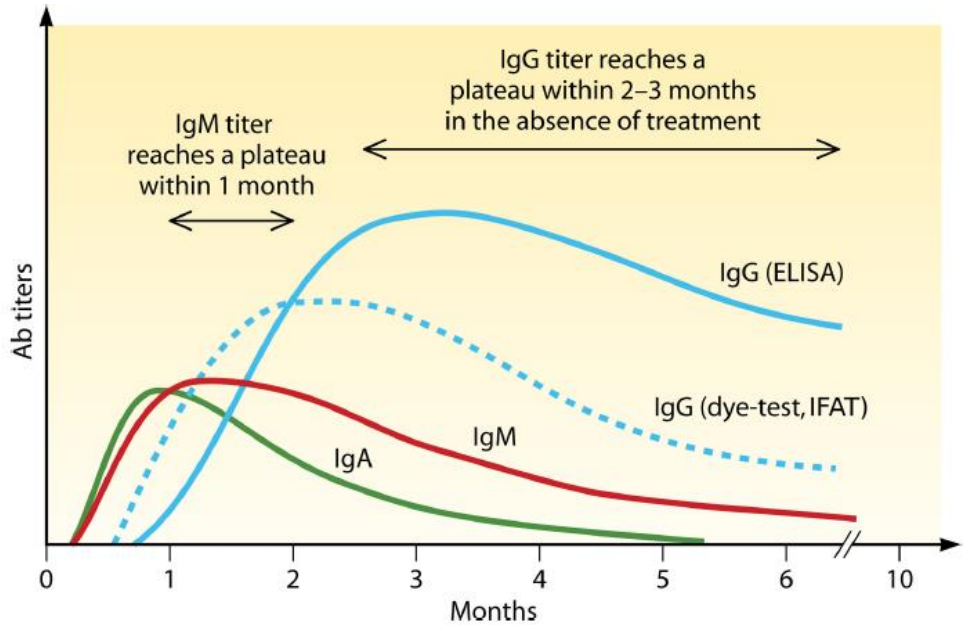

Figure 10. Kinetics of antibody responses against *T. gondii*. IgM titer peaks at the first 1 to 2 months and declines 1 to 6 months after infection. However, IgM may persist one year or longer. IgA peaks within 1 month and declines 1-3 months after infection, sometimes it may still be detected after 9 months. Specific IgG can be measured by many techniques including ELISA, Sabin Feldman dye assay, immunofluorescence antibody test (IFAT). Despite techniques, IgG peaks within 2-3 months in the absence of antiparasitic treatment. Reprinted with permission from Robert-Gangneux F, Darde ML. 2012. Epidemiology of and diagnostic strategies for toxoplasmosis. *Clin Microbiol Rev* 25:264-96.

Since anti-*T. gondii* IgM may persist for months after initial exposure to the pathogen as well as being elicited by recurrent infection, a result of positive IgM should be retested for IgG avidity to rule out primary infection. As a rule, a high IgG avidity index indicates past infection. However, low or intermediate avidity indices cannot prove a recent infection (114). IgG maturation seems to be delayed especially in pregnant women, and the process can be further slowed down due to spiramycin treatment (117, 118). Another approach determining the stage of infection is to detect rising IgG titers between two consecutive serum samples obtained at 3-week intervals, but the antiparasitic treatment may also hamper the IgG-titers. Therefore, a combination of different diagnostic tools for precise interpretations is required to achieve accurate timing of infection (114).

3. Human polyomaviruses

Polyomaviruses belong to the family *Polyomaviridae*. The first polyomavirus was identified in 1953 when Ludwik Gross noticed tumours in parotid glands after injecting leukemic extracts into animals. He soon published this finding and named this agent parotid tumour virus (119-121). Later, Sarah Stewart and Bernice Eddy observed similar results in mice and renamed this agent SE (Stewart and Eddy) polyoma (poly =multiple, tumours=oma) virus (122). Eventually, virologists agreed to adopt the name “polyoma virus” (121). To date, polyomaviruses have been found in a wide range of hosts including humans, primates, birds, reptiles and rodents.

To date, 14 human polyomaviruses (HPyVs) have been discovered. All HPyVs except the newest agent Lyon IARC polyomavirus (LIPyV) were assigned as polyomavirus species (Table 1). Based on the amino acid identity of the large tumor antigen (LTag), HPyVs have been grouped by the ICTV into three genera: *Alphapolyomavirus* (*HPyVs 5, 8, 9, 12, 13*), *Betapolyomavirus* (*HPyVs 1, 2, 3, 4*) and *Deltapolyomavirus* (*HPyVs 6, 7, 10, 11*) (123). Although all HPyVs share a similar genomic structure, they have distinct biological properties, for instance, disease associations, tissue tropism and epidemiology (124).

3.1 Overview of human polyomaviruses

All the HPyVs are listed in Table 1. The first two HPyVs, BK (BKPyV) polyomavirus and JC polyomavirus (JCPyV) were isolated and characterised in 1971 (124, 125). BKPyV (*HPyV1*) and JCPyV (*HPyV2*) were named for the initials of patients from whom the viruses were found. The third and fourth HPyVs, Karolinska Institute polyomavirus (KIPyV, *HPyV3*) (126) and Washington University polyomavirus (WUPyV, *HPyV4*) (127), were found in 2007, 36 years after the first two. KIPyV and WUPyV were identified from nasopharyngeal aspirates of children with respiratory tract infection, but no solid evidence yet links the viruses with the symptoms. One year later, the carcinogenic Merkel cell polyomavirus (MCPyV, *HPyV5*) was identified from a rare, but aggressive skin cancer, Merkel cell carcinoma (MCC) and was shown to be mutated and chromosomally integrated into most cases of MCC (128, 129). So far this is the only HPyV causally associated with cancer. In 2010, two other HPyVs, human polyomaviruses 6 and 7 (*HPyV6, HPyV7*), were found in skin swabs of healthy volunteers (130). They were considered normal skin viral flora until two recent studies (131, 132) proposed the two to be associated with pruritic skin eruptions during immunosuppression. In 2010, another HPyV, trichodysplasia spinulosa polyomavirus (TSPyV, *HPyV8*), was discovered and isolated from the face of an immunocompromised patient with the rare skin disease trichodysplasia spinulosa (TS) (133). In 2011, human polyomavirus 9 (*HPyV9*) was

amplified from the blood and urine of an asymptomatic renal transplant recipient (134). Subsequently, in 2012, human polyomavirus 10 (*HPyV10*) / Malawi polyomavirus (MWPyV) / Mexico polyomavirus (MXPyV) was found and reported by several research groups (135-137). This virus was identified in stool samples of children with diarrhoea and in condyloma from an immunocompromised patient with warts, hypogammaglobulinaemia, infections and myelokathexis (WHIM) syndrome. The two isolates MWPyV and MXPyV were nearly identical and were proved to belong to a single species. In late 2012, the 11th human polyomavirus (Saint Louis polyomavirus, STLPyV, *HPyV11*) was isolated from stool samples of children with diarrhoea as well as healthy children (138). In 2013, human polyomavirus 12 (HPyV12) was identified in resected human liver tissue (139). In the following year, another novel human polyomavirus New Jersey polyomavirus (NJPyV, HPyV 13) was identified in a pancreatic transplant recipient. The patient harboured several clinical conditions (140). Finally in 2017, the latest novel human polyomavirus, LIPyV was discovered in human skin samples and its DNA has been detected at low prevalence (0.2%-2.1%) in skin swabs, oral gargles and eyebrow hair of cancer-free individuals (141).

3.2 Epidemiology of human polyomaviruses

Seroprevalences of HPyVs are presented in Table 1. HPyV serological studies are mainly based on IgG seroresponses against VP1, the immunodominant major capsid protein (32, 142-144). Studies have shown the HPyV infections to be ubiquitous and to be acquired during childhood, as indicated by a rapid increase in seropositivity during the first years of life. For instance, our group showed the MCPyV-IgG prevalence to be 9% at 1-4 years and 35% at 4-13 years (144); whereas TSPyV-IgG prevalence was 5% at 1-4 years, rising to 48% at 6-10 years and reaching 70% among adults (143). Generally, the geographical differences in HPyV seroprevalences seem small, however, the seroprevalences of the HPyV species do differ. A comprehensive study (32) revealed high seroprevalences of HPyVs among Dutch blood donors (60-100%). However, the most recently identified HPyV12, NJPyV and LIPyV showed both low seroprevalences (<5%) and low seroreactivities (32). The low HPyV12 seroprevalence fits with the recent notion of HPyV12 representing a shrew-derived virus (145). The NJPyV seroprevalence is not fully settled; this virus likely does not circulate widely in Europe (32).

Table 1. Fourteen human polyomaviruses so far discovered

Species	Virus name (abbreviation)	Year identified	Method of identification	Source of isolation	Associated diseases	Genome length (bp)	Seroprevalence
HPyV1	BK polyomavirus (BKPyV)	1971	Cell culture	Urine (125)	Nephropathy	5153	80-100% (146-149)
HPyV2	JC polyomavirus (JCPyV)	1971	Cell culture	Brain (PML), Urine (124)	Progressive multifocal leukoencephalopathy	5130	40-80% (146-149)
HPyV3	Karolinska Institute polyomavirus (KIPyV)	2007	Deep sequencing	Nasopharynx (150)	Not defined	5040	40-95% (146, 151, 152)
HPyV4	Washington University polyomavirus (WUPyV)	2007	Deep sequencing	Nasopharynx (127)	Not defined	5229	60-90% (146, 151, 152)
HPyV5	Merkel cell polyomavirus (MCPyV)	2008	Digital transcriptome substraction	Skin (Merkel cell carcinoma) (129)	Mekel cell carcinoma	5387	40-80% (146, 151, 153-155)
HPyV6	Human polyomavirus (HPyV6)	2010	Rolling-circle amplification	Skin (130)	Pruritic rash	4926	70-85% (130, 151, 153, 155, 156)
HPyV7	Human polyomavirus (HPyV7)	2010	Rolling-circle amplification	Skin (130)	Pruritic rash, Thymic epithelial tumours	4952	35-65% (130, 153, 155, 156)
HPyV8	Trichodysplasia spinulosa polyomavirus (TSPyV)	2010	Rolling-circle amplification	Skin (TS spicule) (133)	Trichodysplasia spinulosa	5232	70-85% (151, 153, 155, 157, 158)
HPyV9	Human polyomavirus 9	2011	Consensus PCR and deep sequencing	Serum (134)	Not defined	5026	20-70% (151, 153, 155, 156, 159)

Species	Virus name (abbreviation)	Year identified	Method of identification	Source of isolation	Associated diseases	Genome length (bp)	Seroprevalence
HPyV10	MW polyomavirus (MWPyV) *	2012	Rolling-circle amplification, multiple displacement amplification, Random PCR	Stool / Skin (anal condyloma) (136, 137)	Not defined	4927	40-99% (151, 160, 161)
HPyV11	Saint Louis polyomavirus (STLPyV)	2012	Pyrosequencing and multiple displacement amplification	Stool (138)	Not defined	4776	70% (162)
HPyV12	Human polyomavirus 12 (HPyV12)	2013	Generic PCR	Liver (139)	Not defined	5033	23-33% (139, 156)
HPyV13	New Jersey polyomavirus (NJPyV)	2014	High-throughput sequencing	Muscle (140)	Not defined	5108	Unknown
**	Lyon IARC polyomavirus (LIPyV)	2017	Degenerate PCR combined with next-generation sequencing	Skin (141)	Not defined	5263	Unknown

* Human polyomavirus (HPyV10) / Malawi polyomavirus (MWPyV) / Mexico polyomavirus (MXPyV) are the same virus species.
** LIPyV has not been assigned as a polyomavirus species.
Note added after completion of our work, Ondov et al. (*Genome Biology 2019*, https://doi.org/10.1186/s13059-019-1841-x) found 15th human polyomavirus Quebec polyomavirus (QPyV, GenBank BK010702) in fecal samples from a 85-year-old hospital patient in Montreal, Canada.

3.3 Molecular biology of human polyomaviruses

Polyomaviruses are relatively small (~40-45 nm in diameter) (163), non-enveloped viruses containing a circular double-stranded DNA genome (~5.2kb). Polyomavirus capsids have an icosahedral symmetry structure with 72 capsomers in a skewed (T=7) arrangement (164). All polyomaviruses share a similar genomic organisation with two distinct transcriptional regions on opposite strands: early region and late region. Between the early and late gene regions is a non-coding control region (NCCR) (Fig. 11). This regulatory region contains the origin of DNA replication as well as promoters for transcription of the early and late viral transcripts.

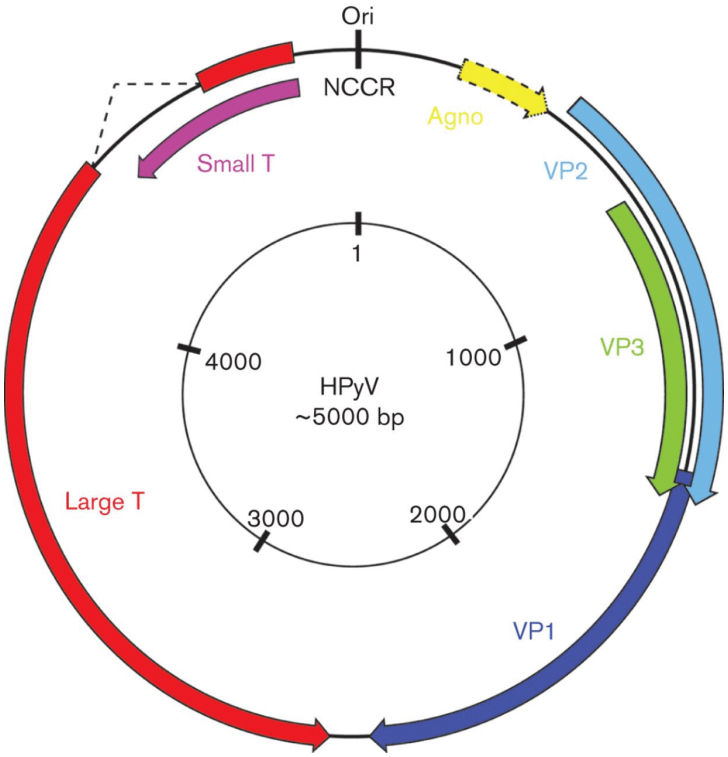

Figure 11. Schematic presentation of the circular double-stranded DNA genome of human polyomaviruses. The genome has three main regions: a non-coding control region containing the early and late promoters; an early region encoding large T antigen and small T antigen and an alternatively spliced LTag; and a late region encoding the viral proteins VP1, VP2 and VP3. The agnoprotein is by far only found in JCPyV and BKPyV genome. Reproduced with permission from Feltkamp M.C.W, Kazem S. et al., 2013 From Stockholm to Malawi: recent developments in studying human polyomaviruses. *J GEN VIROL* 94(Pt 3):482-96.

The early gene regions of HPyVs encode LTAg and small tumour antigen (STAg) (Fig. 11). These two antigens share 75-80 aa at their N termini, with a unique LTAg C-terminus (165). Some HPyVs also harbour open frames for middle T antigen (TSPyV, STLPyV) and / or alternate frame of the LTag reading frame, ALTO (MCPyV, NJPyV, TSPyV) (138, 140, 166, 167). Besides,

MCPyV and TSPyV produce truncated spliced LTag, 57kT and 21kT, respectively (167, 168). The late gene regions of HPyVs encode the capsid proteins, viral protein (VP)1, VP2 and VP3 (Fig. 11). Exceptionally, MCPyV lacks a VP3 minor capsid protein (169). VP1 is the major structural protein, making up more than 70% of the total protein of the virus particle. The HPyV capsid contains 72 capsomers, each of which contains 5 VP1s and 1 VP2 or VP3. Only VP1 is exposed on the capsid surface (170).

3.4 Host cells and suggested routes of transmission

Like other non-enveloped DNA viruses, polyomaviruses are extremely resistant to environmental and chemical influences (171, 172). They are also resistant to UV-C irradiation like other non-enveloped viruses such as parvo- and caliciviruses. Although the interactions of newly found HPyVs and the host cells or tissues *in vivo* are largely unknown, collective information from several studies suggests that the horizontal transmission route of HPyVs may be direct contact or aerosol or faecal-oral (164, 173, 174). For example BKPyV and JCPyV are known to persist in the reno-urinary tract and can be excreted in the urine. Exposure to the virus-containing excreta could be a source of infection. JCPyV DNA has also been found in tonsillar stromal and B cells (175). Under experimental conditions, JCPyV can productively infect tonsillar stromal cells. Likewise, BKPyV DNA has been detected in the lung tissue, in the respiratory tract, and tonsillar tissue, and has a preferential tropism for human salivary glands (176-178). WUPyV DNA was detected in tonsils and nasopharyngeal lymphoid tissue of immunocompetent children (179). Of the HPyVs, MCPyV, HPyV6, and HPyV7 are frequently found in skin whereas TSPyV, HPyV9, HPyV10, NJPyV, LIPyV have also been sporadically reported in skin (141, 180-182). MCPyV DNA was also found in tonsillar tissue from tonsillectomy patients and in nasopharyngeal aspirates from wheezing children (183). Moreover, MWPyV DNA has been found in faecal and respiratory samples of healthy children (136, 184), suggesting respiratory or faecal-oral transmission.

On the other hand, environmental studies have proposed another potential source, water. BKPyV, JCPyV, MCPyV, KIPyV, and WUPyV are routinely found in sewage water (171, 172). In addition, a review summarized the recent environmental studies and the collective data showing that HPyVs can be detected in almost all types of water, includes wastewater, coastal seawater, stormwater, river water, and even drinking water, suggesting a water-source transmission pathway for HPyV infections (174). Nevertheless, intensive molecular and serological studies are

required to determine the route of transmission and the site of primary infection for the newly discovered HPyVs.

AIMS OF THE STUDY

The specific aims of this thesis were:

1) To develop and evaluate microsphere-based Suspension Immune Assays (SIAs) for IgG, IgM and IgG-avidity for B19V, HCMV and *T. gondii*

2) To assess the diagnostic performances of the SIAs in diagnosis and timing of the infections by B19V, HCMV and *T. gondii*

3) To set up and evaluate microsphere-based multiplex PCR assays for the detection of DNAs of 13 HPyVs

4) To explore the occurrences of HPyV viral DNAs in tonsillar tissues and to determine to what extent the lymphocyte system plays a role in HPyV infections and persistence

5) To investigate the occurrences of the HPyVs in skin biopsies from liver transplant recipients versus healthy controls, in order to determine whether the HPyVs are etiologically associated with squamous cell carcinoma.

MATERIALS AND METHODS

1. Materials

1.1 Patients and clinical samples (I-IV)

Table 2. Clinical samples used in studies I-IV.

Study	Study cohort	Sample n=	Sample type
I	Archival samples from HUSLAB	80	Serum
	80 follow-up patients with B19V infection	143	Serum
	104 Medical students	104	Serum
II	Archival samples from HUSLAB	97	Serum
	Archival samples from HUSLAB	94	Serum
	Archival samples from HUSLAB	40	Serum
	66 follow-up children and adults with B19V infection	126	Serum
	52 follow-up patients with HCMV infection	149	Serum
	22 follow-up pregnant women with *T. gondii* infection	116	Serum
	87 Medical students	87	Serum
III	78 children and adults with tonsillitis or tonsillar hypertrophy	78	Fresh-frozen tonsillar tissue
IV	126 follow-up adult liver transplant recipients	14 127	Fresh-frozen lesional skin Fresh-frozen healthy skin
		118	Serum
	80 immunocompetent adults	80	Fresh-frozen healthy skin

Archival serum samples from HUSLAB (I, II)

Archival samples (-20°C) were obtained from Helsinki University Central Hospital Laboratory Service (HUSLAB) collected between 2003 and 2013. In study I, carried out with IgG-SIAs, 80 samples from 60 subjects had been tested for IgGs by *in-house* B19V-EIA and by Vidas HCMV and Toxo ELFAs. In study II, carried out with IgM- and IgG-avidity-SIAs, 231 samples were studied for IgMs and IgG-avidity against B19V (n=40), HCMV (n=97) and *T. gondii* (n=94) by *in-house* B19V-EIAs, Biotrin's B19V-IgM EIA, Architect HCMV CMIAs and Vidas Toxo ELFAs. The reference assays are listed in Supplementary, Table S1.

Children and adults with B19V infection (I, II)

Serum samples from children or adults (2 to 58 years of age, median 10 years) with symptomatic B19V infection were collected between 1992 and 2001. Study I, for B19V IgG-SIA, included 143 samples from 80 subjects, followed up serologically for up to 700 days after primary infection. Study II, for B19V IgM-SIA and IgG-avidity-SIA, included 126 samples from 66 subjects, followed up serologically for up to 700 days after primary infection. The diagnostic criteria for B19V infection were the presence of B19V-IgM, B19V-IgG seroconversion or a significant rise of B19 IgG and low avidity of B19V IgG in the first seropositive sample (67, 68, 185).

Patients with HCMV infection (II)

In study II, for HCMV IgM and IgG-avidity-SIAs, 149 samples were available from 52 patients with HCMV infection: 108 samples from 39 patients with HCMV primary infection (186, 187) and 41 samples from 13 patients with HCMV secondary infection (exogenous reinfection or endogenous reactivation) (187). The sera had been collected between 1986 and 1997, and their sample number per patient ranged from one to six. The diagnostic criteria for HCMV primary infection were positive or borderline IgM in the first sample, seroconversion or, significant rise of IgG and low avidity of IgG in the first seropositive sample. The diagnostic criteria for HCMV secondary infection were a four-fold or greater increase in IgG in a serum pair, high avidity of IgG in the first serum and positive or borderline IgM (186, 187).

Pregnant women with T. gondii infection (II)

In study II, 116 samples were from 22 pregnant women with *T. gondii* primary infection. Of the patients, 9 individuals (sample n=48) presented specific IgG in the first sample and the other 13 individuals (sample n=68) were seroconverters. The sera were collected between 1989 and 1990. The number of sera per patient ranged from two to seven. The diagnostic criteria for *T. gondii* primary infection were positive or borderline IgM, seroconversion or a significant rise of *T. gondii* IgG and low avidity of IgG in the first sample (188). All the patients presented positive or borderline IgM during follow-up, albeit a single IgG seroconverter.

Medical students (I, II)

For control in B19V study, serum samples from medical students were included. The seroprevalences of B19V and several emerging viruses (143, 189) have been previously determined in these samples. Study I, with B19V IgG-SIA, included single sera from 104 medical

students. Study II, with corresponding IgM-SIA, included single sera from 87 medical students; and with IgG-avidity-SIA, single sera from 57 students who had anti-B19-VP1-IgG.

Children and adults with tonsillitis or tonsillar hypertrophy (III)

In study III, tonsillar tissue from 78 subjects (31 children and 47 adults) was used. The paediatric donors ranged in age from 2 to 15 years (average, 6.6) and the adults from 16 to 69 (average, 30.3). The tonsillectomies and tonsillotomies had in most cases been performed due to chronic tonsillitis or tonsillar hypertrophy (190). The tonsillar tissues had been obtained directly after surgical resection at the operation theatre.

Liver transplant recipients (IV)

In study IV, 126 adult liver transplant recipients (LiTRs) were included. All the LiTRs had been recruited for follow-up skin examination at Helsinki University Hospital between October 2012 and December 2016. The histological examinations were conducted and documented by dermatologists from the Dermatology Unit. Of the LiTRs, 12 had squamous cell carcinoma *in situ* (SCCis) or actinic keratosis (AK), with a median age at diagnosis of 68 years and a median post-transplant (post-tx) time of 11 years. The remaining 114 LiTRs not developing SCCis or AK during follow-up had a median age at diagnosis of 62 years and a median post-tx time of 10 years. Altogether, 14 punch biopsies were collected from lesional sites and 127 from non-lesional sites and were stored at -70 °C. At least one biopsy of healthy skin was taken from each LiTR. Additionally, sera were available from 118 LiTRs.

Fresh-frozen skin biopsies of immunocompetent adults (IV)

For control, 80 immunocompetent adults (median age 43) who participated in epicutaneous testing were included in study IV. Cutavirus DNA has previously been studied in this cohort (191). Skin biopsies taken from the back of the individuals were stored in RNA-later at -80 °C.

1.2 Antigens (I, II)

The antigens used in study I or II are listed in Table 3. B19V recombinant VP2-VLPs were expressed with baculovirus system as described in (67, 69). B19V VP1u recombinant fusion protein including the unique region of B19V minor capsid protein (VP1) was expressed in *E.coli* as described in (68, 69, 187).

Table 3. Antigens used in studies I-II.

SIAs	Antigen (Ag)	Source
B19V IgG	Insect cell recombinant VP2-VLP	*In-house*
HCMV IgG	Viral lysate (strain AD 169)	Commercial
T. gondii IgG	*T. gondii* (RH strain) tachyzoite lysate	Commercial
B19 VP2 IgM	Insect cell recombinant VP2-VLP	*In-house*
HCMV IgM	Viral Lysate (strain AD 169)	Commercial
T. gondii IgM	*T. gondii* (RH strain) lysate enriched in membrane fraction	Commercial
B19 VP1u-IgG-avidity	Prokaryotic recombinant fusion protein containing the B19 VP1 unique region	*In-house*
HCMV IgG-avidity	Viral Lysate (strain AD 169)	Commercial
T. gondii IgG-avidity	*T. gondii* (RH strain) tachyzoite lysate	Commercial

1.3 Plasmids, primers and probes (III, IV)

Plasmids, primers and probes in the HPyV genoprevalence study are presented in Table 4. The first 13 HPyVs were tested in multiplex and the newest HPyV, LIPyV, separately. The primers and probes for the first 10, except MCPyV, were from Gustafsson et al. (192) and for LIPyV was from T. Gheit et al. (141). For MCPyV, STLPyV, HPyV12 and NJPyV, the primers and probes were designed for this study. Each probe sequence represented the reverse complement to the target region of the biotinylated PCR product. All the reverse primers of VP1 region were labelled with biotin at 5'-end and all the probes were 5′ amine-C12-modified.

Plasmids containing a HPyV genome were used as positive controls and to determine assay sensitivities by limiting dilution analysis. A 10-fold dilution series from 10^8 to 10^0 copies/µl of HPyV-DNA was prepared for each of the 14 HPyVs in PCR-grade H_2O and another 10-fold dilution series from 10^6 to 10^0 copies/µL of combined DNAs for all the first 13 HPyVs in PCR-grade H_2O. All the plasmid dilutions were aliquoted and stored at -20 °C.

Table 4. Sequences of primers and probes, amplicon sizes, amplicon positions in target genome and reference strains in study III-IV.

Species	Virus	Forward primers sequence (5'-3') Reverse primers sequence (5´ -3') Probe sequence (5'-3')	Ampli-con length (bp)	Amplicon position in target genome (bp)	Reference strain (GenBank accession no.)
HPyV1	BKPyV	ACAGAGGTTATTGGAATAACTAG ACTCCCTGCATTTCCAAGGG CTTAACCTTCATGCAGGGTC	143	1915-2057	V01108
HPyV2	JCPyV	AATGAGGATCTAACCTGTGGAA CTGCACCATTGTCATGAGTTGCTTG ATGAATGTGCACTCTAATGG	127	1742-1868	J02226
HPyV3	KIPyV	TTGGATGAAAATGGCATTGG TAACCCTTCTTTGTCTAAAATGTAGCC CTTGGAACAGCTAATAGTAGAATC	142	2263-2404	EF127906
HPyV4	WUPyV	TTGGATGAAAATGGCATTGG TAACCCTTCTTTGTCTAAAATGTAGCC GAGTACATACAGGGCTTTCCAG	142	2411-2552	EF444554
HPyV5	MCPyV	TTCCATCTTTATCTAATTTTGCTT AGGCCTAGTTTTAGATTACCAGAC GTAATAGGCCCACCATTTGT	146	3755-3900	JF813003
HPyV6	HPyV6	TTGCTTCTGGATCCAATACTGC GGCCTCAGGAATTTCAGGCAA TGGATGCTGGTTCATCTCTG	131	1426-1556	HM011558
HPyV7	HPyV7	AAGCAGCTACAACTGGGAACTT GGCCTCAGGAATTTCAGGCAA GCCTACCTTATCCTATGAGTG	125	1450-1574	HM011566
HPyV8	TSPyV	AGAATGTATGATGACAAAGGTAT TCTGTAGTTTCCAGTTAGAAAC TGAGGGAATGAATTTCCATATGTT	111	1722-1832	GU989205
HPyV9	HPyV9	ATCTATGGCTCATCCTCAGG GTAGAGCTAGCAACTAGGCCT AGTGCAGGGTACCACTCTC	107	1862-1968	KC831440
HPyV10	MWPyV	GTCCAGTTCCTACTAAAGTTCCT TACATCATTGCCCATCCTTGGTT GCCGGACACCACAATGACA	128	1501-1628	JQ898292
HPyV11	STLPyV	TGAATATGATCCGTGCCAAA ACTGCATCAGGGCCTACTTG CCTCCTCCAACATGTGTTCC	129	1318-1446	JX463184
HPyV12	HPyV12	GTAATGGCACCCAAGAGGAA GGGGATTTAGAAAGGCCTCA CCCAGCAGTGTCCCTAAATT	157	1402-1558	JX308829
HPyV13	NJPyV	TGTGTGCCAAAGAAGTGTCCT TCTGTCACCTGTTGGAGCATT CTGATGCTACTACTGAAATTGAA	159	1113-1271	KF954417
*****	LIPyV	CAAGCCTTGCTGCAGCATTCCTAG ATCTTTGTTTTGTCCTCTAGAACCCT ATTGCCCCCAAGATAGAT	155	3088-3242 (LT region) (141)	KY404016

***** unassigned polyomavirus species

2. Microsphere-based antibody assay (I, II)

2.1 Coupling of antigens to xMAP microspheres (I, II)

The xMAP microsphere (Luminex Corp., USA) coupling was performed according to the manufacturer protocol (29). To minimise nonspecific background, in each coupling, a total of 1.25 × 10^6 microspheres were coated with the corresponding antigen, followed by blocking with Tris buffer (PBS + 50 mM Tris + 0.5 ml/l Tween-20). The coupled microspheres were washed and stored in StabilGuard® Immunoassay Stabilizer (SG, SurModics, USA) at 4°C in the dark. As a control in IgM-SIA, each sample was run with human IgG (Sigma-Aldrich, USA) -coupled microspheres. In the coupling, 6 µg of human IgG was used to coat 10^6 microspheres and the coupled microspheres were stored in 1 ml SG at 4°C in the dark.

2.2 IgG-SIAs (I)

The detection of IgG antibodies against B19V, HCMV and *T. gondii* was based on indirect SIAs format (Fig. 12). In brief, 50 µl of diluted sera in PBST (dilution 1:20) was added into each well of a 96-well flat-bottom plate. Then the diluted sera were incubated with B19V, HCMV, *T. gondii*-antigen coated and naked microspheres for 45 minutes in the dark. After 3 washing cycles with Bio-Plex wash buffer (Bio-Rad, USA), 50 µl of 2 µg/ml biotinylated protein G (Thermo Scientific, USA) was added. The plate was thoroughly mixed and kept for 30 minutes in the dark. After 3 washing cycles, 50 µl of 4 µg/ml SAPE (Life Technologies, USA) in PBST was added and kept for 30 minutes in the dark. After final washes, each well was resuspended with 120 µl of PBST and the median fluorescence intensities (MFIs) were measured with a Bio-Plex®200 instrument.

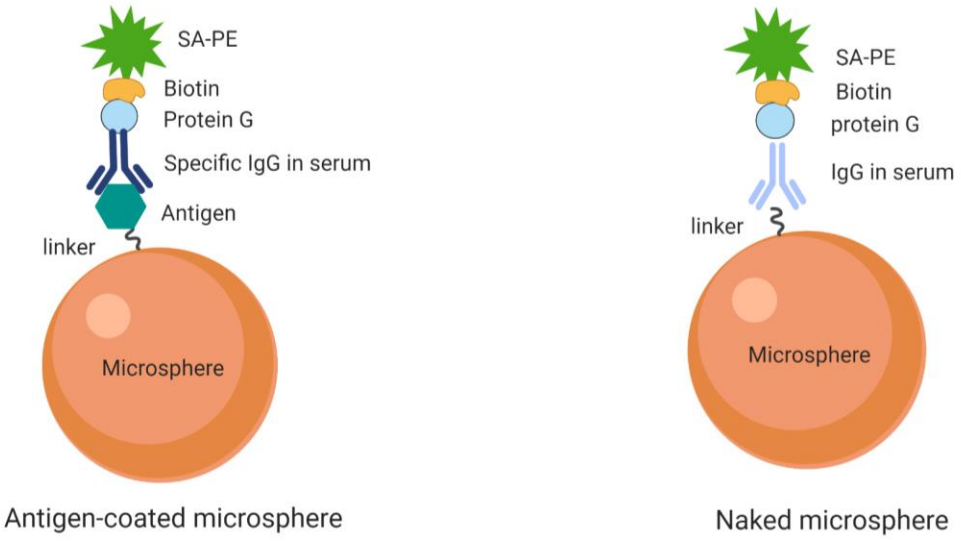

Figure 12. Schematic presentation of indirect IgG-SIA. Microsphere-based assays for the detection of IgG antibodies against B19V, HCMV and *T. gondii* were developed by using antigen recombinant VLPs made up of the B19V-VP2, HCMV viral lysate (strain AD 169) or *T. gondii* (RH strain) tachyzoite lysate. The IgG-SIA is based on the detection of specific IgG captured by an antigen-coated microsphere and then the specific IgG can be measured when it links to the biotinylated protein G and SAPE (Left). Each sample was run together with uncoupled ("naked") microspheres (Right) to estimate nonspecific binding in the SIAs.

2.3 IgM-SIAs (II)

The detection of IgM antibodies was based on indirect SIAs format (Fig.13). IgM-SIAs included IgG removal with GullSORB (Meridian Bioscience, USA) and two internal controls (naked-microsphere and Rheumatoid Factor (RF) control). Uncoupled ("naked") microspheres were used to estimate nonspecific binding in the SIAs and RF control was designed employing human IgG (Sigma-Aldrich, USA) -coupled microspheres to monitor the effectiveness of IgG and RF removal in each sample (Fig.13). In brief, GullSORB was mixed with the sera, making a serum dilution of 1:20 (193). The mixture was kept at room temperature for 1h and centrifuged at 14,000 x g for one minute to remove precipitates. The supernatant was further diluted four-fold with PBST to yield a serum dilution of 1:80. Then 50 µl of diluted sera was dispersed into a 96-well flat-bottom plate and the B19V, HCMV, *T. gondii*-antigen and human IgG-coated as well as naked microspheres were added for 45 min. After washes, 50 µl of biotinylated anti-human IgM (Sigma, USA) at 3 µg/ml was added for 30 min. After washes, 50µl of 6 µg/ml SAPE (Life Technologies, USA) in PBST was applied for 20 min. After final washes, the wells were resuspended in 120 µl of PBST and the MFI values were measured.

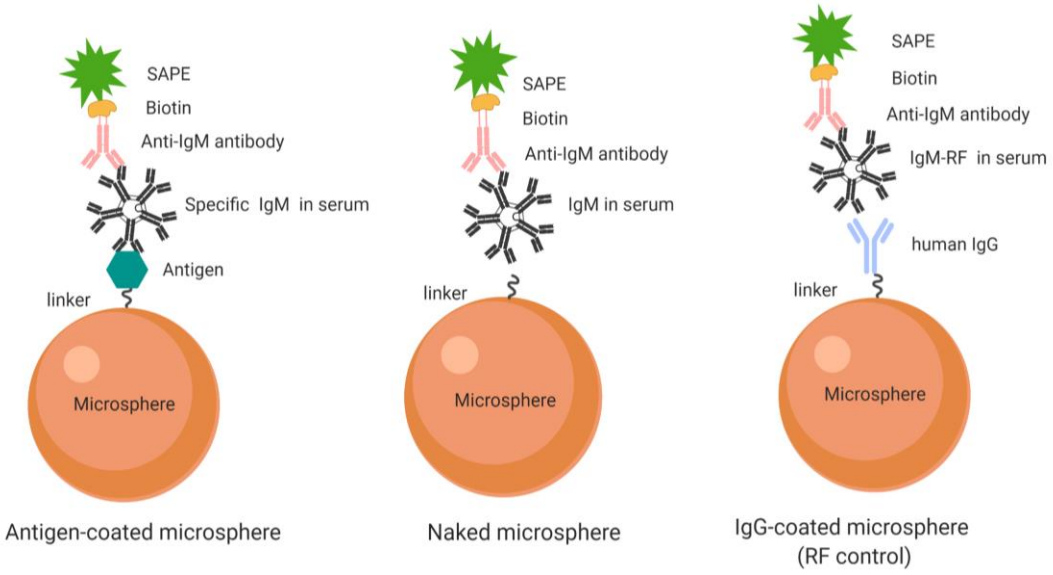

Figure 13 Schematic presentation of indirect IgM-SIA. Microsphere-based assays for the detection of IgM antibodies against B19V, HCMV and *T. gondii* were developed by applying HCMV viral lysate (strain AD 169), *T. gondii* (RH strain) tachyzoite lysate enriched in membrane fraction including the apical complex, or recombinant VLPs made up of the B19V-VP2. The IgM-SIA is based on detection of specific antimicrobial IgM antibodies when they are captured by corresponding antigen-coated microspheres. Then the captured antimicrobial IgM is targeted by adding biotinylated goat anti-human IgM (μ-chain specific) antibody. Finally, specific antimicrobial IgM can be measured when biotinylated anti-human IgM conjugates with SAPE (Left). Each sample was run together with uncoupled ("naked") microspheres (Middle) to estimate nonspecific binding in the SIAs. In addition, each sample was run with human IgG (Sigma-Aldrich, USA) -coupled microspheres (right). This control was used to monitor the effectiveness of IgG and RF removal.

2.4 IgG-avidity-SIAs (II)

The IgG-avidity-SIAs are based on the principle of elution of antigen-bound antibodies by the protein-denaturing agent, urea (Fig.14). An IgG-avidity-SIA in singleplex format was performed with either B19V, HCMV or *T. gondii*-antigen coated microspheres and in multiplex format with the combination of two or three of them. Briefly, from each serum two dilution series were made in PBST, series 1 (1:20, 1:80, 1:320, 1:1280) and series 2 (1:80, 1:320, 1:1280, 1:5120). These dilutions were placed in a 96-well plate and incubated with the antigen-coated microspheres for 45 min. Then, series 1 was washed three times for five minutes with freshly prepared 6M urea (Promega, USA) in PBS, and series 2 was washed with PBS only. After 3 washes, protein G (Thermo Scientific, USA) and SAPE were added as in IgG-SIAs, and the MFI values measured. Avidity value was the ratio of endpoint titer (EPR) of series 1 (urea treated) over series 2 (no-urea treated), calculated by a curve-fitting software (Avidity 1.2) (187).

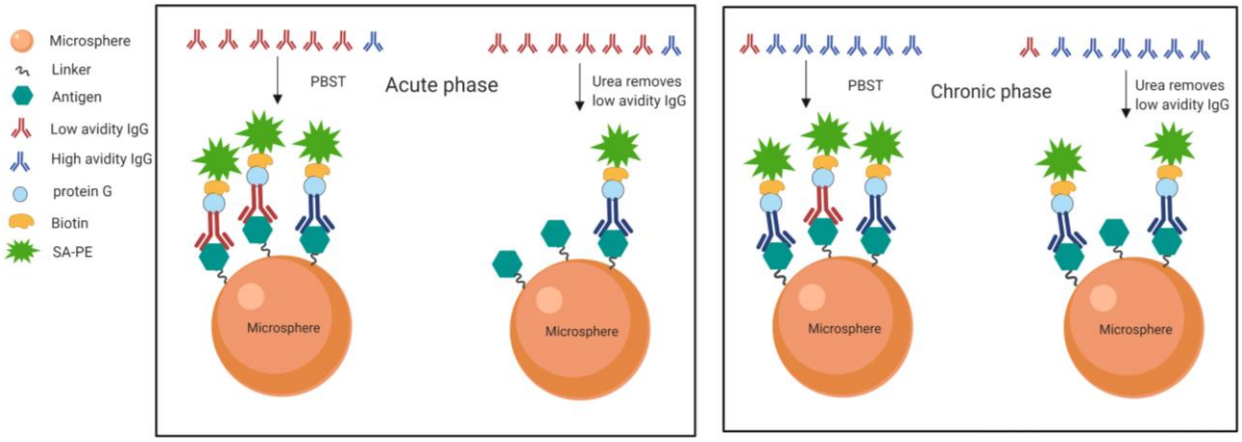

Figure 14. Principle of IgG-avidity-SIA. Chaotrope-based IgG-avidity-SIAs are developed by exploiting HCMV viral lysate (strain AD 169), *T. gondii* (RH strain) tachyzoite lysate or recombinant fusion protein containing the B19 VP1 unique region. The measurement of IgG avidity in SIA was based on the endpoint titration of serially diluted sera and elution of low avidity antibodies by a protein-denaturing agent, urea. Specifically, the antigen-bound antibodies are treated in parallel with or without urea. As a result, the low-avidity antibodies are eluted away while the high-avidity antibodies are retained and measured.

2.5 Reference serological tests (I, II)

Reference serological tests (Table S1) were used to evaluate performances of the IgG (I), IgM (II), IgG-avidity (II) SIAs.

2.6 Statistical analysis (I)

The square of the Pearson's correlation coefficient, R^2, was calculated by Graph-Pad Prism version 6 for Mac (GraphPad Software, USA) to determine the correlation of results between singleplex and multiplex IgG-SIAs. The positive, negative and overall percent agreements were calculated between SIAs and reference assays. In statistical calculations, borderline values in IgG and IgM SIAs were counted as positive given the primary role of IgG and IgM assays in screening. In IgG avidity SIAs, in turn, borderline avidity values were considered high-avidity due to the role of the assays in ruling out recent primary infections. In study I, two-way contingency table analysis in 'Vassar-Stats' was used for the calculation. In study II, contingency table analysis in GraphPad Prism version 7.00 for Windows (GraphPad Software, USA) was used. The agreements between SIAs and EIAs were evaluated by kappa coefficient and defined as (194).

3. Microsphere-based multiplex nucleic acid assay (III, IV)

3.1 DNA extraction (III, IV)

In study III, all tonsillar tissues were sliced with disposable scalpels and cell suspensions were prepared by mechanical homogenisation with a syringe plunge, followed by PBS wash and filtration through a 70 µm mesh (Corning Life Sciences). The cells were resuspended into a final volume of 100 µl PBS. Whole DNA was extracted by the KingFisher Duo DNA Extraction Kit (Thermo Fisher Scientific) according to the manufacturer instructions. The extracted DNA was stored at −20 °C.

In study IV, all the skin specimens were sliced with disposable scalpels and digested with proteinase K overnight. DNA was isolated with Qiagen DNA mini kit (Qiagen, Hilden, Germany) according to the manufacturer instructions. The isolated DNA was eluted in 60 µl of AE buffer (Qiagen) and stored at -20°C. The DNA was also isolated from serum of 37 LiTRs with HPyV-DNA in biopsies. The DNA from each serum (200 µl) was extracted with Qiagen DNA blood mini kit (Qiagen). The yield was eluted in 100 µl of AE buffer (Qiagen) and stored at -20 °C.

3.2 Coupling of oligonucleotides to xMAP microspheres (III, IV)

Oligonucleotide probes (Sigma-Aldrich, UK) for target viruses were assigned to individual xMAP microsphere (Luminex Corp., USA) sets. The coupling of oligonucleotides to microspheres was done according to the manufacturer instructions. The probe amounts ranged from 138 to 300 pmol per coupling (10^6 microspheres). The probe-coupled microspheres were stored in 500 µl TE buffer at +4 °C in the dark.

3.3 Microsphere-based multiplex HPyV-DNA test (III, IV)

Multiplex nucleic acid amplification: In brief, 5 µl DNA templates were mixed in a 20 µl multiplex reaction consisting of 12.5 µl of 2× multiplex PCR mastermix (Qiagen, USA), 0.2 µM of each forward primer (Sigma-Aldrich, UK) and 1 µM of each biotinylated reverse primer (Sigma-Aldrich, UK). The amplification conditions were 95 °C for 15 min, 40 cycles at 94°C for 20 s, 50°C for 90 s, 71°C for 80 s, and a final extension at 71°C for 10 min. In study IV, multiplex nucleic acid amplification for the 13 HPyVs was performed as described in study III except that annealing temperature was 57.5°C. Each run included as positive controls the plasmids of all 13 HPyVs. In

addition, a separate singleplex PCR for the LIPyV was done as described (141), and each PCR run included plasmid with LIPyV complete genome as a positive control.

Hybridisation (Fig. 15): Followed by PCR amplification, type-specific oligonucleotide probes-coated microspheres and PCR products were hybridised as described in (192) except that the SAPE (Invitrogen) incubation temperature was 48 °C. In brief, a total of 5µl of PCR products were mixed with 45 µl of tetramethyl ammonium chloride (TMAC) hybridization buffer (195) containing probes-coated microspheres (study I: probes of HPyV1-13; study II: probes of HPyV1-13 or LIPyV). The mixture was added into a 96-well V-bottomed plate and heated to 95°C for 10 min. After a cool down on the ice for a minute, the plate was incubated for 30 min at 48°C in the dark with shaking. After three washes, 4 µg/ml SAPE in staining buffer (195) was added for 20 min at 48°C in the dark with shaking. After three washes, the microspheres were analysed in Bio-Plex 200 (Bio-Rad).

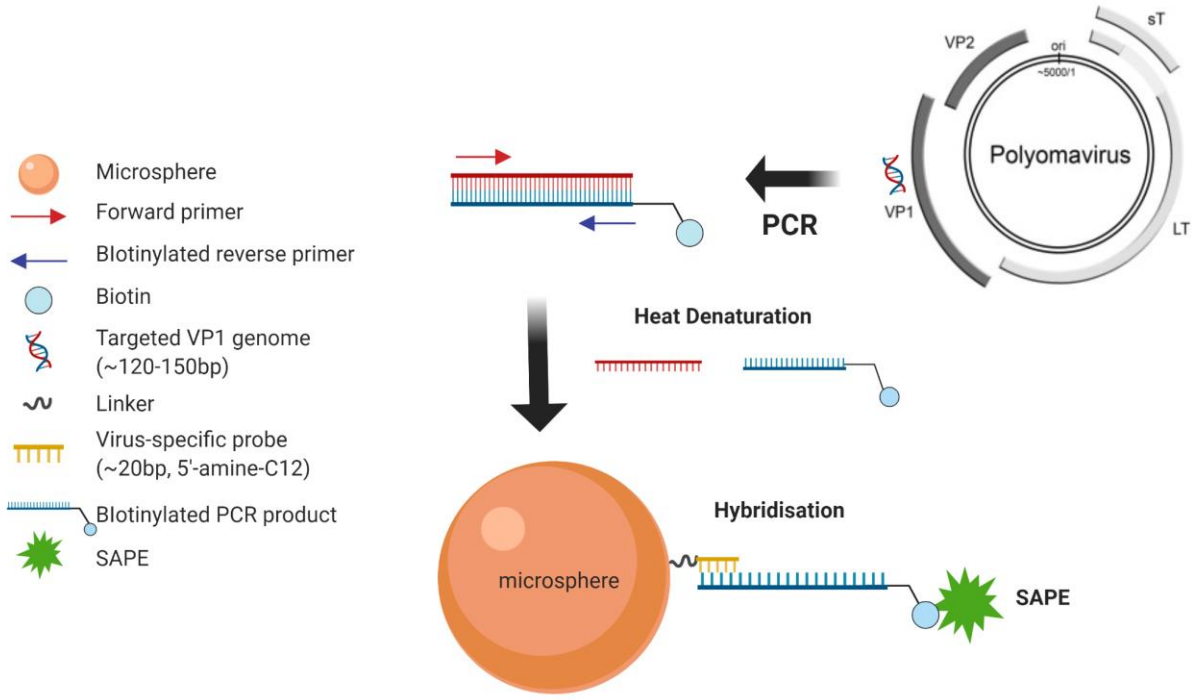

Figure 15. Microsphere-based multiplex HPyV-DNA test. The multiplex HPyV-DNA test involves the amplification of target genes and the following hybridisation links the amplified target strand to a specific probe on the microsphere. In our study, the test was designed using primer pairs and probes targeting the respective HPyV viral protein 1 (VP1) genes. The PCR amplification with one of the primers was labelled with biotin at 5' end. After heat denaturation, dsDNAs were separated and the biotin-labelled target strands bind to specific probes linked on microspheres. Finally, SAPE was added to detect and semi-quantify the target genes.

3.4 Microsphere-based singleplex HPyV-DNA test (III, IV)

Microsphere-based singleplex HPyV-DNA test was performed as described in multiplex format except using one pair of primers for DNA amplification and a single probe for DNA detection.

3.5 Cut-off determination (III, IV)

The cut-offs of microsphere-based HPyV-DNA assays were defined as two times background means plus 15 MFI.

3.6 Singleplex PCR (III)

In study III, to confirm each positive HPyV-DNA finding in tonsillar tissue (JCPyV, WUPyV, MCPyV, HPyV and TSPyV), all the samples with positive findings were retested with singleplex PCR and agarose gel electrophoresis. To enrich the band signal, a second run of PCR was used employing the product of the first PCR as template. In brief, 5µl of DNA template was mixed in a 20 µL multiplex reaction consisting of 12.5 µL of 2 x multiplex PCR mastermix (Qiagen), 0.2 µM of the corresponding forward primer and 0.2 µM of the corresponding biotinylated reverse primer. The amplification conditions were the same as described in the microsphere-based multiplex PCR. The second PCR run was performed as the first run except for using 3µl of template. Each run included PCR-grade water as negative control, as well as single plasmid of corresponding HPyV as positive control.

3.7 Quantitative singleplex PCR (IV)

To quantify and confirm the microsphere-based DNA findings in study IV, samples with positive results were re-examined with the corresponding qPCRs as described (133, 196, 197). The viral DNA loads were given per million cells, determined with the human house-keeping gene RNaseP (198).

3.8 DNA sequencing and sequence analyses (IV)

The PCR product of the LIPyV-positive sample was purified with Diffinity RapidTip (Sigma-Aldrich, St. Louis, MO, USA) and Sanger sequenced. The resulting sequences were compared with the reference DNA sequences of the NCBI Entrez Nucleotide database (accession number KY404016 (141), using the NCBI Blast program.

3.9 Statistical analysis (IV)

We performed Fisher's exact test, Mann–Whitney U test, chi-squared test, unpaired nonparametric Kruskal–Wallis test and Dunn's multiple comparison test to compare the prevalences or loads of MCPyV or HPyV6 DNA in skin biopsies from the lesion and/or non-lesion sites in LiTRs and immunocompetent individuals. All the statistical tests were performed using GraphPad Prism version 7.00 (GraphPad Software, La Jolla, CA, USA). A P-value <0.05 was considered significant.

4. Ethical statements

The Helsinki University Hospital Ethics Committee approved the use of all clinical samples included in this study. All the clinical samples were collected and handled following the ethical rules of the Ethics Committee of Helsinki and Uusimaa Hospital District. The medical students had provided informed consent for the collection, storage and use of their samples.

RESULTS AND DISCUSSION

1. Microsphere-based serological assays (I, II)

EIA- or immunofluorescence- based assays have been used mainly in singleplex format. Singleplex testing has its limitations, such as low throughput, cost and labour. The microsphere-based methodology offers a simplified working platform by multiplexing assays, as well as a wide dynamic range of 3 to 4 logs (26). Regarding expenditure, the cost per sample in IgG-SIA was calculated as an example in study I, and estimated to be per sample 0.20€ for singleplex and 0.35€ for a triplex, making these tools beneficial also financially.

B19, HCMV and *T. gondii* infections can cause severe complications to foetuses or congenital abnormalities. It is important to determine whether or when a pregnant woman has acquired the infection. Combinations of serological tests (IgG, IgM and IgG-avidity) are practicable in the detection of infections during pregnancy (69, 199-201). Specific IgM can persist long after the initial antigenic challenge (112, 202) and also re-appear in HCMV or *T. gondii* reactivations. In such cases, measurement of the antigen-binding avidity of the antimicrobial IgG is necessary in the second line for the distinction of primary infection from long-term B-cell immunity. Current serodiagnosis approaches, e.g. ELISA, are mostly confined to detection of one pathogen at a time. To improve the efficiency in the detection of infections, in study I and II, we described the development of microsphere-based assays for detection of IgG antibodies, IgM antibodies and IgG-avidity against the three important pathogens in multiplex and monoplex format.

1.1 Development of SIAs (I, II)

Optimisation of SIAs

The development of each SIA involved the optimisation of antigen concentrations, serum dilutions, secondary antibody concentration, SAPE concentration, GullSORB treatment and post-coat blocking. All the SIAs were first optimised individually and then were combined into a multiplex format. The optimal assay conditions for each SIA are listed in Table 5.

Table 5. Optimal assay conditions

Assays	Pathogens	Ag amount (µg per 10^6 beads)	Serum dilution	Secondary antibody (µg/ml)	SAPE (µg/ml)
IgG-SIAs	B19V	50	1:20	2	4
	HCMV	20	1:20	2	4
	T. gondii	50	1:20	2	4
IgM-SIAs	B19V	6	1:80	3	6
	HCMV	25	1:80	3	6
	T. gondii	6	1:80	3	6
IgG-avidity-SIAs	B19V	50	1:20-1:5120	2	4
	HCMV	20	1:20-1:5120	2	4
	T. gondii	12.5	1:20-1:5120	2	4

SIA microsphere-based suspension immunoassay; Ag antigen; SAPE streptavidin-phycoerythrin

Our results showed that IgG absorption by GullSORB in each sample corrects the results for rheumatoid factor (RF) interference (unpublished data). Also, the GullSORB pre-treatment was shown to promote not only the specificity, but also the sensitivity of the IgM assays (study II, Fig. S3). It is well known that the interference through endogenous antibodies, e.g. RF can cause unspecific false-positive IgM results by bridging the serum IgG and the secondary antibody. Besides, the antimicrobial IgG can compete for the binding site with homologous IgM which shares the same antigen determinants. The GullSORB treatment has been utilised widely to eliminate the false-positive IgM result caused by RF (203, 204).

The post-coat blocking of the microsphere was tested with bovine serum albumin (BSA) and Tris buffer. We noticed that post-coat blocking with bovine serum albumin (BSA) yielded inappropriately high background in some individuals. Instead, the replacement of BSA with Tris significantly improved the signal-to-noise ratios. Tris contains a primary amine, and it can specifically bind the spare reactive intermediate (sulfo-NHS-ester intermediate) on the antigen-coated microsphere and hinder nonspecific binding in the following assays. The Tris buffer post-coat blocking has also been successfully applied in (205).

Cut-off determination (I, II)

The SIA cut-offs were calculated by the means and standard deviations (SDs) of MFI values or avidity values. The cut-off criteria and values are presented in Table 6. For B19V IgG-SIA (I) and IgM-SIA (II), the cut-offs were determined with sera tested B19V seronegative by both Biotrin's (Diasorin, Ireland) and *in-house* B19V IgG and IgM EIAs. For HCMV- and *T. gondii*-IgG and -IgM-SIAs, the cut-offs were defined with separate sets of 60 sera shown to lack the respective antibodies by the corresponding Architect IgG and IgM tests (Abbott, USA). The cut-offs of low

and high avidity (II) were determined with the B19V or HCMV primary infection samples taken within 28-50 days after onset of symptoms, and with *T. gondii* using the first IgG-containing samples in < 3 month-seroconversion.

Table 6. **Cut-offs in SIAs**

Assays	Pathogens	Unit	Cutoff criterion	Cutoff value	Seronegative / Primary infection n=
IgG-SIAs	B19V	MFI	4 SD 5 SD	Negative < 453 Positive > 532	72
	HCMV	MFI	4 SD 5 SD	Negative < 650 Positive > 800	60
	T. gondii	MFI	4 SD 4 SD	Negative < 234 Positive > 234	60
IgM-SIAs	B19V	MFI	4 SD 5 SD	Positive, ≤714 Negative, >831	86
	HCMV	MFI	2 SD 3 SD	Positive, ≤518 Negative, >631	60
	T. gondii	MFI	4 SD 5 SD	Positive, ≤938 Negative, >1056	60
IgG-avidity-SIAs	B19V	Index	2.5 SD 3.5 SD	Acute, ≤35 Past, >44	59 (≤28 days of onset)
	HCMV	Index	1.5 SD 3 SD	Acute, ≤15 Past, >24	52 (≤50 days of onset)
	T. gondii	Index	1.5 SD 2.5 SD	Acute, ≤21 Past, >27	40 (<3 months after IgG-seroconversion)

Reproducibility (I, II)

In IgG-SIAs (I), the intra-assay variability was calculated with 8 replicates in the same run, and the inter-assay variability with 6 distinct runs, using serum pools containing or lacking the respective IgG. The intra-assay and inter-assay variability of HCMV-, *T. gondii*- and B19V-IgG-SIAs were 3-7%, 7-12%, 3-8%; and 4-9%, 8-15%, 1-12%, respectively. In IgM-SIAs (II), the intra-assay variability was calculated with 8 replicates in the same run, and the inter-assay variability with 6 distinct runs, employing serum pools containing or lacking the respective IgM. The respective intra-assay CVs of HCMV-, *T. gondii*-, B19V-IgM-SIAs were 2-9%, 9-11% and 6-9%; and the inter-assay CVs, 9-12%, 11-16% and 11-14%. In IgG-avidity-SIAs (II), inter-assay variability was calculated with 6-8 distinct runs over three months, using acute-phase and past-infection serum pools. The respective inter-assay CVs of HCMV-, *T. gondii*-, B19V-VP1-IgG-avidity-SIAs – assessed using acute-phase and past infection serum pools – were 9-18%, 14-19% and 14-17%. All SIAs showed good within- and between-run precisions, demonstrating the reliabilities of the assays.

1.2 Diagnostic performance of SIAs (I, II)

To validate the established assays, serum samples from well-characterized clinical cohorts were applied. All the samples were analysed by *in-house* or commercial reference serological tests (Table S1). The positive, negative and overall percent agreements of SIAs in comparison to reference assays are presented in Table 7.

Table 7. Positive percent, negative percent and overall agreements of SIAs in study I-II

Assays	Pathogens	Sample n=	Positive percent agreement (95% CI)	Negative percent agreement (95% CI)	Kappa coefficient (95% CI)
IgG-SIAs	B19V	247	98 (97-100)	98 (95-99)	0.99 (0.95-1.0)
	HCMV	79	100 (92-100)	100 (80-100)	1.0 (1.0-1.0)
	T. gondii	77	100 (90-100)	100 (85-100)	1.0 (1.0-1.0)
IgM-SIAs	B19V	127	95 (83-99)	100 (96-100)	0.96 (0.91-1.0)
	HCMV	97	98 (88-100)	98 (90-100)	0.96 (0.90-1)
	T. gondii	94	100 (92-100)	100 (92-100)	1.0 (0.95-1.0)
IgG-avidity-SIAs	B19V	94	92 (79-98)	100 (94-100)	0.93 (0.86-1.0)
	HCMV	97	100 (91-100)	95 (86-99)	0.91 (0.83-1)
	T. gondii	94	100 (92-100)	100 (92-100)	1.0 (0.95-1.0)

IgG-SIAs (I)

In total, the agreement between B19V IgG-SIA and VP2-IgG-EIA tests was 99.2% (245/247). Full agreement between B19V SIA and EIA resulted in the cohort of the healthy medical student. Two discrepancies were found between B19V SIA and EIA: one (SIA-, EIA+) was collected on day 4 and another (SIA+, EIA-) collected on day 1 after onset. In B19V-IgG-SIA, all the samples collected >10 days after onset were positive; and the four borderlines were collected within 6 days of onset (Fig 1. in study I). HCMV and *T. gondii* IgG-SIAs were 100% concordant with those obtained with Vidas ELFAs. Moreover, the multiplex IgG-SIAs were compared with singleplex SIAs and reference assays with 80 sera of known IgG reactivities against three pathogens (Fig 4. in study I). Pearson's correlation coefficients between multiplex and singleplex SIAs were 0.961-0.977. With multiplex IgG-SIAs, B19V, HCMV, *T. gondii* IgG seropositivity corresponded perfectly with those obtained with reference assays (singleplex), except for a single discrepancy (SIA+, EIA-).

All IgG-SIAs were highly sensitive and specific in comparison to reference assays. Great correlation between the multiplex and singleplex assays indicated no interference among the three IgG SIAs. The few discrepancies in B19V are likely due to low antibody affinity as the samples were collected from very early infection. Moreover, the explanations for the discrepancies may also be due to the intrinsic differences between assays: fluorescence vs. colourimetric substrate detection, antigen coupling covalently onto magnetic microspheres vs. via adsorption and antibody detection with protein G vs. anti-human IgG.

IgM-SIAs (II)

The overall agreement between B19V SIA and Biotrin's B19V IgM EIA tests were 98.4% (125/127). Both SIA and *in-house* IgM-VP2-EIA showed the absence of B19V-IgM in all 87 samples from medical students. HCMV IgM-SIA agreed with the corresponding Architect IgM test in 97.9% (94/96) of samples. *T. gondii* IgM-SIA resulted in 100% (94/94) concordance with the corresponding VIDAS results.

All in all, excellent agreements were observed between SIAs and reference assays in the detection of IgM. Of note, the antigens used in *T. gondii* IgM detection are usually tachyzoite lysates or recombinant proteins (16, 188, 206). Here we employed a tachyzoite lysate enriched in membrane fractions including the apical complex. Kumolosasi et el. (207) have shown that the apical complex is associated with active motility during parasite invasion and is a strong immunogen for IgM antibodies. Notably, the presently generated IgM-SIA based on this antigen showed full agreement with the Vidas Toxo IgM test employing the tachyzoite lysate.

IgG-avidity-SIAs (II)

With B19V, excluding three sera with insufficient VP1u-IgG in SIA, a total of 96.8% (91/94 samples) agreement was seen between IgG-avidity-SIA and VP2-ETS-EIA. All the seropositive samples from students showed high avidity in B19-IgG-SIA and B19V-VP1u-IgG-avidity-EIA. HCMV IgG-avidity-SIA agreed with the Architect IgG avidity test in 95.9% (93/97 samples). Of the four discordances between HCMV SIA vs. Architect, three were SIA low vs. Architect high and one was SIA borderline vs. Architect low. The four samples were retested with Vidas IgG avidity assay and exhibited low avidity (n=2) and borderline avidity (n=2). With *T. gondii* IgG-avidity SIA, a full agreement was observed between IgG-avidity-SIA and Vidas IgG avidity ELFA, giving a 100% of positive as well as negative percent agreements.

Altogether, IgG-avidity-SIAs results were highly concordant with the results obtained from reference assays. Notably, the B19V VP1u-IgG-avidity-SIA showed good agreement with the *in-*

house EIA measuring the “conformation-dependence” of VP2-IgG (67, 69, 185), and altogether, pinpointed the time of B19V infection accurately. With regard to HCMV, notwithstanding the test type divergence, in clinical performance avidity-SIA (based on chaotrope-elution) agreed very well with the corresponding Architect (based on antigen-competition).

In IgG-avidity SIAs, we used endpoint titration of serially diluted sera which has been considered as gold standard so far for IgG avidity. Accordingly, the avidity result is calculated by the ratio of end-point titers obtained from the generated titration curves. A simpler, but popular approach, the “avidity indices” (AI) are derived from single dilutions of serum. With our data, the AI approach may not be sufficient to calculate IgG-avidity SIAs (unpublished data). Moreover, our recent studies have verified and extended the long-term notion (10) that the AI approach is influenced by the IgG concentration (208).

1.3 IgM and IgG-avidity SIAs for the timing of infection (II)

To study the IgM and IgG-avidity-SIAs in the timing of infection, we examined 391 follow-up serum samples from 140 patients with infection by HCMV (186, 187), *T. gondii* (188, 209) or B19V (67, 68, 185). The IgM and avidity results are summarised in Table 8. Of the samples collected within three months of infections by HCMV, *T. gondii* or B19V, multiplex IgM-SIAs detected the corresponding IgM (including borderline IgM results) in 87.4% (83/95), 87.5% (33/40) and 100% (82/82) samples; and low avidities of IgG were also shown in 86.9% (53/61), 88.6% (31/35) and 93.2% (68/73) among these samples. With HCMV and B19V IgG-avidity-SIAs, high avidities were shown in 95.4% (42/44) and 90.7% (49/54) of samples collected beyond three months of primary infection (including HCMV secondary infection), respectively. All the samples collected beyond 200 days were high avidity in HCMV and B19V IgG-avidity-SIAs. With *T. gondii* IgG-avidity SIA, 82% (9/50) exhibited high (70%, 35/50) or borderline avidity (12%, 6/50) among the samples collected beyond 200 days, albeit five patients exhibited persistent low avidity IgG.

The IgM as well as the IgG-avidity-SIAs showed high clinical sensitivities among the samples collected within three months of primary infection by HCMV, *T. gondii* or B19V. Only beyond two months onset of B19V and HCMV infections did the first examples of high avidity appear. As both persisting and re-appearing IgMs were observed among these samples, the need for infection time verification became substantiated. With the IgG-avidity-SIAs, more than 90% of samples collected beyond three months of primary infection by B19V or HCMV (including secondary responses of the latter) were correctly identified (high avidity) as past infection. Likewise, *T. gondii* IgG-avidity-SIA could effectively distinguish acute from latent/chronic *T. gondii* infections,

however, low-avidity IgG was seen in five patients beyond 200 days of primary infection. Persistence of low-avidity IgG in *T. gondii* infection has been seen in many studies, especially among pregnant women and in medicated patients (210-213). Therefore, as pointed out (214), measurement of *T. gondii* IgG avidity serves better in ruling out than ruling in the recent acquisition of infection.

Table 8. SIA-based IgM and IgG-avidity determination for dating infection

	IgM-SIA, n (%)			IgG-avidity-SIA, n (%)		
	Positive	**Borderline**	**Negative**	**Low**	**Borderline**	**High**
CMV						
< 3 mo	83 (87.4%)	0	12 (12.6%)	53 (86.9%)	3 (4.9%)	5 (8.2%)
> 3 mo*	13 (24.1%)	4 (7.4%)	37 (68.5%)	4 (7.4%)	1 (1.9%)	49 (90.7%)
T. gondii						
< 3 mo	33 (82.5%)	2 (5%)	5 (12.5%)	31 (88.6%)	4 (11.4%)	0
> 200 days	27 (54%)	2 (4%)	21 (42%)	9 (18%)	6 (12%)	35 (70%)
B19V						
< 3 mo	82 (100%)	0	0	68 (93.2%)	4 (5.5%)	1 (1.4%)
> 3 mo	11 (25%)	1 (2.3%)	32 (72.7%)	0	2 (4.5%)	42 (95.5%)

* Samples collected from beyond three months of HCMV primary and from HCMV secondary seroresponses.

1.4 Polyclonal immunoreactivity (II)

Heterologous IgM reactivity among the three microbes was found in 3.5% (25/709) of samples in study II. To identify the original immunoreactivity, multiplex IgG-avidity SIAs were applied. Among the 25 IgM-immunoreactive samples, 13 lacked the corresponding IgG, and the other samples showed high avidity to exclude recent primary infection. Interestingly, of the samples presented with homologous (with respect to the IgM-reactivity) IgG, two samples from a patient with a profile of HCMV secondary infection also displayed IgG and IgM SIA reactivities against B19-VP2. However, both of the samples lacked B19 VP1u-IgG (required for IgG-avidity determination). Retested by EIA, they turned out to have B19V primary infection (VP2 IgM-EIA positive and VP2-IgG ETS index <10). The results suggested that this patient may have had a B19V (primary infection) inducing a serological pattern of HCMV secondary infection.

IgM antibodies appear in circulation not only in acute (primary) and secondary infection, but also due to polyclonal B-cell stimulation (215). Transient heterologous IgM reactivity induced by HCMV or B19V primary infections have been long known (216). Here, the measurement of

qualitative characteristic of the antimicrobial IgG (19) by multiplex IgG-avidity-SIA were shown suitable for identification of the infection origin.

1.5 Conclusion (I, II)

In our study, the strategy of IgG-IgM multiplex screening followed by IgG-avidity reflex testing can provide a high-throughput and accurate means for detection and stage determination of B19V, HCMV*, T. gondii* infections. Altogether, the IgG, IgM and IgG-avidity-SIAs were in diagnostic performance closely comparable to high-quality reference assays, providing a reliable and cost-effective means for diagnosis of B19V, HCMV, *T. gondii* infections. All IgG and IgM-SIAs were highly sensitive, and antibodies were detectable even on one day after the onset of symptoms. The IgG-avidity-SIAs were highly efficient in the differentiation of recent primary and secondary infections.

2. HPyVs and multiplex DNA detection (III, IV)

Classical PCR-based single-reaction techniques have been widely used in clinical laboratories for detection and genotyping of pathogens. The ability to detect multiple targets in a single reaction is a great leap forward in nucleic acid detection. Probe-based quantitative real-time PCR provides a quantitative analysis for targets; it is widely used, but is of limited multiplexing capacity. Next Generation Sequencing-based applications can reveal the entire nucleic acid content of pathogens in a sample, whereas they are currently not routinely employed in clinical microbial diagnosis because of challenges on turnaround time, cost per sample and enormous bioinformatic data analysis. A major advantage of microsphere-based DNA detection is having a high level of multiplexing.

Many emerging human viruses were discovered rapidly by advanced molecular techniques. During the past 12 years, virus hunting has led to the discovery of 12 new HPyVs. So far, six HPyVs have been linked with diseases, especially MCPyV associated with skin cancer, emphasises the oncogenic potential of HPyVs. Seroepidemiologcal evidence indicated that most cases of HPyV primary infection occur asymptomatically in childhood (32, 143, 144). All the novel and highly divergent HPyVs call for in-depth studies regarding their tissue tropism, route of transmission, epidemiology, latency, reactivation and clinical impact.

2.1 Development of microsphere-based HPyV-DNA detection (III, IV)

To study the disease associations for HPyVs, previous studies have developed and validated several PCR protocols for nucleic acid detection (183, 217, 218). However, the existing PCR assays are of limited value in the multi-HPyV assessment. A microsphere-based DNA detection assay has been set up for the detection of 10 HPyVs (192). To optimize and extend this assay, we developed a method for the detection of all 13 HPyVs known before 2017.

In the early assay development, we noticed asymmetric PCR as opposed to standard PCR significantly increased the sensitivity of assays (unpublished data). The explanation is that the biotinylated strand preferentially binds to its complement strand rather than the probe sequence on the microsphere. In this regard, asymmetric PCR for build-up of the excess biotinylated strands can overcome the competition during hybridisation (219).

Detection limit (III, IV)

Detection limits of microsphere-based HPyV-DNA assays were determined with 10-fold serial dilutions of DNA standards. Each HPyV plasmid was diluted serially from 10^8 to 10^0 and a mixture of all HPyV plasmids diluted serially from 10^6 to 10^0 in TE buffer. Detection limits were measured at the PCR annealing temperature 50°C (III) or 57.5°C (IV) in singleplex and multiplex formats. The limit of detection was defined as the dilution containing the fewest copies of a viral genome that still gave a positive result in duplicates. Detection limits of all the assays are listed in Table 9. Increased sensitivity was seen when raising the annealing temperature from 50°C to 57.5°C. The explanation for this improvement could be that at higher temperature the mixed primers are less prone to form primer-dimers.

Table 9. Limits of detection of microsphere-based HPyV PCR at annealing temperature 50°C (study III) and 57.5°C (study IV).

	Limits of detection (DNA amount per µl)					
	Annealing 50°C			Annealing 57.5°C		
HPyV	**Singleplex**	**Multiplex (single plasmid)**	**Multiplex (mixed 13 plasmids)**	**Singleplex**	**Multiplex (single plasmid)**	**Multiplex (mixed 13 plasmids)**
BKPyV	10	10	10	1	1	1
JCPyV	10	10	10	1	1	1
KIPyV	10	10	10	1	1	1
WUPyV	10	10	10	1	1	1
MCPyV	10	10	100	1	1	1
HPyV6	10	10	10	1	1	10
HPyV7	100	100	100	1	1	1
TSPyV	10	10	10	1	1	1
HPyV9	10	10	100	1	1	10
MWPyV	1	1	10	1	1	1
STLPyV	10	100	100	1	1	10
HPyV12	1	10	10	1	1	100
NJPyV	10	10	1	1	1	10
LIPyV	-	-	-	1	-	-

Specificity (III, IV)

The specificity of multiplex PCR at the two annealing temperatures was evaluated with DNA purified from virus-free SF9 and HEK 293 cells. Neither of the two annealing temperatures showed observable amplification with these specimens. Cross-reactivity in microsphere-based HPyV-DNA tests was studied with plasmids of each HPyV alone and with 13 plasmids combined as a template to hybridise with a mixture of 13 type-specific probe-microspheres. The multiplex PCR at both annealing temperatures identified all 13 target sequences correctly, with no observable cross-amplification.

To conclude, singleplex and multiplex PCR assays were developed for the DNA detection of 13 HPyVs. The multiplex format provides a flexible and low-cost platform for the known and yet undiscovered HPyVs. The newly developed multiplex assays are highly sensitive and specific, suitable for epidemiological and diagnostic studies to address whether any of the emerging HPyVs are associated with disease.

2.2 HPyV-DNA in tonsillar samples (III)

HPyVs can establish persistent infections. The mechanism behind the persistence involves the equilibrium between viral replication and the efficiency of the host immune response (220). It is not known so far which precise cell types serve as reservoirs for the persistence of HPyV-DNAs and which specific sites play roles in HPyV reactivation, especially under weakened immune conditions. The sites for persistence may differ among HPyV species, and can serve as the source of the reactivated virus and potentially also the disease sites (221). HPyV-DNAs have been found widely in the human body, including in lymphoid organs, albeit in low copy numbers (183, 222, 223). Whereas JCPyV, BKPyV, MCPyV, HPyV6, HPyV7 and TSPyV are known to be associated with diseases, the others are orphan regarding clinical manifestations.

By applying the newly developed multiplex PCR, we studied tonsillar tissue from 78 subjects (31 children and 47 adults) mostly with tonsillitis or tonsillar hypertrophy. Positive findings were seen in 13 specimens: JCPyV (1/78, 1.3%), WUPyV (3/78, 3.8%), MCPyV (1/78, 1.3%), HPyV6 (6/78, 7.7%), TSPyV (3/78, 3.8%). JCPyV, MCPyV and HPyV6 DNAs were found in juveniles or adults and WUPyV and TSPyV DNA in young children. Co-infection with WUPyV and TSPyV was found in a 6-y child with hypertrophy. The positive findings were confirmed with corresponding singleplex PCRs and agarose gel electrophoresis.

A total of five HPyVs (JCPyV, WUPyV, MCPyV, HPyV6 and TSPyV) were found in tonsillar tissue in this study. JCPyV DNA has been found in tonsillar tissue in several studies (222, 224), and tonsillar stromal cells have been shown to be susceptible to JCPyV infection. In a previous study (183), WUPyV and MPyV DNA was detected in 3.5% (8/229) and 2.2% (5/229) respectively of tonsillar tissues by using nested singleplex PCR. Moreover, a study investigated 229 tonsillar biopsies for the presence of TSPyV, finding TSPyV DNA in eight (3.5%) tonsils (218). A German tonsillar HPyV-DNA prevalence study, using real-time quantitative PCRs in singleplex format, found JCPyV (1/40, 2.5%), WUPyV (3/40, 7.5%), MCPyV (4/40, 10%), HPyV6 (1/40, 2.5%) in non-malignant tonsillar tissue, with overall very low HPyV DNA amounts (225). Their viral prevalence findings are highly similar to ours. Other studies of HPyV finding in tonsils are listed in Table 10. Genoprevalence of HPyV in tonsillar tissue varies in different studies and in various geographic locations. Nevertheless, in line with other studies, the result confirmed and suggested that the lymphoid system plays a crucial role in HPyV biology as the site of initial infection or reactivation. Of note, HPyV12, NJPyV and LIPyV have not been detected in tonsillar tissues in present or previous studies (225-227).

To conclude, the frequent occurrence of HPyVs in human tonsils provided evidence that the lymphoid tissue plays an important role for these viruses. However, whether or not the undetected HPyVs share the same infection route requires more investigation with different sample types.

Table 10. Genoprevalence of HPyV in tonsillar tissue by PCR assays

Virus *Species*	Sample n	Children / Adults	Sample type	Prevalence (%)			Study	Country
				Children	Adults	Total		
BKPyV	220	Children	FFPE	0.5		0.5	(228)	USA
(*HPyV1*)	78	Children and Adults	FFPE	-	-	5.1	(229)	Italy
	29	Children and Adults	Frozen	-	-	0	(230)	Italy
	57	Children	Fresh	5.3		5.3	(231)	Italy
	50	Children	Frozen	6.0		6.0	(179)	Italy
	40	Children and Adults	ND	-	-	0	(225)	Germany
	99	Children	Swab	0		0	(227)	China
	100	Children	Fresh	0		0	(223)	Italy
	689	Children and Adults	Brushing	12.3	0.2	2.6	(226)	France
JCPyV	220	Children	FFPE	0		0	(228)	USA
(*HPyV2*)	57	Children	Fresh	0		0	(231)	Italy
	50	Children	Frozen	0		0	(179)	Italy
	40	Children and Adults	ND	-	-	2.5	(225)	Germany
	99	Children	Swab	0		0	(227)	China
	100	Children	Fresh	0		0	(223)	Italy
	689	Children and Adults	Brushing	0.7	0.5	0.6	(226)	France
KIPyV	229	Children and Adults	Fresh	-	-	0	(183)	Finland
(*HPyV3*)	78	Children and Adults	FFPE	-	-	12.8	(229)	Italy
	29	Children and Adults	Frozen	7.7	6.2	6.9	(230)	Italy
	50	Children	Frozen	0		0	(179)	Italy
	51	Children	Frozen	0		0	(232)	Turkey
	99	Children	Swab	2.0		2.0	(227)	China
	40	Children and Adults	ND	-	-	0	(225)	Germany
	689	Children and Adults	Brushing	0	0	0	(226)	France
WUPyV	229	Children and Adults	Fresh	-	-	2.2	(183)	Finland
(*HPyV4*)	78	Children and Adults	FFPE	-	-	5.1	(229)	Italy
	29	Children and Adults	Frozen	-	-	0	(230)	Italy
	50	Children	Frozen	12.0		12.0	(179)	Italy
	51	Children	Frozen	3.9		3.9	(232)	Tukey
	99	Children	Swab	13.1		13.1	(227)	China
	40	Children and Adults	ND	-	-	7.5	(225)	Germany
	689	Children and Adults	Brushing	0	1.6	1.3	(226)	France
MCPyV	229	Children and Adults	Fresh	-	-	3.5	(183)	Finland
(*HPyV5*)	78	Children and Adults	FFPE	-	-	0	(229)	Italy
	40	Children and Adults	ND	-	-	10.0	(225)	Germany
	103	Adults	FFPE		10.2	10.2	(233)	Czech
	99	Children	Fresh	6.0		6.0	(227)	China
	689	Children and Adults	Brushing	9.4	16.0	14.7	(226)	France
HPyV6	40	Children and Adults	ND	-	-	2.5	(225)	Germany
(*HPyV6*)	103	Adults	FFPE		4.6	4.6	(233)	Czech
	99	Children	Fresh	0		0	(227)	China
	689	Children and Adults	Brushing	9.4	18.1	16.4	(226)	France

Virus *Species*	Sample n	Children / Adults	Sample type	Prevalence (%) Children	Adults	Total	Study	Country
(*HPyV7*)	103	Adults	FFPE		0.9	0.9	(233)	Czech
	99	Children	Swab	0		0	(227)	China
	689	Children and Adults	Brushing	1.4	0.7	0.9	(226)	France
TSPyV	40	Children and Adults	ND	-	-	0	(225)	Germany
(*HPyV8*)	689	Children and Adults	Brushing	21.0	1.1	5.1	(226)	France
HPyV9	40	Children and Adults	ND	-	-	0	(225)	Germany
(*HPyV9*)	99	Children	Swab	0		0	(227)	China
	689	Children and Adults	Brushing	0.7	1.1	1.0	(226)	France
MWPyV	100	Children	Fresh	6.0		6.0	(223)	Italy
(*HPyV10*)	99	Children	Swab	2.0		2.0	(227)	China
	40	Children and Adults	ND	-	-	0	(225)	Germany
	689	Children and Adults	Brushing	0	0	0	(226)	France
STLPyV	40	Children and Adults	ND	-	-	0	(225)	Germany
(HPyV11)	99	Children	Swab	2.0		2.0	(227)	China
HPyV12	40	Children and Adults	ND	-	-	0	(225)	Germany
(HPyV12)	99	Children	Swab	0			(227)	China
	689	Children and Adults	Brushing	0	0	0	(226)	France
NJPyV (*HPyV13*)	40	Children and Adults	ND	-	-	0	(225)	Germany
LIPyV	689	Children and Adults	Brushing	0	0	0	(226)	France

ND no data; FFPE formalin-fixed paraffin-embedded

2.3 HPyV-DNA in the skin of liver transplant recipients (IV)

To determine the occurrences of the HPyVs in skin and possible clinical associations, we applied multiplex PCR and singleplex qPCR assays to study HPyV genoprevalences in SCCis or AK and benign skin in LiTRs and in healthy skin of immunocompetent adults. Furthermore, DNA was isolated from the serum of LiTRs with HPyV-DNA detectable in biopsies. All the samples were first tested using the new multiplex PCR assay for 13 HPyVs, followed by singleplex qPCRs to quantify the viral DNAs. The detection of LIPyV was performed in singleplex format and then further confirmed by sequencing because no published quantitative PCR method is available for detection of LIPyV DNA.

In 126 LiTRs, a total of 14 punch biopsies collected from lesional and 127 from non-lesional sites were studied (Fig.16). The occurrences of MCPyV DNA in lesions versus non-lesions were similar, with no significant statistical difference. TSPyV DNA was detected in a single biopsy, at extremely low level (1.1 copies per 10^6 cells). HPyV 6 and HPyV7 DNAs were present in only healthy skin. The viral loads of the two viruses were similar. One biopsy from a LiTR with no premalignant lesions was tested LIPyV positive. The PCR product was confirmed by sequencing, showing 100% identity to the reference LIPyV genome (KY404016). For control, skin biopsies from 80 immunocompetent adults having participated in epicutaneous irritant testing were studied.

MCPyV and HPyV6 DNAs were found in 15% (12/80) and 2.5% (2/80) of skin biopsies, respectively.

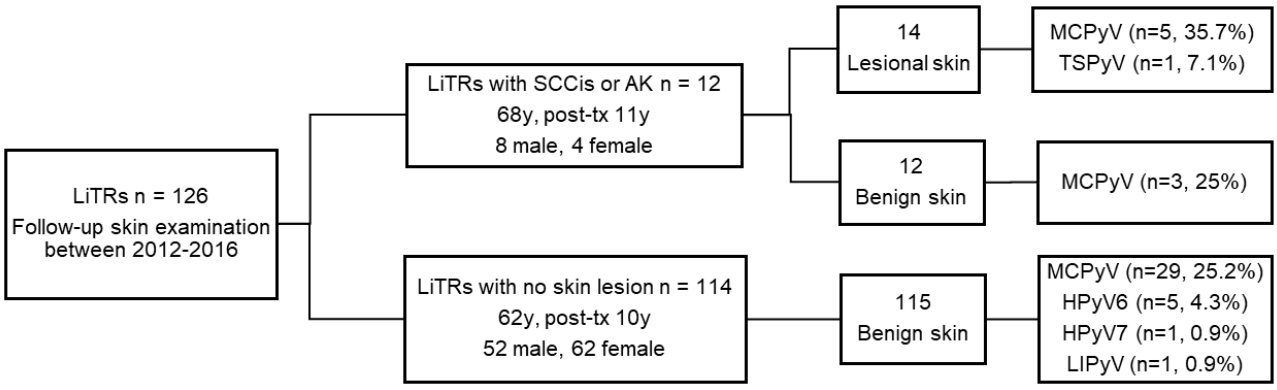

Figure 16. HPyVs genoprevalence in lesional and benign skin biopsies collected from liver transplant recipients.

Overall, HPyV-DNA was found in skin biopsies of 38 LiTRs including five patients with pre-stage SCC. Except for two patients with HPyV-DNA present exclusively in pre-stage SCC, in all other 10 pre-stage SCC patients the viral DNA findings were alike in both premalignant and healthy tissues. The MCPyV-DNA-positive individuals with lesion(s) vs. non-lesion(s) and HPyV6 and HPyV7 DNA-positive-individuals matched in ages. Co-infection was seen in two LiTRs with no premalignant lesions. The sera of all 37 biopsy-HPyV-positive LiTRs tested DNA negative for all 14 HPyVs.

Previous studies of HPyV in cutaneous SCC or pre-stage SCC are listed in Table 11. In all, our data on HPyVs in SCC precursors and SCC are in line with previous studies, and point to virus latency or shedding, rather than activation. The diverse genoprevalence among studies may be related to the sample size per patient, sample type, methods of analysis and study population. In this study, MCPyV DNA was detected in both premalignant and benign skin with no statistically significant difference in viral DNA prevalence or load, speaking against a role for this carcinogenic virus in SCC development. In our much larger series, HPyV6 and HPyV7 were present exclusively in non-diseased skin. As in previous studies (234, 235), our low prevalences of HPyV6 and HPyV7 do not point to SCC pathology among LiTRs. LIPyV was discovered quite recently, at low genoprevalence in skin swabs of cancer-free individuals (141). In our cohort, LIPyV DNA was found in skin tissue of a single LiTR, but not in her serum, and the seroprevalence of LIPyV seems to be low (32, 142). Interestingly, a very recent study showed LIPyV DNA in faeces in an outbreak of feline diarrhoea (236), suggesting that LIPyV might be a feline-origin polyomavirus. The medical impact of LIPyV in humans or in felines remains to be determined in forthcoming geno- and seroprevalence studies.

As a summary, the data in this thesis work does not support a role for any of the 14 HPyVs in SCC pathogenesis. In light of the large number of existing human cancer types and their multifactorial pathogenesis, inclusion of additional risk factors and their combinations with HPyV types could provide new information on the driving forces of cancer development.

Table 11. Occurrences of HPyVs in cutaneous SCCs and pre-stage cutaneous SCCs by PCR assays

Patients	Lesion	Sample n	Sample type	HPyV	Prevalence (%)	Study
immunocompetent	SCC	177	FFPE	MCPyV	15	(237)
immunosuppressed	SCC	25	FFPE	MCPyV	52	(238)
immunocompetent	SCC	28	FFPE	MCPyV	25	
immunosuppressed	SCCis	13	FFPE	MCPyV	69	
immunocompetent	SCCis	23	FFPE	MCPyV	17.4	
immunosuppressed	SCCis	21	FFPE	MCPyV	9.5	(239)
immunocompetent	SCCis	24	FFPE	MCPyV	8.3	
immunocompetent	SCC	30	FFPE	MCPyV	13	(240)
immunocompetent and immunosuppressed	SCC	185	Fresh-frozen	MCPyV	37	(241)
				JCPyV	0	
				BKPyV	0	
				KIPyV	0	
				WUPyV	0	
ND	SCC	21	FFPE	HPyV6	33	(234)
				HPyV7	4.7	
immunocompetent	SCCis	8	FFPE	MCPyV	25	(235)
				HPyV6	12	
				HPyV7	0	
				TSPyV	0	
				HPyV9	0	
immunocompetent	SCC	52	FFPE	MCPyV	27	
				HPyV6	4	
				HPyV7	0	
				TSPyV	0	
				HPyV9	0	
immunocompetent	AK	31	FFPE	MCPyV	19	
				HPyV6	3	
				HPyV7	0	
				TSPyV	0	
				HPyV9	0	
immunocompetent and immunosuppressed	SCC	75	FFPE	MCPyV	28	(242)
immunocompetent	SCC	11	Fresh-frozen	MCPyV	18	(243)
ND	SCC	34	FFPE	MCPyV	18	(244)

ND no data; FFPE formalin-fixed paraffin-embedded; SCC squamous cell carcinoma; SCCis squamous cell carcinoma in situ; AK actinic keratosis

2.4 Conclusion (III, IV)

The new multiplex assay was successfully applied to detect viral DNA in various clinical materials, including fresh tissues (III and IV), serum (IV), urine and plasma (245). The existing screening approach can target currently assigned HPyV species in multiplex or LIPyV in singleplex. Comprehensive detection of all currently assigned HPyVs species requires merely 5 µl of DNA template. On the other hand, one should keep in mind the limitations of microsphere-based DNA detection. Despite the possibility of determining DNA quantity according to a calibration curve, the microsphere-based multiplex DNA assay can provide only semi-quantitative data because the PCR amplification step prior to xMAP analysis does not reveal the real DNA copy number in the original sample (25). Also, direct DNA hybridisation is highly specific for selective sequences. Even if able to detect particular virus strains, such approaches can be vulnerable to mutations, like any other sequence-specific nucleic acid detection. Importantly, the existing virus panel can be easily adapted for adding more emerging viruses in the near future.

CONCLUDING REMARKS AND FUTURE PROSPECTIVES

This thesis includes the design and setup of new methods for molecular and serodiagnosis and their clinical utilities. In the studies, I (i) developed serological tests for identification of three intrauterine infections; (ii) evaluated the diagnostic performance of newly developed serological tests; (iii) set up a microsphere-based PCR assays for the detection of 13 HPyVs; (iv) determined the role of lymphoid tissue for HPyV persistence and transmission; and (v) analysed the possible pathological associations between HPyVs and premalignant skin lesions of post-transplantation.

The newly developed antibody tests in both multiplex and singleplex formats were shown to be highly sensitive and specific in comparison to high-standard commercial or *in-house* reference assays (study I, II). The current panels for intrauterine infections are of remarkable potential for other anti-microbial antibodies. Heterologous IgM reactivity was identified by multiplex IgG-avidity-SIA. Other solutions, such as applying recombinant peptides/proteins or design of competition-format-based SIA, may improve IgM detection, yet require forthcoming examination. The current xMAP technology permits only one fluorescent reporter for identification of a single-type capture property (e.g. a given antibody isotype) against different analytes (antigens). Bold thinking on the development of multiplexing serological tests would aim at a variety of capture properties (e.g. IgG, IgM and IgA) against various antigens in a single well, by applying more than one reporter in concert with colour-coded microspheres.

With our microsphere-based multiplex PCR, several HPyVs were found in tonsillar tissues of children and adults, indicating the lymphoid system plays a role in HPyV infections and persistence (study III). Moreover, the resembling presences of HPyV viral DNAs in lesional and non-lesional skin of post-tx patients were shown not to be associated with premalignant pathogenesis (study IV). Since HPyVs are capable of persisting and later reactivating, more studies are warranted to assess the possible clinical impact of new HPyVs concerning immunocompromised or elderly individuals. Furthermore, for the newest members, LIPyV, HPyV12 and NJPyV exhibiting low seroprevalences in the general population, forthcoming studies should focus on identifying their unique transmission routes (if any) and origins of infections. In this regard, the development of cell culture systems would permit us to understand the potential pathogenesis, tissue/cell tropism and specific cell reservoirs for these viruses.

Emerging technologies have achieved increasing feasibility in clinical microbiology, especially as many viruses are challenging to grow in cell culture. Several novel molecular and

serodiagnosis methods are already available. However, the new approaches will not replace, but combine and enhance traditional methods. The combinations of techniques yield a comprehensive diagnostic toolbox, improving our understanding of the association between infectious agents and diseases.

ACKNOWLEDGEMENTS

This study was carried out at the Department of Virology, Medicum, University of Helsinki. I warmly thank the head of the Department, Professor Kalle Saksela for the wonderful working environment.

This study was financially supported by the foundations at Helsinki, Helsinki University Hospital Research & Education and Research & Development Funds; CIMO; Instrumentarium Research Fund; the Academy of Finland; the Sigrid Jusélius Foundation; the Medical Society of Finland (FLS); the Jane and Aatos Erkko Foundation; the Life and Health Medical Association; the Medical Foundation Liv och Hälsa; the Ida Montin Foundation; and the Finnish-Norwegian Medical Foundation.

I would like to express my deepest appreciation to my supervisor, Professor Klaus Hedman, for his support and patient guidance throughout my PhD study. Your knowledge, wisdom, encouragement and positive attitude have greatly inspired me in scientific research and beyond. Your careful editing has contributed enormously to the production of each publication in this study. I am really thankful to be your student. I also wish to express my gratitude to Docent Maria Söderlund-Vernermo for your scientific guidance and support. Your advice has always motived me to explore new ideas during the entire study. I am deeply grateful to my previous supervisor Jonas Blomberg, now sadly deceased. I appreciate his enthusiasm for science stimulated my interest when I was a master student, and his encouragement to follow my own path.

I want to acknowledge the reviewers of this thesis, Professor Tero Soukka and Docent Laura Kakkola, for their advice and insightful comments on the improvement of this work. I also want to thank Docent Matti Lehtinen for accepting the role of opponent for the thesis dissertation. I am thankful to my DPBM thesis committee members, Hannimari Kallio-Kokko & Jussi Merenmies, for their excellent advice and guidance in the annual meetings.

Neither of this book or the work would have existed without the stimulus and supports provided by my colleagues. My deepest thank goes to Lea Hedman, the heart and soul in our lab who provided me enjoyable working environment. Lea, you have given me so much help and support all these years. I wish to give my special gratitude to the former and present co-workers: Mari, Mafe, Xu Man, Elina, Lari, Juuso, Visa, Usha, Mohammadreza, Fu Yu, Tingting, Arun, Kalle, Xuemeng, Benedict and Päivi, for their unwavering support and encouragement. I appreciate all the fun trips and parties we shared together. I want to thank all the co-authors for your kind cooperation during various stages of processing of the manuscript. Warm thanks go to my

badminton partners Rommel, Mafe, Visa and Vincent who have helped me to achieve a weekly work-life balance.

I am grateful to my Chinese friends Qingru, Yajie, Jingyu, Xiaoqing, Yuxia, Zhaozhe for togetherness and social occasions. You guys always provided unconditional help and encouragement in my life.

I would like to express my deepest gratitude to my beloved family, in particular to my parents and brother Xuanjun who always being there for me. I am grateful to my parents-in-law Otto and Kirsti for giving me constant love and care. I want to thank brother-in-law Janne for all the fun family activities. Last but not least, I deeply thank my dear husband Mikko for your understanding, support, patience and love during this entire process. Thank you for being in my life.

Helsinki, March 2020

Yilin Wang

SUPPLEMENTARY DATA

Table S1. Reference assays in study I and II

Study	Manufacturer Assay	Antigen	Assay principles	Unit	Interpretation of results
I	***In-house*** B19V VP2-IgG	Parvovirus B19V recombinant VP2 virus-like particle	EIA	Absorbance	Negative, <0.198 Positive, >0.198
I	**BioMérieux** Vidas HCMV IgG	Viral lysate (AD 169)	ELFA, two-step ELFA with a final fluorescent detection	Titer (IU/mL)	Negative, <4 Positive, ≥6 Equivocal, 4 - <6
I	**BioMérieux** Vidas Toxo IgG	Cell-cultured tachyzoites lysate (RH strain)	ELFA, two-step ELFA with a final fluorescent detection	Titer (IU/mL)	Negative, <4 Positive, ≥8 Equivocal, 4 - <8
II	***In-house*** B19V VP2-IgM	Parvovirus B19V recombinant VP2 virus-like particle	EIA	Absorbance	Negative, <0.17 Positive, >0.22 Equivocal, 0.17-0.22
II	**DiaSorin** LIAISON Biotrin B19V IgM	Parvovirus B19V recombinant VP2 virus-like particle	EIA	Index	Negative <0.9 Positive, >1.1 Equivocal, 0.9-1.1
II	**Abbott** Architect HCMV IgM	Viral lysate (AD 169) and recombinant antigens	CMIA, two steps indirect anti-IgM detection	Index	Negative, <0.85 Positive, ≥1 Equivocal, 0.85-0.99
II	**BioMérieux** Vidas Toxo IgM	Cell-cultured tachyzoites lysate (RH strain)	ELFA, two-step ELFA with a final fluorescent detection	Index	Negative, <0.55 Positive, ≥0.65 Equivocal, 0.55 - <0.65
II	**Abbott** Architect HCMV IgG avidity	Viral lysate (AD 169)	CMIA, two assays with and without liquid HCMV antigen to neutralise high-avidity HCMV antibodies	% Avidity	Low avidity, <50% High avidity, ≥60% Equivocal, 50-59.9%
II	**BioMérieux** Vidas HCMV IgG avidity	Viral lysate	ELFA, two assays with and without 6M urea to dissociate low-avidity antibodies	Avidity index	Low avidity, <0.4; high avidity, ≥0.65; equivocal, 0.4–<0.65
II	**BioMérieux** Vidas Toxo IgG avidity	Cell-cultured tachyzoites lysate (RH strain)	ELFA, two assays with and without 6M urea to dissociate low-avidity antibodies	Avidity index	Low avidity, <0.2 High avidity, >0.3 Equivocal, 0.2 - 0.3

Study	Manufacturer Assay	Antigen	Assay principles	Unit	Interpretation of results
II	***In-house*** B19V VP2-IgG-ETS	Parvovirus B19V VP2 virus-like particles and synthetic peptide KYVTGIN	EIA	ETS Index	Recent infection, ≤10% Past infection, >20% Equivocal, 11-20
II	***In-house*** B19V VP1-IgG-avidity	Prokaryotic recombinant fusion protein containing the B19 VP1 unique region	EIA	Index	Recent infection, ≤15% Past infection, >25% Equivocal, >15 - 25%

CMIA, chemiluminescent microparticle immunoassay; ELFA, enzyme-linked fluorescent assay;

REFERENCES

1. Cunha BA. 2004. Historical aspects of infectious diseases, part I. Infect Dis Clin North Am 18:XI-V.
2. Heesterbeek H, Anderson RM, Andreasen V, Bansal S, De Angelis D, Dye C, Eames KT, Edmunds WJ, Frost SD, Funk S, Hollingsworth TD, House T, Isham V, Klepac P, Lessler J, Lloyd-Smith JO, Metcalf CJ, Mollison D, Pellis L, Pulliam JR, Roberts MG, Viboud C, Isaac Newton Institute IDDC. 2015. Modeling infectious disease dynamics in the complex landscape of global health. Science 347:aaa4339.
3. World Health Organization. 2013. Mortality and global health estimates 2013, *on* WHO. http://apps.who.int/gho/data/node.main.686?lang=en. Accessed
4. Goldwasser RA, Kissling RE. 1958. Fluorescent antibody staining of street and fixed rabies virus antigens. Proc Soc Exp Biol Med 98:219-23.
5. Kadi Z, Dali S, Bakouri S, Bouguermouh A. 1986. Rapid diagnosis of respiratory syncytial virus infection by antigen immunofluorescence detection with monoclonal antibodies and immunoglobulin M immunofluorescence test. J Clin Microbiol 24:1038-40.
6. Kasempimolporn S, Saengseesom W, Lumlertdacha B, Sitprija V. 2000. Detection of rabies virus antigen in dog saliva using a latex agglutination test. J Clin Microbiol 38:3098-9.
7. Kindt T, Goldsby R, Osborne B, Kuby J. 2003. Antibodies: Structure and Function, Kuby Immunology 5th ed. W.H. Freeman, 2003., New York.
8. Hornick CL, Karuch F. 1972. Antibody affinity. 3. The role of multivalance. Immunochemistry 9:325-40.
9. Van Regenmortel MH, Hardie G. 1976. Immunochemical studies of tobacco mosaic virus--II. Univalent and monogamous bivalent binding of IgG antibody. Immunochemistry 13:503-7.
10. Hedman K, Lappalainen M, Söderlund M, and Hedman L. 1993. Avidity of IgG in serodiagnosis of infectious diseases. Clin Microbiol Rev 4:123-129.
11. Jacob J, Miller C, Kelsoe G. 1992. In situ studies of the antigen-driven somatic hypermutation of immunoglobulin genes. Immunol Cell Biol 70 (Pt 2):145-52.
12. Dal Porto JM, Haberman AM, Shlomchik MJ, Kelsoe G. 1998. Antigen drives very low affinity B cells to become plasmacytes and enter germinal centers. J Immunol 161:5373-5381.
13. Engvall E, Perlmann P. 1972. Enzyme-linked immunosorbent assay, Elisa. 3. Quantitation of specific antibodies by enzyme-labeled anti-immunoglobulin in antigen-coated tubes. J Immunol 109:129-35.
14. Procop GW, Church DL, Hall GS, Janda WM, Koneman EW, Schreckenberger PC, Woods GL. 2017. Laboratory Diagnosis by Immunologic Methods, p 277-331, Koneman's color atlas and textbook of diagnostic microbiology
15. Hedman K, Seppala I. 1988. Recent rubella virus infection indicated by a low avidity of specific IgG. J Clin Immunol 8:214-21.
16. Curdt I, Praast G, Sickinger E, Schultess J, Herold I, Braun HB, Bernhardt S, Maine GT, Smith DD, Hsu S, Christ HM, Pucci D, Hausmann M, Herzogenrath J. 2009. Development of fully automated determination of marker-specific immunoglobulin G (IgG) avidity based on the avidity competition assay format: application for Abbott Architect cytomegalovirus and Toxo IgG Avidity assays. J Clin Microbiol 47:603-13.
17. Hedman K, Lappalainen M, Seppaia I, Makela O. 1989. Recent primary toxoplasma infection indicated by a low avidity of specific IgG. J Infect Dis 159:736-40.
18. Saiki RK, Scharf S, Faloona F, Mullis KB, Horn GT, Erlich HA, Arnheim N. 1985. Enzymatic amplification of beta-globin genomic sequences and restriction site analysis for diagnosis of sickle cell anemia. Science 230:1350-4.
19. Kralik P, Ricchi M. 2017. A Basic Guide to Real Time PCR in Microbial Diagnostics: Definitions, Parameters, and Everything. Front Microbiol 8:108.
20. Kuypers J, Jerome KR. 2017. Applications of Digital PCR for Clinical Microbiology. J Clin Microbiol 55:1621-1628.

21. Buchan BW, Ledeboer NA. 2014. Emerging technologies for the clinical microbiology laboratory. Clin Microbiol Rev 27:783-822.
22. Ellington AA, Kullo IJ, Bailey KR, Klee GG. 2010. Antibody-based protein multiplex platforms: technical and operational challenges. Clin Chem 56:186-93.
23. Ramanan P, Bryson AL, Binnicker MJ, Pritt BS, Patel R. 2018. Syndromic Panel-Based Testing in Clinical Microbiology. Clin Microbiol Rev 31.
24. Miller MB, Tang YW. 2009. Basic concepts of microarrays and potential applications in clinical microbiology. Clin Microbiol Rev 22:611-33.
25. Reslova N, Michna V, Kasny M, Mikel P, Kralik P. 2017. xMAP Technology: Applications in Detection of Pathogens. Front Microbiol 8:55.
26. Kellar KL, Iannone MA. 2002. Multiplexed microsphere-based flow cytometric assays. Exp Hematol 30:1227-37.
27. Hartmann M, Roeraade J, Stoll D, Templin MF, Joos TO. 2009. Protein microarrays for diagnostic assays. Anal Bioanal Chem 393:1407-16.
28. Nichkova M, Dosev D, Gee SJ, Hammock BD, Kennedy IM. 2007. Multiplexed immunoassays for proteins using magnetic luminescent nanoparticles for internal calibration. Anal Biochem 369:34-40.
29. Angeloni S, Dunbar S, Garcia C, Stone V. 2016. Luminex xMAP® cookbook 4th Edition. Luminex Corporation, www.luminexcorp.com.
30. Iannone MA, Consler TG. 2006. Effect of microsphere binding site density on the apparent affinity of an interaction partner. Cytometry A 69:374-83.
31. Opalka D, Lachman CE, MacMullen SA, Jansen KU, Smith JF, Chirmule N, Esser MT. 2003. Simultaneous quantitation of antibodies to neutralizing epitopes on virus-like particles for human papillomavirus types 6, 11, 16, and 18 by a multiplexed luminex assay. Clin Diagn Lab Immunol 10:108-15.
32. Kamminga S, van der Meijden E, Feltkamp MCW, Zaaijer HL. 2018. Seroprevalence of fourteen human polyomaviruses determined in blood donors. PLoS One 13:e0206273.
33. Kong W, Li Y, Cheng S, Yan C, An S, Dong Z, Yan L, Yuan Y. 2016. Luminex xMAP combined with Western blot improves HIV diagnostic sensitivity. J Virol Methods 227:1-5.
34. Fonseca BP, Marques CF, Nascimento LD, Mello MB, Silva LB, Rubim NM, Foti L, Silva ED, Ferreira AG, Krieger MA. 2011. Development of a multiplex bead-based assay for detection of hepatitis C virus. Clin Vaccine Immunol 18:802-6.
35. Gu AD, Xie YB, Mo HY, Jia WH, Li MY, Li M, Chen LZ, Feng QS, Liu Q, Qian CN, Zeng YX. 2008. Antibodies against Epstein-Barr virus gp78 antigen: a novel marker for serological diagnosis of nasopharyngeal carcinoma detected by xMAP technology. J Gen Virol 89:1152-8.
36. Bokken GC, Bergwerff AA, van Knapen F. 2012. A novel bead-based assay to detect specific antibody responses against Toxoplasma gondii and Trichinella spiralis simultaneously in sera of experimentally infected swine. BMC Vet Res 8:36.
37. Pabbaraju K, Tokaryk KL, Wong S, Fox JD. 2008. Comparison of the Luminex xTAG respiratory viral panel with in-house nucleic acid amplification tests for diagnosis of respiratory virus infections. J Clin Microbiol 46:3056-62.
38. Zou S, Han J, Wen L, Liu Y, Cronin K, Lum SH, Gao L, Dong J, Zhang Y, Guo Y, Shu Y. 2007. Human influenza A virus (H5N1) detection by a novel multiplex PCR typing method. J Clin Microbiol 45:1889-92.
39. Zubach V, Smart G, Ratnam S, Severini A. 2012. Novel microsphere-based method for detection and typing of 46 mucosal human papillomavirus types. J Clin Microbiol 50:460-4.
40. Reslova N, Huvarova V, Hrdy J, Kasny M, Kralik P. 2019. A novel perspective on MOL-PCR optimization and MAGPIX analysis of in-house multiplex foodborne pathogens detection assay. Sci Rep 9:2719.
41. Hamza IA, Jurzik L, Wilhelm M. 2014. Development of a Luminex assay for the simultaneous detection of human enteric viruses in sewage and river water. J Virol Methods 204:65-72.
42. Nahmias AJ, Walls KW, Stewart JA, Herrmann KL, Flynt WJ. 1971. The ToRCH complex-perinatal infections associated with toxoplasma and rubella, cytomegol- and herpes simplex viruses. Pediatr Res 5:405-406.
43. Arora N, Sadovsky Y, Dermody TS, Coyne CB. 2017. Microbial Vertical Transmission during Human Pregnancy. Cell Host Microbe 21:561-567.

44. Luo M, Tsao J, Rossmann MG, Basak S, Compans RW. 1988. Preliminary X-ray crystallographic analysis of canine parvovirus crystals. J Mol Biol 200:209-11.
45. Cossart YE, Field AM, Cant B, Widdows D. 1975. Parvovirus-like particles in human sera. Lancet 1:72-3.
46. Young NS, Brown KE. 2004. Parvovirus B19. N Engl J Med 350:586-97.
47. Brown KE, Young NS. 1997. Parvovirus B19 in human disease. Annu Rev Med 48:59-67.
48. FIELDS BN, KNIPE DM, HOWLEY PM. 2013. Parvoviridae, p 1812-1835, Fields Virology 6th ed, vol Volume 2. Philadelphia : Wolters Kluwer Health/Lippincott Williams & Wilkins, 2013.
49. Qiu J, Söderlund-Venermo M, Young NS. 2017. Human Parvoviruses. Clin Microbiol Rev 30:43-113.
50. Broliden K, Tolfvenstam T, Norbeck O. 2006. Clinical aspects of parvovirus B19 infection. J Intern Med 260:285-304.
51. Ergaz Z, Ornoy A. 2006. Parvovirus B19 in pregnancy. Reprod Toxicol 21:421-35.
52. Gray JJ, Cohen BJ, Desselberger U. 1993. Detection of human parvovirus B19-specific IgM and IgG antibodies using a recombinant viral VP1 antigen expressed in insect cells and estimation of time of infection by testing for antibody avidity. J Virol Methods 44:11-23.
53. Gray ES. 1987. Human parvovirus infection. J Pathol 153:310-2.
54. Gray ES, Davidson RJ, Anand A. 1987. Human parvovirus and fetal anaemia. Lancet 1:1144.
55. Anand A, Gray ES, Brown T, Clewley JP, Cohen BJ. 1987. Human parvovirus infection in pregnancy and hydrops fetalis. N Engl J Med 316:183-6.
56. Gratacos E, Torres PJ, Vidal J, Antolin E, Costa J, Jimenez de Anta MT, Cararach V, Alonso PL, Fortuny A. 1995. The incidence of human parvovirus B19 infection during pregnancy and its impact on perinatal outcome. J Infect Dis 171:1360-3.
57. Koch WC, Harger JH, Barnstein B, Adler SP. 1998. Serologic and virologic evidence for frequent intrauterine transmission of human parvovirus B19 with a primary maternal infection during pregnancy. Pediatr Infect Dis J 17:489-94.
58. Kerr JR, O'Neill HJ, Coyle PV, Thompson W. 1994. An outbreak of parvovirus B19 infection; a study of clinical manifestations and the incidence of fetal loss. Ir J Med Sci 163:65-7.
59. Hall SM. 1990. Prospective-Study of Human Parvovirus (B19) Infection in Pregnancy. Bmj-British Medical Journal 300:1166-1170.
60. Lamont RF, Sobel JD, Vaisbuch E, Kusanovic JP, Mazaki-Tovi S, Kim SK, Uldbjerg N, Romero R. 2011. Parvovirus B19 infection in human pregnancy. BJOG 118:175-86.
61. Jensen IP, Thorsen P, Jeune B, Moller BR, Vestergaard BF. 2000. An epidemic of parvovirus B19 in a population of 3,596 pregnant women: a study of sociodemographic and medical risk factors. BJOG 107:637-43.
62. Mossong J, Hens N, Friederichs V, Davidkin I, Broman M, Litwinska B, Siennicka J, Trzcinska A, P VAND, Beutels P, Vyse A, Shkedy Z, Aerts M, Massari M, Gabutti G. 2008. Parvovirus B19 infection in five European countries: seroepidemiology, force of infection and maternal risk of infection. Epidemiol Infect 136:1059-68.
63. Kurtzman GJ, Cohen BJ, Field AM, Oseas R, Blaese RM, Young NS. 1989. Immune response to B19 parvovirus and an antibody defect in persistent viral infection. J Clin Invest 84:1114-23.
64. Söderlund M, Brown KE, Meurman O, Hedman K. 1992. Prokaryotic expression of a VP1 polypeptide antigen for diagnosis by a human parvovirus B19 antibody enzyme immunoassay. J Clin Microbiol 30:305-11.
65. Peterlana D, Puccetti A, Corrocher R, Lunardi C. 2006. Serologic and molecular detection of human Parvovirus B19 infection. Clin Chim Acta 372:14-23.
66. Söderlund M, Brown CS, Spaan WJ, Hedman L, Hedman K. 1995. Epitope type-specific IgG responses to capsid proteins VP1 and VP2 of human parvovirus B19. J Infect Dis 172:1431-6.
67. Kaikkonen L, Lankinen H, Harjunpaa I, Hokynar K, Söderlund-Venermo M, Oker-Blom C, Hedman L, Hedman K. 1999. Acute-phase-specific heptapeptide epitope for diagnosis of parvovirus B19 infection. J Clin Microbiol 37:3952-6.
68. Söderlund M, Brown CS, Cohen BJ, Hedman K. 1995. Accurate serodiagnosis of B19 parvovirus infections by measurement of IgG avidity. J Infect Dis 171:710-3.
69. Maple PA, Hedman L, Dhanilall P, Kantola K, Nurmi V, Söderlund-Venermo M, Brown KE, Hedman K. 2014. Identification of past and recent parvovirus B19 infection in immunocompetent

individuals by quantitative PCR and enzyme immunoassays: a dual-laboratory study. J Clin Microbiol 52:947-56.
70. Enders M, Weidner A, Rosenthal T, Baisch C, Hedman L, Söderlund-Venermo M, Hedman K. 2008. Improved diagnosis of gestational parvovirus B19 infection at the time of nonimmune fetal hydrops. J Infect Dis 197:58-62.
71. FIELDS BN, KNIPE DM, HOWLEY PM. 2013. Cytomegaloviruses, p 2004-2582, Fields Virology 6th ed, vol Volume 2. Philadelphia : Wolters Kluwer Health/Lippincott Williams & Wilkins, 2013.
72. Yu X, Jih J, Jiang J, Zhou ZH. 2017. Atomic structure of the human cytomegalovirus capsid with its securing tegument layer of pp150. Science 356:6345.
73. Schottstedt V, Blumel J, Burger R, Drosten C, Groner A, Gurtler L, Heiden M, Hildebrandt M, Jansen B, Montag-Lessing T, Offergeld R, Pauli G, Seitz R, Schlenkrich U, Strobel J, Willkommen H, von Konig CH. 2010. Human Cytomegalovirus (HCMV) - Revised. Transfus Med Hemother 37:365-375.
74. Morton CC, Nance WE. 2006. Newborn hearing screening--a silent revolution. N Engl J Med 354:2151-64.
75. Jeon J, Victor M, Adler SP, Arwady A, Demmler G, Fowler K, Goldfarb J, Keyserling H, Massoudi M, Richards K, Staras SA, Cannon MJ. 2006. Knowledge and awareness of congenital cytomegalovirus among women. Infect Dis Obstet Gynecol 2006:80383.
76. Oliver SE, Cloud GA, Sanchez PJ, Demmler GJ, Dankner W, Shelton M, Jacobs RF, Vaudry W, Pass RF, Soong SJ, Whitley RJ, Kimberlin DW, National Institute of Allergy IDCASG. 2009. Neurodevelopmental outcomes following ganciclovir therapy in symptomatic congenital cytomegalovirus infections involving the central nervous system. J Clin Virol 46 Suppl 4:S22-6.
77. Manicklal S, Emery VC, Lazzarotto T, Boppana SB, Gupta RK. 2013. The "silent" global burden of congenital cytomegalovirus. Clin Microbiol Rev 26:86-102.
78. Adler SP, Nigro G. 2013. Prevention of maternal-fetal transmission of cytomegalovirus. Clin Infect Dis 57 Suppl 4:S189-92.
79. Society for Maternal-Fetal M, Hughes BL, Gyamfi-Bannerman C. 2016. Diagnosis and antenatal management of congenital cytomegalovirus infection. Am J Obstet Gynecol 214:B5-B11.
80. Schopfer K, Lauber E, Krech U. 1978. Congenital cytomegalovirus infection in newborn infants of mothers infected before pregnancy. Arch Dis Child 53:536-9.
81. Simonazzi G, Curti A, Cervi F, Gabrielli L, Contoli M, Capretti MG, Rizzo N, Guerra B, Farina A, Lazzarotto T. 2018. Perinatal Outcomes of Non-Primary Maternal Cytomegalovirus Infection: A 15-Year Experience. Fetal Diagn Ther 43:138-142.
82. Kenneson A, Cannon MJ. 2007. Review and meta-analysis of the epidemiology of congenital cytomegalovirus (CMV) infection. Rev Med Virol 17:253-76.
83. Fowler KB, Stagno S, Pass RF, Britt WJ, Boll TJ, Alford CA. 1992. The outcome of congenital cytomegalovirus infection in relation to maternal antibody status. N Engl J Med 326:663-7.
84. Daiminger A, Bader U, Enders G. 2005. Pre- and periconceptional primary cytomegalovirus infection: risk of vertical transmission and congenital disease. BJOG 112:166-72.
85. Griffiths PD, Baboonian C. 1984. A prospective study of primary cytomegalovirus infection during pregnancy: final report. Br J Obstet Gynaecol 91:307-15.
86. Gindes L, Teperberg-Oikawa M, Sherman D, Pardo J, Rahav G. 2008. Congenital cytomegalovirus infection following primary maternal infection in the third trimester. BJOG 115:830-5.
87. Enders G, Daiminger A, Bader U, Exler S, Enders M. 2011. Intrauterine transmission and clinical outcome of 248 pregnancies with primary cytomegalovirus infection in relation to gestational age. J Clin Virol 52:244-6.
88. Liesnard C, Donner C, Brancart F, Gosselin F, Delforge ML, Rodesch F. 2000. Prenatal diagnosis of congenital cytomegalovirus infection: prospective study of 237 pregnancies at risk. Obstet Gynecol 95:881-8.
89. Puhakka L, Renko M, Helminen M, Peltola V, Heiskanen-Kosma T, Lappalainen M, Surcel HM, Lonnqvist T, Saxen H. 2017. Primary versus non-primary maternal cytomegalovirus infection as a cause of symptomatic congenital infection - register-based study from Finland. Infect Dis (Lond) 49:445-453.

90. Istas AS, Demmler GJ, Dobbins JG, Stewart JA. 1995. Surveillance for congenital cytomegalovirus disease: a report from the National Congenital Cytomegalovirus Disease Registry. Clin Infect Dis 20:665-70.
91. Dollard SC, Grosse SD, Ross DS. 2007. New estimates of the prevalence of neurological and sensory sequelae and mortality associated with congenital cytomegalovirus infection. Rev Med Virol 17:355-63.
92. Lazzarotto T, Guerra B, Spezzacatena P, Varani S, Gabrielli L, Pradelli P, Rumpianesi F, Banzi C, Bovicelli L, Landini MP. 1998. Prenatal diagnosis of congenital cytomegalovirus infection. J Clin Microbiol 36:3540-4.
93. Stagno S, Tinker MK, Elrod C, Fuccillo DA, Cloud G, O'Beirne AJ. 1985. Immunoglobulin M antibodies detected by enzyme-linked immunosorbent assay and radioimmunoassay in the diagnosis of cytomegalovirus infections in pregnant women and newborn infants. J Clin Microbiol 21:930-5.
94. Lazzarotto T, Varani S, Spezzacatena P, Gabrielli L, Pradelli P, Guerra B, Landini MP. 2000. Maternal IgG avidity and IgM detected by blot as diagnostic tools to identify pregnant women at risk of transmitting cytomegalovirus. Viral Immunol 13:137-41.
95. Castellani A. 1914. Note on certain protozoa-like bodies in a case of protracted fever and splenomegaly. J Trop Med 17:113-114
96. Wolf A, Cowen, D., Paige, B.,. 1939a. Human toxoplasmosis: occurrence in infants as an encephalomyelitis verification by transmission to animals. Science 89:226-227.
97. Wolf A, Cowen, D., Paige, B.H.,. 1939b. Toxoplasmic encephalomyelitis. III. A new case of granulomatous encephalomyelitis due to a protozoon. Am J Pathol:657–694.
98. Frenkel JK, Dubey JP, Miller NL. 1970. Toxoplasma gondii in cats: fecal stages identified as coccidian oocysts. Science 167:893-6.
99. Jacobs L. 1967. Toxoplasma and toxoplasmosis. Adv Parasitol 5:1-45.
100. Montoya JG, Liesenfeld O. 2004. Toxoplasmosis. Lancet 363:1965-76.
101. Tenter AM, Heckeroth AR, Weiss LM. 2000. Toxoplasma gondii: from animals to humans. Int J Parasitol 30:1217-58.
102. Remington JD, G. 1990. Toxoplasmosis., p 89-195. *In* In: Remington JK, JO., editors. (ed), Infectious diseases of the fetus and newborn infant, Philadelphia: WB Saunders.
103. Ebbesen P. 2000. Placenta physiology., p 27-35. *In* In: Ambroise-Thomas PP, E., editors. (ed), Congenital toxoplasmosis: scientific background, clinical management and control, Paris: Springer-Verlag.
104. Dunn D, Wallon M, Peyron F, Petersen E, Peckham C, Gilbert R. 1999. Mother-to-child transmission of toxoplasmosis: risk estimates for clinical counselling. Lancet 353:1829-33.
105. Desmonts G, Couvreur J. 1974. Congenital toxoplasmosis. A prospective study of 378 pregnancies. N Engl J Med 290:1110-6.
106. Holland GN. 1999. Reconsidering the pathogenesis of ocular toxoplasmosis. Am J Ophthalmol 128:502-5.
107. Silveira C, Belfort R, Jr., Burnier M, Jr., Nussenblatt R. 1988. Acquired toxoplasmic infection as the cause of toxoplasmic retinochoroiditis in families. Am J Ophthalmol 106:362-4.
108. Weiss LM, Dubey JP. 2009. Toxoplasmosis: A history of clinical observations. Int J Parasitol 39:895-901.
109. Miro G, Montoya A, Jimenez S, Frisuelos C, Mateo M, Fuentes I. 2004. Prevalence of antibodies to Toxoplasma gondii and intestinal parasites in stray, farm and household cats in Spain. Vet Parasitol 126:249-55.
110. Phan L, Kasza K, Jalbrzikowski J, Noble AG, Latkany P, Kuo A, Mieler W, Meyers S, Rabiah P, Boyer K, Swisher C, Mets M, Roizen N, Cezar S, Sautter M, Remington J, Meier P, McLeod R, Toxoplasmosis Study G. 2008. Longitudinal study of new eye lesions in children with toxoplasmosis who were not treated during the first year of life. Am J Ophthalmol 146:375-384.
111. Torgerson PR, Mastroiacovo P. 2013. The global burden of congenital toxoplasmosis: a systematic review. Bull World Health Organ 91:501-8.
112. Gras L, Gilbert RE, Wallon M, Peyron F, Cortina-Borja M. 2004. Duration of the IgM response in women acquiring Toxoplasma gondii during pregnancy: implications for clinical practice and cross-sectional incidence studies. Epidemiol Infect 132:541-8.

113. Nascimento FS, Suzuki LA, Rossi CL. 2008. Assessment of the value of detecting specific IgA antibodies for the diagnosis of a recently acquired primary Toxoplasma infection. Prenat Diagn 28:749-52.
114. Robert-Gangneux F, Darde ML. 2012. Epidemiology of and diagnostic strategies for toxoplasmosis. Clin Microbiol Rev 25:264-96.
115. Sabin AB, Feldman HA. 1948. Dyes as Microchemical Indicators of a New Immunity Phenomenon Affecting a Protozoon Parasite (Toxoplasma). Science 108:660-3.
116. Schreiber RD, Feldman HA. 1980. Identification of the activator system for antibody to Toxoplasma as the classical complement pathway. J Infect Dis 141:366-9.
117. Peyron F, Lefevre-Pettazzoni M, Wallon M, Cozon F, Bissery A, Rabilloud M. 2007. Delayed maturation of toxoplasma immunoglobulin G avidity in pregnant women: impact of spiramycin treatment and gestational age. Int J Antimicrob Agents 29:S123-S124.
118. Lefevre-Pettazzoni M, Bissery A, Wallon M, Cozon G, Peyron F, Rabilloud M. 2007. Impact of spiramycin treatment and gestational age on maturation of Toxoplasma gondii immunoglobulin G avidity in pregnant women. Clin Vaccine Immunol 14:239-43.
119. Gross L. 1953. A filterable agent, recovered from Ak leukemic extracts, causing salivary gland carcinomas in C3H mice. Proc Soc Exp Biol Med 83:414-21.
120. Gross L. 1953. Neck tumors, or leukemia, developing in adult C3H mice following inoculation, in early infancy, with filtered (Berkefeld N), or centrifugated (144,000 X g), Ak-leukemic extracts. Cancer 6:948-58.
121. Morgan GJ. 2014. Ludwik Gross, Sarah Stewart, and the 1950s discoveries of Gross murine leukemia virus and polyoma virus. Stud Hist Philos Biol Biomed Sci 48 Pt B:200-9.
122. Eddy BE, Rowe WP, Hartley JW, Stewart SE, Huebner RJ. 1958. Hemagglutination with the SE polyoma virus. Virology 6:290-1.
123. International Committee on Taxonomy of Viruses. 2018. Virus Taxonomy: 2018b Release, *on* ICTV. https://talk.ictvonline.org/taxonomy/. Accessed
124. Padgett BL, Walker DL, ZuRhein GM, Eckroade RJ, Dessel BH. 1971. Cultivation of papova-like virus from human brain with progressive multifocal leucoencephalopathy. Lancet 1:1257-60.
125. Gardner SD, Field AM, Coleman DV, Hulme B. 1971. New human papovavirus (B.K.) isolated from urine after renal transplantation. Lancet 1:1253-7.
126. Allander T, Andreasson K, Gupta S, Bjerkner A, Bogdanovic G, Persson MA, Dalianis T, Ramqvist T, Andersson B. 2007. Identification of a third human polyomavirus. J Virol 81:4130-6.
127. Gaynor AM, Nissen MD, Whiley DM, Mackay IM, Lambert SB, Wu G, Brennan DC, Storch GA, Sloots TP, Wang D. 2007. Identification of a novel polyomavirus from patients with acute respiratory tract infections. PLoS Pathog 3:e64.
128. Shuda M, Feng H, Kwun HJ, Rosen ST, Gjoerup O, Moore PS, Chang Y. 2008. T antigen mutations are a human tumor-specific signature for Merkel cell polyomavirus. Proc Natl Acad Sci U S A 105:16272-7.
129. Feng H, Shuda M, Chang Y, Moore PS. 2008. Clonal integration of a polyomavirus in human Merkel cell carcinoma. Science 319:1096-100.
130. Schowalter RM, Pastrana DV, Pumphrey KA, Moyer AL, Buck CB. 2010. Merkel cell polyomavirus and two previously unknown polyomaviruses are chronically shed from human skin. Cell Host Microbe 7:509-15.
131. Ho J, Jedrych JJ, Feng H, Natalie AA, Grandinetti L, Mirvish E, Crespo MM, Yadav D, Fasanella KE, Proksell S, Kuan SF, Pastrana DV, Buck CB, Shuda Y, Moore PS, Chang Y. 2015. Human polyomavirus 7-associated pruritic rash and viremia in transplant recipients. J Infect Dis 211:1560-5.
132. Nguyen KD, Lee EE, Yue Y, Stork J, Pock L, North JP, Vandergriff T, Cockerell C, Hosler GA, Pastrana DV, Buck CB, Wang RC. 2017. Human polyomavirus 6 and 7 are associated with pruritic and dyskeratotic dermatoses. J Am Acad Dermatol 76:932-940 e3.
133. van der Meijden E, Janssens RW, Lauber C, Bouwes Bavinck JN, Gorbalenya AE, Feltkamp MC. 2010. Discovery of a new human polyomavirus associated with trichodysplasia spinulosa in an immunocompromized patient. PLoS Pathog 6:e1001024.
134. Scuda N, Hofmann J, Calvignac-Spencer S, Ruprecht K, Liman P, Kuhn J, Hengel H, Ehlers B. 2011. A novel human polyomavirus closely related to the african green monkey-derived lymphotropic polyomavirus. J Virol 85:4586-90.

135. Yu G, Greninger AL, Isa P, Phan TG, Martinez MA, de la Luz Sanchez M, Contreras JF, Santos-Preciado JI, Parsonnet J, Miller S, DeRisi JL, Delwart E, Arias CF, Chiu CY. 2012. Discovery of a novel polyomavirus in acute diarrheal samples from children. PLoS One 7:e49449.
136. Siebrasse EA, Reyes A, Lim ES, Zhao G, Mkakosya RS, Manary MJ, Gordon JI, Wang D. 2012. Identification of MW polyomavirus, a novel polyomavirus in human stool. J Virol 86:10321-6.
137. Buck CB, Phan GQ, Raiji MT, Murphy PM, McDermott DH, McBride AA. 2012. Complete genome sequence of a tenth human polyomavirus. J Virol 86:10887.
138. Lim ES, Reyes A, Antonio M, Saha D, Ikumapayi UN, Adeyemi M, Stine OC, Skelton R, Brennan DC, Mkakosya RS, Manary MJ, Gordon JI, Wang D. 2013. Discovery of STL polyomavirus, a polyomavirus of ancestral recombinant origin that encodes a unique T antigen by alternative splicing. Virology 436:295-303.
139. Korup S, Rietscher J, Calvignac-Spencer S, Trusch F, Hofmann J, Moens U, Sauer I, Voigt S, Schmuck R, Ehlers B. 2013. Identification of a novel human polyomavirus in organs of the gastrointestinal tract. PLoS One 8:e58021.
140. Mishra N, Pereira M, Rhodes RH, An P, Pipas JM, Jain K, Kapoor A, Briese T, Faust PL, Lipkin WI. 2014. Identification of a novel polyomavirus in a pancreatic transplant recipient with retinal blindness and vasculitic myopathy. J Infect Dis 210:1595-9.
141. Gheit T, Dutta S, Oliver J, Robitaille A, Hampras S, Combes JD, McKay-Chopin S, Le Calvez-Kelm F, Fenske N, Cherpelis B, Giuliano AR, Franceschi S, McKay J, Rollison DE, Tommasino M. 2017. Isolation and characterization of a novel putative human polyomavirus. Virology 506:45-54.
142. Kamminga S, van der Meijden E, Wunderink HF, Touze A, Zaaijer HL, Feltkamp MCW. 2018. Development and Evaluation of a Broad Bead-Based Multiplex Immunoassay To Measure IgG Seroreactivity against Human Polyomaviruses. J Clin Microbiol 56:01566-17.
143. Chen T, Mattila PS, Jartti T, Ruuskanen O, Söderlund-Venermo M, Hedman K. 2011. Seroepidemiology of the newly found trichodysplasia spinulosa-associated polyomavirus. J Infect Dis 204:1523-6.
144. Chen T, Hedman L, Mattila PS, Jartti T, Ruuskanen O, Söderlund-Venermo M, Hedman K. 2011. Serological evidence of Merkel cell polyomavirus primary infections in childhood. J Clin Virol 50:125-9.
145. Gedvilaite A, Tryland M, Ulrich RG, Schneider J, Kurmauskaite V, Moens U, Preugschas H, Calvignac-Spencer S, Ehlers B. 2017. Novel polyomaviruses in shrews (Soricidae) with close similarity to human polyomavirus 12. J Gen Virol 98:3060-3067.
146. Kean JM, Rao S, Wang M, Garcea RL. 2009. Seroepidemiology of human polyomaviruses. PLoS Pathog 5:e1000363.
147. Lundstig A, Dillner J. 2006. Serological diagnosis of human polyomavirus infection. Adv Exp Med Biol 577:96-101.
148. Moens U, Van Ghelue M, Song X, Ehlers B. 2013. Serological cross-reactivity between human polyomaviruses. Rev Med Virol 23:250-64.
149. Stolt A, Sasnauskas K, Koskela P, Lehtinen M, Dillner J. 2003. Seroepidemiology of the human polyomaviruses. J Gen Virol 84:1499-504.
150. Allander T, Jartti T, Gupta S, Niesters HG, Lehtinen P, Osterback R, Vuorinen T, Waris M, Bjerkner A, Tiveljung-Lindell A, van den Hoogen BG, Hyypia T, Ruuskanen O. 2007. Human bocavirus and acute wheezing in children. Clin Infect Dis 44:904-10.
151. Gossai A, Waterboer T, Nelson HH, Michel A, Willhauck-Fleckenstein M, Farzan SF, Hoen AG, Christensen BC, Kelsey KT, Marsit CJ, Pawlita M, Karagas MR. 2016. Seroepidemiology of Human Polyomaviruses in a US Population. Am J Epidemiol 183:61-9.
152. Neske F, Prifert C, Scheiner B, Ewald M, Schubert J, Opitz A, Weissbrich B. 2010. High prevalence of antibodies against polyomavirus WU, polyomavirus KI, and human bocavirus in German blood donors. BMC Infect Dis 10:215.
153. Nicol JT, Robinot R, Carpentier A, Carandina G, Mazzoni E, Tognon M, Touze A, Coursaget P. 2013. Age-specific seroprevalences of merkel cell polyomavirus, human polyomaviruses 6, 7, and 9, and trichodysplasia spinulosa-associated polyomavirus. Clin Vaccine Immunol 20:363-8.
154. Pastrana DV, Tolstov YL, Becker JC, Moore PS, Chang Y, Buck CB. 2009. Quantitation of human seroresponsiveness to Merkel cell polyomavirus. PLoS Pathog 5:e1000578.

155. van der Meijden E, Bialasiewicz S, Rockett RJ, Tozer SJ, Sloots TP, Feltkamp MC. 2013. Different serologic behavior of MCPyV, TSPyV, HPyV6, HPyV7 and HPyV9 polyomaviruses found on the skin. PLoS One 8:e81078.
156. Ehlers B, Wieland U. 2013. The novel human polyomaviruses HPyV6, 7, 9 and beyond. APMIS 121:783-95.
157. van der Meijden E, Kazem S, Burgers MM, Janssens R, Bouwes Bavinck JN, de Melker H, Feltkamp MC. 2011. Seroprevalence of trichodysplasia spinulosa-associated polyomavirus. Emerg Infect Dis 17:1355-63.
158. Pedergnana V, Martel-Jantin C, Nicol JTJ, Leblond V, Tortevoye P, Coursaget P, Touze A, Abel L, Gessain A. 2017. Trichodysplasia Spinulosa Polyomavirus Infection Occurs during Early Childhood with Intrafamilial Transmission, Especially from Mother to Child. J Invest Dermatol 137:1181-1183.
159. Nicol JT, Touze A, Robinot R, Arnold F, Mazzoni E, Tognon M, Coursaget P. 2012. Seroprevalence and cross-reactivity of human polyomavirus 9. Emerg Infect Dis 18:1329-32.
160. Nicol JT, Leblond V, Arnold F, Guerra G, Mazzoni E, Tognon M, Coursaget P, Touze A. 2014. Seroprevalence of human Malawi polyomavirus. J Clin Microbiol 52:321-3.
161. Berrios C, Jung J, Primi B, Wang M, Pedamallu C, Duke F, Marcelus C, Cheng J, Garcea RL, Meyerson M, DeCaprio JA. 2015. Malawi polyomavirus is a prevalent human virus that interacts with known tumor suppressors. J Virol 89:857-62.
162. Lim ES, Meinerz NM, Primi B, Wang D, Garcea RL. 2014. Common exposure to STL polyomavirus during childhood. Emerg Infect Dis 20:1559-61.
163. Baker TS, Drak J, Bina M. 1989. The capsid of small papova viruses contains 72 pentameric capsomeres: direct evidence from cryo-electron-microscopy of simian virus 40. Biophys J 55:243-53.
164. FIELDS BN, KNIPE DM, HOWLEY PM. 2013. Polyomavirus, p 1633-1661, Fields Virology 6th ed, vol Volume 2. Philadelphia : Wolters Kluwer Health/Lippincott Williams & Wilkins, 2013.
165. Van Ghelue M, Khan MT, Ehlers B, Moens U. 2012. Genome analysis of the new human polyomaviruses. Rev Med Virol 22:354-77.
166. Carter JJ, Daugherty MD, Qi X, Bheda-Malge A, Wipf GC, Robinson K, Roman A, Malik HS, Galloway DA. 2013. Identification of an overprinting gene in Merkel cell polyomavirus provides evolutionary insight into the birth of viral genes. Proc Natl Acad Sci U S A 110:12744-9.
167. van der Meijden E, Kazem S, Dargel CA, van Vuren N, Hensbergen PJ, Feltkamp MC. 2015. Characterization of T Antigens, Including Middle T and Alternative T, Expressed by the Human Polyomavirus Associated with Trichodysplasia Spinulosa. J Virol 89:9427-39.
168. Cheng J, Rozenblatt-Rosen O, Paulson KG, Nghiem P, DeCaprio JA. 2013. Merkel cell polyomavirus large T antigen has growth-promoting and inhibitory activities. J Virol 87:6118-26.
169. Schowalter RM, Buck CB. 2013. The Merkel cell polyomavirus minor capsid protein. PLoS Pathog 9:e1003558.
170. Griffith JP, Griffith DL, Rayment I, Murakami WT, Caspar DL. 1992. Inside polyomavirus at 25-A resolution. Nature 355:652-4.
171. Bofill-Mas S, Formiga-Cruz M, Clemente-Casares P, Calafell F, Girones R. 2001. Potential transmission of human polyomaviruses through the gastrointestinal tract after exposure to virions or viral DNA. J Virol 75:10290-9.
172. Bofill-Mas S, Rodriguez-Manzano J, Calgua B, Carratala A, Girones R. 2010. Newly described human polyomaviruses Merkel cell, KI and WU are present in urban sewage and may represent potential environmental contaminants. Virol J 7:141.
173. Dalianis T, Hirsch HH. 2013. Human polyomaviruses in disease and cancer. Virology 437:63-72.
174. Rachmadi AT, Torrey JR, Kitajima M. 2016. Human polyomavirus: Advantages and limitations as a human-specific viral marker in aquatic environments. Water Res 105:456-469.
175. Monaco MC, Atwood WJ, Gravell M, Tornatore CS, Major EO. 1996. JC virus infection of hematopoietic progenitor cells, primary B lymphocytes, and tonsillar stromal cells: implications for viral latency. J Virol 70:7004-12.
176. Goudsmit J, Wertheim-van Dillen P, van Strien A, van der Noordaa J. 1982. The role of BK virus in acute respiratory tract disease and the presence of BKV DNA in tonsils. J Med Virol 10:91-9.
177. Jeffers LK, Madden V, Webster-Cyriaque J. 2009. BK virus has tropism for human salivary gland cells in vitro: implications for transmission. Virology 394:183-93.

178. Burger-Calderon R, Madden V, Hallett RA, Gingerich AD, Nickeleit V, Webster-Cyriaque J. 2014. Replication of oral BK virus in human salivary gland cells. J Virol 88:559-73.
179. Comar M, Zanotta N, Rossi T, Pelos G, D'Agaro P. 2011. Secondary lymphoid tissue as an important site for WU polyomavirus infection in immunocompetent children. J Med Virol 83:1446-50.
180. Sheu JC, Tran J, Rady PL, Dao H, Jr., Tyring SK, Nguyen HP. 2019. Polyomaviruses of the skin: integrating molecular and clinical advances in an emerging class of viruses. Br J Dermatol 180:1302-1311.
181. Hampras SS, Giuliano AR, Lin HY, Fisher KJ, Abrahamsen ME, McKay-Chopin S, Gheit T, Tommasino M, Rollison DE. 2015. Natural history of polyomaviruses in men: the HPV infection in men (HIM) study. J Infect Dis 211:1437-46.
182. Wieland U, Silling S, Hellmich M, Potthoff A, Pfister H, Kreuter A. 2014. Human polyomaviruses 6, 7, 9, 10 and Trichodysplasia spinulosa-associated polyomavirus in HIV-infected men. J Gen Virol 95:928-32.
183. Kantola K, Sadeghi M, Lahtinen A, Koskenvuo M, Aaltonen LM, Mottonen M, Rahiala J, Saarinen-Pihkala U, Riikonen P, Jartti T, Ruuskanen O, Söderlund-Venermo M, Hedman K. 2009. Merkel cell polyomavirus DNA in tumor-free tonsillar tissues and upper respiratory tract samples: implications for respiratory transmission and latency. J Clin Virol 45:292-5.
184. Rockett RJ, Sloots TP, Bowes S, O'Neill N, Ye S, Robson J, Whiley DM, Lambert SB, Wang D, Nissen MD, Bialasiewicz S. 2013. Detection of novel polyomaviruses, TSPyV, HPyV6, HPyV7, HPyV9 and MWPyV in feces, urine, blood, respiratory swabs and cerebrospinal fluid. PLoS One 8:e62764.
185. Enders M, Schalasta G, Baisch C, Weidner A, Pukkila L, Kaikkonen L, Lankinen H, Hedman L, Söderlund-Venermo M, Hedman K. 2006. Human parvovirus B19 infection during pregnancy--value of modern molecular and serological diagnostics. J Clin Virol 35:400-6.
186. Aalto SM, Linnavuori K, Peltola H, Vuori E, Weissbrich B, Schubert J, Hedman L, Hedman K. 1998. Immunoreactivation of Epstein-Barr virus due to cytomegalovirus primary infection. J Med Virol 56:186-91.
187. Korhonen MH, Brunstein J, Haario H, Katnikov A, Rescaldani R, Hedman K. 1999. A new method with general diagnostic utility for the calculation of immunoglobulin G avidity. Clin Diagn Lab Immunol 6:725-8.
188. Lappalainen M, Koskela P, Koskiniemi M, Ammala P, Hiilesmaa V, Teramo K, Raivio KO, Remington JS, Hedman K. 1993. Toxoplasmosis acquired during pregnancy: improved serodiagnosis based on avidity of IgG. J Infect Dis 167:691-7.
189. Söderlund-Venermo M, Lahtinen A, Jartti T, Hedman L, Kemppainen K, Lehtinen P, Allander T, Ruuskanen O, Hedman K. 2009. Clinical assessment and improved diagnosis of bocavirus-induced wheezing in children, Finland. Emerg Infect Dis 15:1423-30.
190. Pyöriä L, Toppinen M, Mantyla E, Hedman L, Aaltonen LM, Vihinen-Ranta M, Ilmarinen T, Söderlund-Venermo M, Hedman K, Perdomo MF. 2017. Extinct type of human parvovirus B19 persists in tonsillar B cells. Nat Commun 8:14930.
191. Vaisanen E, Fu Y, Koskenmies S, Fyhrquist N, Wang Y, Keinonen A, Makisalo H, Vakeva L, Pitkanen S, Ranki A, Hedman K, Söderlund-Venermo M. 2019. Cutavirus DNA in Malignant and Nonmalignant Skin of Cutaneous T-Cell Lymphoma and Organ Transplant Patients but Not of Healthy Adults. Clin Infect Dis 68:1904-1910.
192. Gustafsson B, Priftakis P, Rubin J, Giraud G, Ramqvist T, Dalianis T. 2013. Human polyomaviruses were not detected in cerebrospinal fluid of patients with neurological complications after hematopoietic stem cell transplantation. Future Virol 8:809-814.
193. Martins TB, Jaskowski TD, Mouritsen CL, Hill HR. 1995. An evaluation of the effectiveness of three immunoglobulin G (IgG) removal procedures for routine IgM serological testing. Clin Diagn Lab Immunol 2:98-103.
194. Altman DG. 1991. Statistics in medical journals: developments in the 1980s. Stat Med 10:1897-913.
195. Gustafsson B, Priftakis P, Rubin J, Giraud G, Ramqvist T, Dalianis T. 2013. Human polyomaviruses were not detected in cerebrospinal fluid of patients with neurological complications after hematopoietic stem cell transplantation. Future Virol 8:809-814.

196. Goh S, Lindau C, Tiveljung-Lindell A, Allander T. 2009. Merkel cell polyomavirus in respiratory tract secretions. Emerg Infect Dis 15:489-91.
197. Antonsson A, Bialasiewicz S, Rockett RJ, Jacob K, Bennett IC, Sloots TP. 2012. Exploring the prevalence of ten polyomaviruses and two herpes viruses in breast cancer. PLoS One 7:e39842.
198. Toppinen M, Norja P, Aaltonen LM, Wessberg S, Hedman L, Söderlund-Venermo M, Hedman K. 2015. A new quantitative PCR for human parvovirus B19 genotypes. J Virol Methods 218:40-5.
199. Montoya JG. 2002. Laboratory diagnosis of Toxoplasma gondii infection and toxoplasmosis. J Infect Dis 185 Suppl 1:S73-82.
200. Prince HE, Lape-Nixon M. 2014. Role of cytomegalovirus (CMV) IgG avidity testing in diagnosing primary CMV infection during pregnancy. Clin Vaccine Immunol 21:1377-84.
201. Saldan A, Forner G, Mengoli C, Gussetti N, Palu G, Abate D. 2017. Testing for Cytomegalovirus in Pregnancy. J Clin Microbiol 55:693-702.
202. Erdman DD, Usher MJ, Tsou C, Caul EO, Gary GW, Kajigaya S, Young NS, Anderson LJ. 1991. Human parvovirus B19 specific IgG, IgA, and IgM antibodies and DNA in serum specimens from persons with erythema infectiosum. J Med Virol 35:110-5.
203. Salonen EM, Vaheri A, Suni J, Wager O. 1980. Rheumatoid factor in acute viral infections: interference with determination of IgM, IgG, and IgA antibodies in an enzyme immunoassay. J Infect Dis 142:250-5.
204. Hepojoki S, Hepojoki J, Hedman K, Vapalahti O, Vaheri A. 2015. Rapid homogeneous immunoassay based on time-resolved Forster resonance energy transfer for serodiagnosis of acute hantavirus infection. J Clin Microbiol 53:636-40.
205. Waterboer T, Sehr P, Michael KM, Franceschi S, Nieland JD, Joos TO, Templin MF, Pawlita M. 2005. Multiplex human papillomavirus serology based on in situ-purified glutathione s-transferase fusion proteins. Clin Chem 51:1845-53.
206. Montoya JG, Liesenfeld O, Kinney S, Press C, Remington JS. 2002. VIDAS test for avidity of Toxoplasma-specific immunoglobulin G for confirmatory testing of pregnant women. J Clin Microbiol 40:2504-8.
207. Kumolosasi E, Bonhomme A, Beorchia A, Lepan H, Marx C, Foudrinier F, Pluot M, Pinon JM. 1994. Subcellular localization and quantitative analysis of Toxoplasma gondii target antigens of specific immunoglobulins G, M, A, and E. Microsc Res Tech 29:231-9.
208. Prince HE, Wilson M. 2001. Simplified assay for measuring Toxoplasma gondii immunoglobulin G avidity. Clin Diagn Lab Immunol 8:904-8.
209. Lappalainen M, Koskiniemi M, Hiilesmaa V, Ammala P, Teramo K, Koskela P, Lebech M, Raivio KO, Hedman K. 1995. Outcome of children after maternal primary Toxoplasma infection during pregnancy with emphasis on avidity of specific IgG. The Study Group. Pediatr Infect Dis J 14:354-61.
210. Gay-Andrieu F, Fricker-Hidalgo H, Sickinger E, Espern A, Brenier-Pinchart MP, Braun HB, Pelloux H. 2009. Comparative evaluation of the ARCHITECT Toxo IgG, IgM, and IgG Avidity assays for anti-Toxoplasma antibodies detection in pregnant women sera. Diagn Microbiol Infect Dis 65:279-87.
211. Remington JS, Thulliez P, Montoya JG. 2004. Recent developments for diagnosis of toxoplasmosis. J Clin Microbiol 42:941-5.
212. Lefevre-Pettazzoni M, Le Cam S, Wallon M, Peyron F. 2006. Delayed maturation of immunoglobulin G avidity: implication for the diagnosis of toxoplasmosis in pregnant women. Eur J Clin Microbiol Infect Dis 25:687-93.
213. Fricker-Hidalgo H, Saddoux C, Suchel-Jambon AS, Romand S, Foussadier A, Pelloux H, Thulliez P. 2006. New Vidas assay for Toxoplasma-specific IgG avidity: evaluation on 603 sera. Diagn Microbiol Infect Dis 56:167-72.
214. Lappalainen M, Hedman K. 2004. Serodiagnosis of toxoplasmosis. The impact of measurement of IgG avidity. Ann Ist Super Sanita 40:81-8.
215. Wollheim FA, Williams RC, Jr. 1966. Studies on the macroglobulins of human serum. I. Polyclonal immunoglobulin class M (IgM) increase in infectious mononucleosis. N Engl J Med 274:61-7.
216. Klemola E, von Essen R, Wager O, Haltia K, Koivuniemi A, Salmi I. 1969. Cytomegalovirus mononucleosis in previously healthy individuals. Five new cases and follow-up of 13 previously published cases. Ann Intern Med 71:11-9.

217. Sadeghi M, Aronen M, Chen T, Jartti L, Jartti T, Ruuskanen O, Söderlund-Venermo M, Hedman K. 2012. Merkel cell polyomavirus and trichodysplasia spinulosa-associated polyomavirus DNAs and antibodies in blood among the elderly. BMC Infect Dis 12:383.
218. Sadeghi M, Aaltonen LM, Hedman L, Chen T, Söderlund-Venermo M, Hedman K. 2014. Detection of TS polyomavirus DNA in tonsillar tissues of children and adults: evidence for site of viral latency. J Clin Virol 59:55-8.
219. Ohrmalm C, Eriksson R, Jobs M, Simonson M, Stromme M, Bondeson K, Herrmann B, Melhus A, Blomberg J. 2012. Variation-tolerant capture and multiplex detection of nucleic acids: application to detection of microbes. J Clin Microbiol 50:3208-15.
220. Imperiale MJ, Jiang M. 2016. Polyomavirus Persistence. Annu Rev Virol 3:517-532.
221. DeCaprio JA, Garcea RL. 2013. A cornucopia of human polyomaviruses. Nat Rev Microbiol 11:264-76.
222. Monaco MC, Jensen PN, Hou J, Durham LC, Major EO. 1998. Detection of JC virus DNA in human tonsil tissue: evidence for site of initial viral infection. J Virol 72:9918-23.
223. Papa N, Zanotta N, Knowles A, Orzan E, Comar M. 2016. Detection of Malawi polyomavirus sequences in secondary lymphoid tissues from Italian healthy children: a transient site of infection. Virol J 13:97.
224. Kato A, Kitamura T, Takasaka T, Tominaga T, Ishikawa A, Zheng HY, Yogo Y. 2004. Detection of the archetypal regulatory region of JC virus from the tonsil tissue of patients with tonsillitis and tonsilar hypertrophy. J Neurovirol 10:244-9.
225. Herberhold S, Hellmich M, Panning M, Bartok E, Silling S, Akgul B, Wieland U. 2017. Human polyomavirus and human papillomavirus prevalence and viral load in non-malignant tonsillar tissue and tonsillar carcinoma. Med Microbiol Immunol 206:93-103.
226. Kourieh A, Combes JD, Tommasino M, Dalstein V, Clifford GM, Lacau St Guily J, Clavel C, Franceschi S, Gheit T, For The Split Study G. 2018. Prevalence and risk factors of human polyomavirus infections in non-malignant tonsils and gargles: the SPLIT study. J Gen Virol 99:1686-1698.
227. Peng J, Li K, Zhang C, Jin Q. 2016. MW polyomavirus and STL polyomavirus present in tonsillar tissues from children with chronic tonsillar disease. Clin Microbiol Infect 22:97 e1-97 e3.
228. Patel NC, Vilchez RA, Killen DE, Zanwar P, Sroller V, Eldin KW, Lopez-Terrada D, Butel JS. 2008. Detection of polyomavirus SV40 in tonsils from immunocompetent children. J Clin Virol 43:66-72.
229. Babakir-Mina M, Ciccozzi M, Bonifacio D, Bergallo M, Costa C, Cavallo R, Di Bonito L, Perno CF, Ciotti M. 2009. Identification of the novel KI and WU polyomaviruses in human tonsils. J Clin Virol 46:75-9.
230. Astegiano S, Terlizzi ME, Elia M, Cavallo GP, Costa C, Cavallo R, Bergallo M. 2010. Prevalence of polyomaviruses BK, JC, SV40, KI, and WU in non-malignant tonsil specimens. Minerva Med 101:385-9.
231. Comar M, Zanotta N, Bovenzi M, Campello C. 2010. JCV/BKV and SV40 viral load in lymphoid tissues of young immunocompetent children from an area of north-east Italy. J Med Virol 82:1236-40.
232. Gunel C, Kirdar S, Omurlu IK, Agdas F. 2015. Detection of the Epstein-Barr virus, Human Bocavirus and novel KI and KU polyomaviruses in adenotonsillar tissues. Int J Pediatr Otorhinolaryngol 79:423-7.
233. Salakova M, Koslabova E, Vojtechova Z, Tachezy R, Sroller V. 2016. Detection of human polyomaviruses MCPyV, HPyV6, and HPyV7 in malignant and non-malignant tonsillar tissues. J Med Virol 88:695-702.
234. Schrama D, Buck CB, Houben R, Becker JC. 2012. No evidence for association of HPyV6 or HPyV7 with different skin cancers. J Invest Dermatol 132:239-41.
235. Scola N, Wieland U, Silling S, Altmeyer P, Stucker M, Kreuter A. 2012. Prevalence of human polyomaviruses in common and rare types of non-Merkel cell carcinoma skin cancer. Br J Dermatol 167:1315-20.
236. Fahsbender E, Altan E, Estrada M, Seguin MA, Young P, Leutenegger CM, Delwart E. 2019. Lyon-IARC Polyomavirus DNA in Feces of Diarrheic Cats. Microbiol Resour Announc 8.

237. Dworkin AM, Tseng SY, Allain DC, Iwenofu OH, Peters SB, Toland AE. 2009. Merkel cell polyomavirus in cutaneous squamous cell carcinoma of immunocompetent individuals. J Invest Dermatol 129:2868-74.
238. Kassem A, Technau K, Kurz AK, Pantulu D, Loning M, Kayser G, Stickeler E, Weyers W, Diaz C, Werner M, Nashan D, Zur Hausen A. 2009. Merkel cell polyomavirus sequences are frequently detected in nonmelanoma skin cancer of immunosuppressed patients. Int J Cancer 125:356-61.
239. Mertz KD, Pfaltz M, Junt T, Schmid M, Fernandez Figueras MT, Pfaltz K, Barghorn A, Kempf W. 2010. Merkel cell polyomavirus is present in common warts and carcinoma in situ of the skin. Hum Pathol 41:1369-79.
240. Murakami M, Imajoh M, Ikawa T, Nakajima H, Kamioka M, Nemoto Y, Ujihara T, Uchiyama J, Matsuzaki S, Sano S, Daibata M. 2011. Presence of Merkel cell polyomavirus in Japanese cutaneous squamous cell carcinoma. J Clin Virol 50:37-41.
241. Rollison DE, Giuliano AR, Messina JL, Fenske NA, Cherpelis BS, Sondak VK, Roetzheim RG, Iannacone MR, Michael KM, Gheit T, Waterboer T, Tommasino M, Pawlita M. 2012. Case-control study of Merkel cell polyomavirus infection and cutaneous squamous cell carcinoma. Cancer Epidemiol Biomarkers Prev 21:74-81.
242. Mertz KD, Paasinen A, Arnold A, Baumann M, Offner F, Willi N, Cathomas G. 2013. Merkel cell polyomavirus large T antigen is detected in rare cases of nonmelanoma skin cancer. J Cutan Pathol 40:543-9.
243. Bellott TR, Baez CF, Almeida SG, Venceslau MT, Zalis MG, Guimaraes MA, Rochael MC, Luz FB, Varella RB, Almeida JR. 2017. Molecular prevalence of Merkel cell polyomavirus in nonmelanoma skin cancer in a Brazilian population. Clin Exp Dermatol 42:390-394.
244. Arvia R, Sollai M, Pierucci F, Urso C, Massi D, Zakrzewska K. 2017. Droplet digital PCR (ddPCR) vs quantitative real-time PCR (qPCR) approach for detection and quantification of Merkel cell polyomavirus (MCPyV) DNA in formalin fixed paraffin embedded (FFPE) cutaneous biopsies. J Virol Methods 246:15-20.
245. Wang Y, Strassl R, Helantera I, Aberle SW, Bond G, Hedman K, Weseslindtner L. 2019. Multiplex analysis of Human Polyomavirus diversity in kidney transplant recipients with BK virus replication. J Clin Virol 120:6-11.